For Reference

NOT TO BE TAKEN FROM THIS ROOM

For Reference

NOT TO BE TAKEN FROM THIS ROOM

Ex LIBRIS
UNIVERSITATIS
ALBERTAENSIS

University of Alberta
Printing Department

Digitized by the Internet Archive
in 2019 with funding from
University of Alberta Libraries

https://archive.org/details/martensiteiniron00malc

1963
#7

THE UNIVERSITY OF ALBERTA

MARTENSITE IN IRON, COBALT AND TITANIUM

A Thesis

Submitted to the Faculty of Graduate Studies

In Partial Fulfilment of the Requirements

For the Degree of Master of Science

DEPARTMENT OF MINING AND METALLURGY

by

MALCOLM JOHN BIBBY

EDMONTON, ALBERTA

APRIL 1963

ABSTRACT

A modified gas quenching unit capable of producing cooling rates up to about 60,000°C/sec is described.

The transformation temperatures of iron, cobalt and titanium are given as a function of cooling rate.

Iron containing 0.005 pct carbon is found to have two characteristic temperatures - the massive transformation temperature of 742°C and the martensitic transformation temperature, M_s, of 694°C. The M_s temperature of iron with a carbon concentration of less than 0.0017% carbon is 754°C. The effect of small amounts of carbon on M_s is described.

The transformation temperature - cooling rate characteristics of pure titanium are given. The M_s temperature of titanium at a cooling rate of 200°C/sec is 871°C and decreases almost linearly to 782°C at 64,000°C/sec.

The $\alpha \rightarrow \epsilon$ transformation temperature in cobalt is 382°C at very low cooling rates and decreases to 340°C at 12,000°C/sec. A surface structure, characteristic of martensite reactions, is described and associated with the transformation. Transformation characteristics of cobalt whisker crystals are included and discussed.

The results are rationalized on the basis of existing nucleation theory. Two hypostheses are offered to explain the effect of carbon on the M_s temperature of iron. Crussard's shock wave model of martensite formation is extended.

ACKNOWLEDGEMENTS

The author wishes to express his gratitude to Dr. J. Gordon Parr for his inspiration and guidance in the project and to other staff members for helpful criticisms and suggestions. To Professor E. O. Lilge, Head of the Department of Mining and Metallurgy, University of Alberta, I am indebted for departmental supervision; and am very grateful to Mr. R. M. Scott for his assistance with metallographic techniques. Several members of the department offered helpful criticisms and discussions especially Mr. J. Goldak MSc, Mr. J. R. Cahoon BSc and Mr. Wm. Swanson BSc. A Steel Company of Canada Fellowship and a Consolidated Mining and Smelting Fellowship, as well as the facilities provided by DRB grant 9535-16, are gratefully acknowledged.

TABLE OF CONTENTS

	Page
INTRODUCTION	
GENERAL	1
THE MARTENSITE TRANSFORMATION	4
THE IRON TRANSFORMATION	8
THE TITANIUM TRANSFORMATION	12
THE COBALT TRANSFORMATION	13
WHISKER TRANSFORMATION	13
EXPERIMENTAL	
RAPID COOLING TECHNIQUES	15
WHISKER RESISTANCE MEASUREMENTS	26
RESULTS	
THE IRON TRANSFORMATION	28
A. Transformation Temperature Versus Cooling Rate	30
B. Metallographic Results	34
C. Hardness Measurements	36
THE TITANIUM TRANSFORMATION	37
A. Transformation Temperature Versus Cooling Rate	40
B. Metallographic Results	44
C. Hardness Results	45

TABLE OF CONTENTS

	Page
THE COBALT TRANSFORMATION	46
A. Transformation Temperature Versus Cooling Rate	48
B. Metallographic Results	
C. Hardness Results	52
THE TRANSFORMATION IN COBALT WHISKERS	
A. Resistance Temperature Results	53
DISCUSSION	
THE IRON TRANSFORMATION	60
THE TITANIUM TRANSFORMATION	73
THE COBALT TRANSFORMATION	78
THE TRANSFORMATION IN COBALT WHISKERS	80
GENERAL MARTENSITE TRANSFORMATIONS	82
SUMMARY AND CONCLUSIONS	86
BIBLIOGRAPHY	88
APPENDICES	
APPENDIX I - TABULATION OF TRANSFORMATION TEMPERATURES IN PURE IRON	92
APPENDIX II - TABULATION OF TRANSFORMATION TEMPERATURES IN PURE TITANIUM	95
APPENDIX III - THE SPURIOUS TITANIUM TRANSFORMATION	96

TABLE OF CONTENTS

	Page
APPENDIX IV - TABULATION OF TRANSFORMATION TEMPERATURES IN PURE COBALT	101
APPENDIX V - TABULATION OF WHISKER RESISTANCE RESULTS	102
APPENDIX VI - TABULATION OF MATERIAL COMPOSITION	107
APPENDIX VII - TABULATION OF PUBLICATIONS	109

LIST OF TABLES

		Page
Table 1	A Summary of the M_s Temperatures Obtained in Several Pure Iron Investigations	11
Table 2	Microhardness Measurements of High Purity Iron	36
Table 3	Microhardness Measurements on High Purity Titanium	45
Table 4	Microhardness Measurements on High Purity Cobalt	48
Table 5	Transformation Temperatures of Iron	92
Table 6	Transformation Temperatures of Carburized Iron	94
Table 7	Transformation Temperatures of Titanium	95
Table 8	Transformation Temperatures of Cobalt	101
Table 9	Resistance Measurements of Cobalt Whiskers (Type 1)	102
Table 10	Resistance Measurements of Cycled Cobalt Whiskers	104
Table 11	Resistance Measurements of Cobalt Whiskers (Type 2)	106
Table 12	Material Composition	107

LIST OF ILLUSTRATIONS

		Page
Fig. 1	Gas Quenching Assembly	16
Fig. 2	Quenching Unit	17
Fig. 3	Quenching Jet, Heating Coil and Specimen Assembly	18
Fig. 4	Line Drawing of Quenching Assembly	20
Fig. 5	Scale Drawing of Jet	21
Fig. 6	Oscilloscope Trace of Pure Iron Cooling Curve (44,000°C/sec)	24
Fig. 7	Circuit Diagram For Resistance Measurements of Cobalt Whiskers	27
Fig. 8	$\gamma \rightarrow \alpha$ Transformation in Pure Iron (Rate Range 0-55,000°C/sec)	30
Fig. 9	$\gamma \rightarrow \alpha$ Transformation in Pure Iron (Rate Range 0-10,000°C/sec)	31
Fig. 10	Effect of Carburizing on the Transformation Temperature	32
Fig. 11	M_s Temperatures in Iron - Carbon Alloys	33
Fig. 12	Massive Equiaxed Surface Structure of Iron Cooled at 25,000°C/sec. Transformation Temperature - 742°C	34
Fig. 13	Martensite Surface Structure of Iron Cooled at 50,000°C/sec. Transformation Temperature - 695°C	34
Fig. 14	Martensite Surface Structure of Iron Cooled at 53,000°C/sec. Transformation Temperature - 695°C.	35
Fig. 15	Martensite Surface Structure of Iron Cooled at 10,000°C/sec. Transformation Temperature - 525°C	35
Fig. 16	$\beta \rightarrow \alpha$ Transformation Temperature in Pure Titanium (Rate Range 0-64,000°C/sec)	39

LIST OF ILLUSTRATIONS

		Page
Fig. 17	$\beta \rightarrow \alpha$ Transformation Temperature in Pure Titanium (Rate Range 0-10,000°C/sec)	40
Fig. 18	$\beta \rightarrow \alpha$ Transformation Temperature in Pure Titanium (Rate Range 0-64,000°C/sec) Log Plot	41
Fig. 19	$\beta \rightarrow \alpha$ Time - Temperature - Transformation Curve in Titanium	42
Fig. 20	$\beta \rightarrow \alpha$ Time - Temperature - Transformation Curve in Titanium (Log Plot)	43
Fig. 21	Equiaxed Surface Structure of Titanium Cooled at 10°C/sec. Transformation Temperature - 885°C.	44
Fig. 22	Martensite Surface Structure of Titanium Cooled at 1,000°C/sec Transformation Temperature - 872°C	44
Fig. 23	$\alpha \rightarrow \epsilon$ Transformation Temperature in Pure Cobalt	48
Fig. 24	Surface Structure of Cobalt Cooled at 100°C/sec. Transformation Temperature - 382°C	49
Fig. 25	Surface Structure of Cobalt Cooled at 2,000°C/sec. Transformation Temperature - 380°C	49
Fig. 26	Surface Structure of Cobalt Cooled at 10,000°C/sec. Transformation Temperature - 348°	50
Fig. 27	Surface Structure of Cobalt Showing Transformed Region	50
Fig. 28	Surface Structure of Cobalt Showing Relief Triangles	51
Fig. 29	Cobalt Whisker	51
Fig. 30	Initial Resistance - Temperature Curves for Whisker (Type 1)	55

LIST OF ILLUSTRATIONS

		Page
Fig. 31	Resistance Temperature Curves (Heating) for Whisker (Type 1)	56
Fig. 32	Initial Resistance - Temperature Curves for Whisker (Type 2)	57
Fig. 33	Increase in Resistance of Cycled Whisker (Type 1)	58
Fig. 34	Free Energy Change Accompanying the Martensite Transformation	65
Fig. 35	Schematic Representation of the Variation in Free Energy with Martensite Shear	66
Fig. 36	Effect of Matrix Constraints on the Free Energy of Martensite Formation (After Cohen)	66
Fig. 37	Energy Representation of a Nickel Atom Pair as a Function of Atomic Separation (After Mott and Jones)	70
Fig. 38	Two Dimensional Schematic Representation of the Iron Lattice After Addition of One Carbon Atom	70
Fig. 39	Two Dimensional Schematic Representation of the Iron Lattice After Addition of Two Carbon Atoms	71
Fig. 40	Characteristic Isothermal Transformation Decay Curves	75
Fig. 41	Schematic Representation of Wave Propagation During the Iron Transformation	85
Fig. 42	Oscilloscope Trace of Titanium Cooling Curve Using Chromel - Alumel Thermocouple Wire	98
Fig. 43	Oscilloscope Trace of Titanium Cooling Curve Using Platinum - Platinum Rhodium Thermocouple Wire	98
Fig. 44	Surface Structure of Polished Titanium Showing Base Metal Thermocouple Region	99

LIST OF ILLUSTRATIONS

		Page
Fig. 45	Surface Structure of Polished Titanium Showing Platinum - Platinum Rhodium Thermocouple Region	99
Fig. 46	Surface Structure of Polished Titanium Showing Hardness Indentations in the Base Metal Thermocouple Region	100

INTRODUCTION

GENERAL

The many elements that have allotropic modifications are not to be found in any particular section of the periodic table nor are they limited to any particular structure type. Since free energy changes accompanying transformation processes are usually very small, first principle calculations based on quantum theory must be very exact before a change in the relative stabilities of crystal structures can be predicted. It is, therefore, not surprising that progress has been largely experimental.

Iron, titanium, zirconium, thallium, lithium and sodium transform from a body centered cubic structure stable at high temperatures to a close packed structure stable at lower temperatures. In a body centered cubic structure the atoms are farther apart than in a close packed structure and provide opportunity for greater thermal vibrations. Zener[1] has shown that a 0.35 shear in the (110) plane and the $(1\bar{1}0)$ direction will produce an atomic arrangement that is very nearly face centered cubic. The stiffness factor for this shear is $\frac{1}{2}(c_{11}-c_{12})$ which is relatively small for body centered cubic metals. Thus, the amplitude of thermal vibrations in the $[1\bar{1}0]$ direction is large -- consequently, a greater entropy factor. Because of the large entropy associated with a body centered cubic lattice, free energy is lowered with increasing temperature more rapidly than it is in a close packed structure. Thus, a close packed structure is the more stable at lower temperatures while the body centered structure is stable at high temperatures.

Although iron transforms on cooling from δ, a body centered cubic structure at 1400°C, to γ a face centered cubic structure at 910°C

it reverts back to a body centered cubic structure at 910°C.[2] The upper transformation may be interpreted in terms of the foregoing discussion. Zener[3] has attributed the lower transformation to the electronic structure of iron. Body centered cubic iron becomes spontaneously magnetized at the curie temperature and such magnetization is associated with a lowering of the free energy. According to this viewpoint the transformation might be expected to occur at the curie point. The fact that it actually occurs 150°C above the curie point has been attributed to a local correlation between neighbouring spins.[3]

Calcium, scandium and lanthanum are close packed hexagonal at high temperatures and are face centered cubic at lower temperatures, while the opposite is true in cobalt[4]. There are 12 nearest neighbours, 6 second near neighbours and 8 third near neighbours in the face centered cubic structure. In a close packed hexagonal structure, again there are 12 nearest neighbours and 6 second near neighbours but only 2 third near neighbours. It is not surprising that allotropy is common among close packed structures since third and higher order interactions probably control the relative energetics of the crystal structure. It would appear from experiment, however, that the face centered cubic structure is the more stable at lower temperatures.

It is interesting to note that the $\alpha \rightarrow \epsilon$ transformation temperature in cobalt corresponds to the first electronic transition in the temperature - transition series. Seeger[5] has suggested that the major part of the binding energy in cobalt is associated with the directional (homopolar) interaction of d shell electrons and that the transformation is the result of a d shell electronic transition.

The effect of high cooling rates on transformation temperature is particularly intriguing because of the very rapid transfer of energy. In this respect there is a greater preponderance of experimental data in the literature than of consistent rationalization.

Quite apart from the scientific curiosity aroused by such transformations the strengthening mechanisms of iron alloys and the properties of cobalt and titanium base alloys may depend upon microconstituents formed during rapid cooling. If the martensitic process is to be fully utilized it must be more completely understood. The complications introduced by adding alloy atoms into the crystal do not assist this understanding and, therefore, the work to be described in this investigation is concerned with martensites in pure metals.

THE MARTENSITE TRANSFORMATION

Originally, martensite referred to a microstructure in quenched steels; but this is now much too restrictive to serve as a basis for a definition.

Most recent definitions emphasize two main features [6,7].

The atomic displacements are such as to produce shear that is manifested by a homogeneous tilt on a free metal surface. This feature is often used as a premise for recognizing a martensitic transformation. Secondly, all atomic displacements are less than one interatomic distance so that the transformation is diffusionless. Bilby and Christian [7] emphasized, however, that the only essential feature of the martensite transformation is a tilt on the free surface; the diffusionless nature of the transformation being a consequence of the homogeneous tilt.

Apart from the necessary surface tilt, martensite transformations are usually characterized by the following unique features:

(1) As a result of the diffusionless nature of the transformation there can be no change in chemical composition between the martensitic structure and parent matrix [8].

(2) The tilted regions basically are ellipsoidal or lenticular in shape -- a result of the opposing stress set up by the surrounding matrix [7].

(3) Fundamental to the martensite transformation is the concept of the habit plane [7]. The habit plane is a plane that remains unrotated and undistorted during the transformation. The shear component of transformation is parallel to this habit plane while the dilatational component is perpendicular to the habit plane. As a result, the

matrix - martensite interface remains unrotated.

(4) In many cases each martensite platelet is a result of homogeneous shear[9]. This is a consequence of homogeneous strain, in which the entire transformed region moves as a unit. However, it can be shown that, in order to account for atomic positions in many transformations, a homogeneous shear, as well as a shuffling of atoms, is necessary.

(5) Bilby and Christian[7] have been able to rationalize the crystallography of the transformation by proposing that the matensite reaction is the result of a propagating interface spreading through the parent matrix and leaving martensite behind. Frank[10] proposes a dislocation model for this advancing interface which could account for the resulting homogeneous strains.

(6) Martensite propagates at rates approaching the speed of sound in the material, even at temperatures near absolute zero[11,12]. It may be concluded that the activation energy for such a process is very small.

(7) Many martensites exhibit so called "athermal" kinetics. Athermal martensites are unique in two ways. First, the M_s temperature (temperature at which martensite starts to transform) is independent of cooling rate. Secondly, the transformation proceeds only while the metal is being cooled. This type of behavior is typical of iron base alloys. There are, however, well known isothermal martensities,[13,14,15,16] where transformation proceeds with time at temperature and where the M_s temperature can be depressed with increasing cooling rate. It is noteworthy that there are two modes of athermal formation. For example, martensite in iron - nickel alloys[17] is produced by the formation of new plates which shoot out to their final size in one burst, whereas,

athermal martensite plates of the AuCd type[18] form by a series of propagating steps. Iron - nickel martensites are characterized by a large degree of supercooling and a high driving force, whereas, martensites typical of the AuCd type show little supercooling and a small driving force. The validity of the last statement is subject to some doubt in the light of recent experiments by Singh and Parr[60]. Both types disappear on heating in approximately the opposite order of formation.

(8) Athermal transformations are assumed to proceed only while the metal is being cooled and to stop when cooling is halted. When cooling is resumed, transformation does not usually begin immediately but at some temperature lower than the holding temperature. This phenomenon is known as stabilization[19].

(9) Martensite may form smoothly or entire regions may burst forth[20]. The burst phenomenon is a result of preferred nucleation in the parent matrix near transformed areas. Plates are often observed to propagate end to end because of preferred nucleation near the tip of an existing plate.

(10) Martensite is usually considered to be a metastable phase in iron-base alloys between the parent matrix and the final equilibrium product[21].

(11) The M_s temperature is usually uniquely defined by composition and is generally lowered with increasing solute content.

(12) Some martensites have been shown to be "crystallographically reversible" during heating[22].

(13) The martensite start temperature is increased when the transforming specimen is subjected to applied stress[23,24,25]. The maximum

transformation temperature attainable is the so-called M_d temperature.

(14) Iron - carbon martensites possess a hardness which results from stress in the parent matrix[26]. This is, however, not a feature of all martensites.

Closely associated with the martensitic transformation is the massive transformation[27]. In a recent discussion Owen[28] pointed out the following features of the massive transformation.

(1) The massive structure is a diffusionless transformation product. If differs from martensite, however, in that there is no shape change involved.

(2) The massive structure occurs at intermediate cooling rates and can be depressed by rapid cooling which implies that it is thermally activated.

(3) The characteristic transformation temperature of a massive structure occurs at a higher temperature than does the M_s, and the suggestion has, therefore, been made that the driving force required to start the massive transformation is less than that required to start the martensite transformation.

THE IRON TRANSFORMATION

Iron has a body centered cubic lattice (α) below 910°C, a face centered cubic above 910°C (γ) and is again body centered cubic (δ) between 1403°C and the melting point of 1537°C . The lattice parameter of iron is 2.86A° at room temperature[29]. As the temperature is raised the lattice expands until it transforms at 910°C. Thermal expansion continues in the γ and δ regions. If the lattice parameter of the low temperature body centered cubic structure is plotted against temperature and extrapolated to high temperatures the line representing expansion in the δ phase is an extension of the α line[29]. This suggests that the two lattice types α and δ are identical, a contention that is confirmed by the fact that when a sufficient amount of Al, Cr, Mo, P, S, Sn, W, or V is alloyed with iron the two body centered cubic forms are merged and there is no evidence of any transformation in passing from the high temperature body centered cubic structure to the low temperature body centered cubic structure.

The 910°C transformation that takes place under near equilibrium conditions proceeds by a diffusion mechanism with a diffusion path that depends upon time at temperature. As cooling rate increases the transformation temperature is decreased until a critical rate is reached. At rates higher than this critical rate the transformation temperature remains essentially constant and a tilt is manifested on free metal surfaces. The transformation at this point is martensitic.

If one applies the shape change criterion to the photomicrographs taken by Sauveur and Chou in 1929[30], there is no doubt that the transformation produced in electrolytic iron, quenched in mercury from 1000°C was, indeed, martensitic. However, in 1929 the constitution of martensite was still in doubt; the shear mechanism of formation had not been proposed

and transformation temperatures had not, apparently, been measured.

Consider, first of all, iron - carbon alloys. Face centered cubic iron will accept interstitially a carbon concentration up to 2 pct. Carbon is, however, relatively insoluble in body centered cubic iron. When a solution of carbon in γ iron is cooled slowly carbon is deposited from solution as Fe_3C. Increasing the rate makes it impossible for carbon to be precipitated in the time available and the result is that the sample reaches room temperature with carbon still in solid solution. As the martensite lattice accepts carbon in solid solution one side of the cube decreases while the other side of the cube expands. The axial ratio increases from 1 for pure iron to 1.068 at a carbon concentration of 1.4 pct[29]. Concurrently, the transformation temperature is lowered (Figure 11). Extrapolation of the transformation temperature data to 0 pct carbon varies considerably with different investigations. However, the best extrapolation in the literature suggests that the transformation occurs at 520°C. Iron - nickel and iron mangonese data, on the other hand, extrapolate to 747°C[31]. The recent work of Swanson, however, show that iron - nickel data extrapolate to approximately 680°C[32].

Previous measurements of M_s in pure iron have been made by Esser, et al[33], Duwez[34], Gilbert and Owen[28], and Srivastava and Parr[35]. Table (1) summarizes the values of M_s obtained, the cooling rates at which transformation occurred and the purity of the iron. Two qualifications must be kept in mind, however, when the data in Table (1) are evaluated:

(a) The expressed composition of the iron is not inevitably correct. Carbon analyses at low values are not always reliable; the bar composition may not be typical of the sample used in the experiment, because of local segregation effect.

(b) There is no record of martensite formation being confirmed by metallographic examination for a shape change in any of the work quoted other than that of Srivastava and Parr[35].

The crystallography of iron - carbon martensite transformations has been a subject of intensive research for a number of years. An excellent review article of this is given by Bilby and Christian[7]. The accepted mechanism for carbon steels can be attributed to Greninger and Troiano[9] who postulated it on the basis of relief on polished surfaces and crystallographic relationships. It will suffice to say here that the mechanism is a result of a homogeneous shear followed by a heterogeneous reshuffling of atoms. The mechanism of transformation in pure iron is as yet uncertain, but, according to Barrett[21], is probably similar to the 1.4° pct carbon process.

The conflicting evidence in the literature on the M_s value for pure iron prompted an investigation into the transformation characteristics of pure iron at very high quenching rates.

TABLE I

M_s VALUES OBTAINED IN VARIOUS INVESTIGATIONS

Investigation	Transformation Temperature		Metal Analysis
	M_s	Rate	
Esser, Elender and Spenel[33]	520°C	18,000°C/sec	Carbon - 0.017% No record of Metallics
Gilbert and Owen[28]	560°C	5,500°C/sec	Carbon = 0.010% Si = 0.005% O_2 = 0.006 S = 0.004 P = 0.002
Duwez[34]	750°C	12,000°C/sec	Carbon - 0.001% Trace Metallic impurities each less than 0.001% O_2 less than 0.02%
Srivastava and Parr[35]	519°C	10,000°C/sec	Carbon - 0.005 Si = 0.02 Ni = 0.06

THE TITANIUM TRANSFORMATION

Titanium undergoes an equilibrium transformation at 882°C from the high temperature body centered cubic structure β to the low temperature modification, close packed hexagonal, α . The transformation is diffusion controlled at rates up to 100°C/sec. At this rate the diffusion path is reduced to one interatomic distance and the transformation exhibits martensite characteristics.

Studies on the crystallography of the $\beta \rightarrow \alpha$ transformation have been made by Burgers [39], Newkirk and Geisler [40], and by McHargue [41]. They are led to believe that the transformation mechanism is homogeneous and can be accounted for by a simple homogeneous shear mechanism. However, the problem has not been completely solved.

Duwez [34] found that the transformation temperature was depressed from 882°C to 850°C at rates up to 12,000°C/sec. Srivastava found that the transformation temperature could be depressed to 873° by quenching at rates up to 10,000°C/sec [35].

In view of this depression in M_s with increasing rates, it was decided to investigate the transformation temperature at high quenching rates, up to 65,000°C/sec.

THE COBALT TRANSFORMATION

The stable form of cobalt is close packed hexagonal (ϵ) at low temperatures, and face centered cubic (α) at temperatures above 417°C [42]. Some investigators feel that cobalt transforms to (ϵ) again near the curie point of 1120°C [43, 44]. This suggestion is, however, controversial.

The 417°C transformation has been called martensitic and proceeds by the shear of close packed planes. The transformation is sluggish, in that much of the high temperature phase is retained even at room temperature. The retained face centered cubic phase may be altered to the close packed hexagonal phase by cold work.

A criterion of martensite transformations is the shape changethat produces relief on a polished surface. Bibring, Sebilleau and Buckle [45] in their investigation of the $\alpha \rightarrow \epsilon \rightarrow \alpha$ transformation by micrographical methods observed fine parallel striations that ran almost completely across the crystals. Secondary striations were observed at an angle to the first but were shorter, thicker and less numerous than the primary set. The primary markings appear during the $\alpha \rightarrow \epsilon$ transformation on heating and represent complete crystal transformation; the secondary markings appear on cooling ($\alpha \rightarrow \epsilon$) and are due to local incomplete transformation. Interferometric measurements showed that in the regions of secondary striations, surface tilting had occurred. Takeuch and Honma [46] considered the possibility that surface appearance might indicate a martensitic shear process. They were able to conclude that the mechanism in Co - Ni alloys was indeed martensitic but were unable to draw the same conclusions for pure cobalt.

Troiano and Tockich [47] investigated the transformation temperature at various cooling rates and found the transformation to be athermal at rates up to 3,000°C/sec. This, together with the observation of Edwards

and Lipson[48] that the transformation stops when cooling stops, led Troiano and Tockich[47] to class the transformation as martensitic.

In view of these observations, it was decided to investigate the effect of high quenching rates on the transformation as well as polished surface features. Also, some transformation characteristics of cobalt whiskers were determined.

EXPERIMENTAL

GAS QUENCHING

The rate data obtained in this investigation were obtained by a high velocity gas quenching apparatus. Figure 4 is a scale drawing of the essential components.

The design of the unit is based on the original by Greninger [49] and the modified design by Duwez [34] and by Srivastava [35]. Greninger originally held the sample to be quenched in an inert atmosphere, while the unit used by Duwez was designed so that the specimen was held in a vacuum of 10^{-5} mm Hg or less. Greninger was able to quench at rates up to 3,000°C/sec while Duwez obtained rates of 15,000°C/sec.

The essential features of the gas quenching unit are:

(a) a high vacuum system to avoid oxygen contamination of the specimen,

(b) a means of supporting and heating the specimen to the desired soaking temperature,

(c) a quench jet fed by helium gas under high pressure,

(d) a means of recording the cooling curves.

A. THE VACUUM SYSTEM

The vacuum system comprises a Dia Kia Japanese 150 liter/sec mechanical pump and a two inch M.C.F. 65 liter/second frationating oil diffusion pump. A "Balzers" hot cathode ionization gauge type J.M.G.1 is used to measure the pressure of the system.

B. THE QUENCHING UNIT

The quench unit, Figure 2, comprises a bell jar sealed by an L ring on a flat finely machined brass flange plate. This plate is bolted

Figure 1 Gas Quenching Assembly

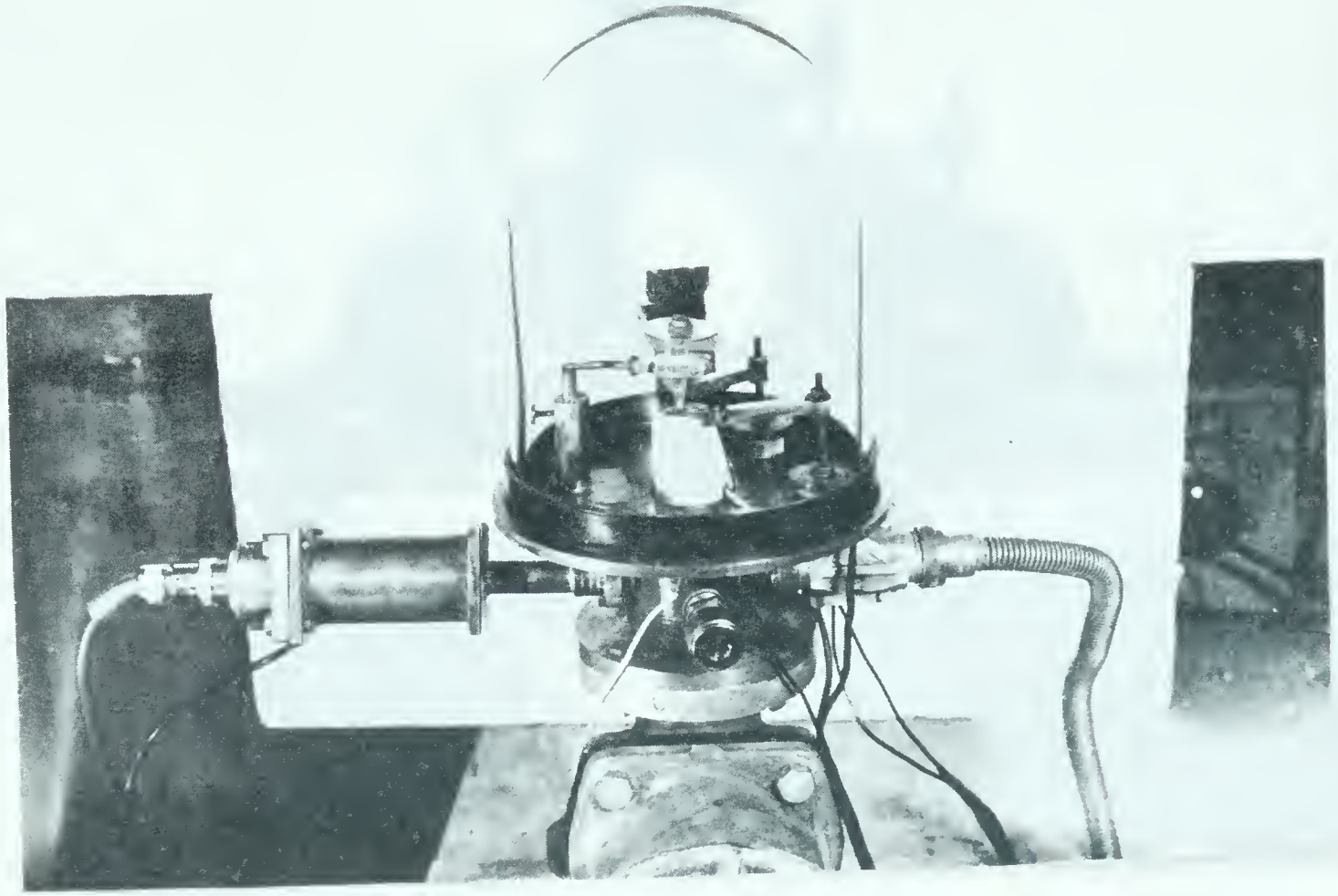

Figure 2 Quenching Unit

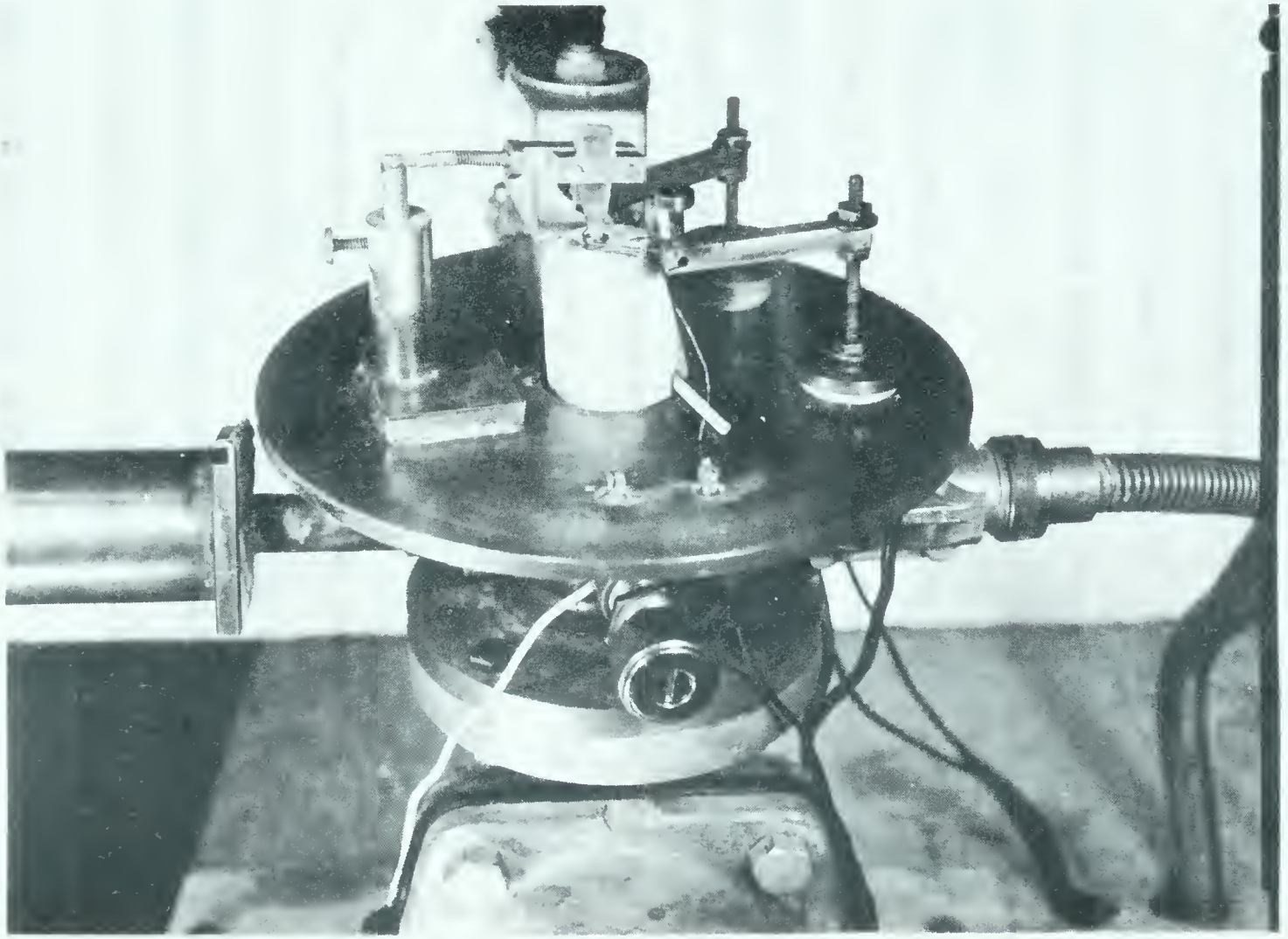

Figure 3 Quenching Jet, Specimen Assembly and Heating Coil

to a small chamber and vacuum sealed by means of O rings. The chamber has four vacuum outlets

(a) to the helium gas quench bottle

(b) to the Balzers vacuum gauge

(c) to a vacuum release valve

(d) to a rough vacuum by-pass line

The chamber is sealed to the vacuum pumping system via a two-inch vacuum speedivac valve.

Kovar glass metal insulators are used to introduce thermocouple wires into the system through the brass flange plate; similarly, two heavy vacuum sealed current terminals are introduced through the flange. Heating is accomplished by supplying current through these leads to a $\frac{1}{4}$ inch diameter tungsten coil of $2\frac{1}{2}$ turns.

The coil is fed by a 300 VA - 110 volt primary, 15 volt secondary variable transformer. This, in turn, is in series with a variac 0-140 volts.

The specimen is held inside the tungsten coil by thermocouple wires that extended from the center of the specimen. A quartz member is placed between the thermocouple wires to help support the sample. This, in turn, is fastened to a cross bar and pillar.

C. THE QUENCH JET AND HELIUM LINE

Beneath the specimen is the quench jet used for rapid cooling. The jet extends through one of the outlets in the chamber below the brass flange plate to a $\frac{1}{2}$ inch vacuum line and solenoid valve used to control the gas flow. The valve is an Asco valve designed for a pressure differential of 200 psi. A $\frac{1}{2}$ inch vacuum line extends from the solenoid valve to a regulated high pressure helium bottle. The downstream pressure

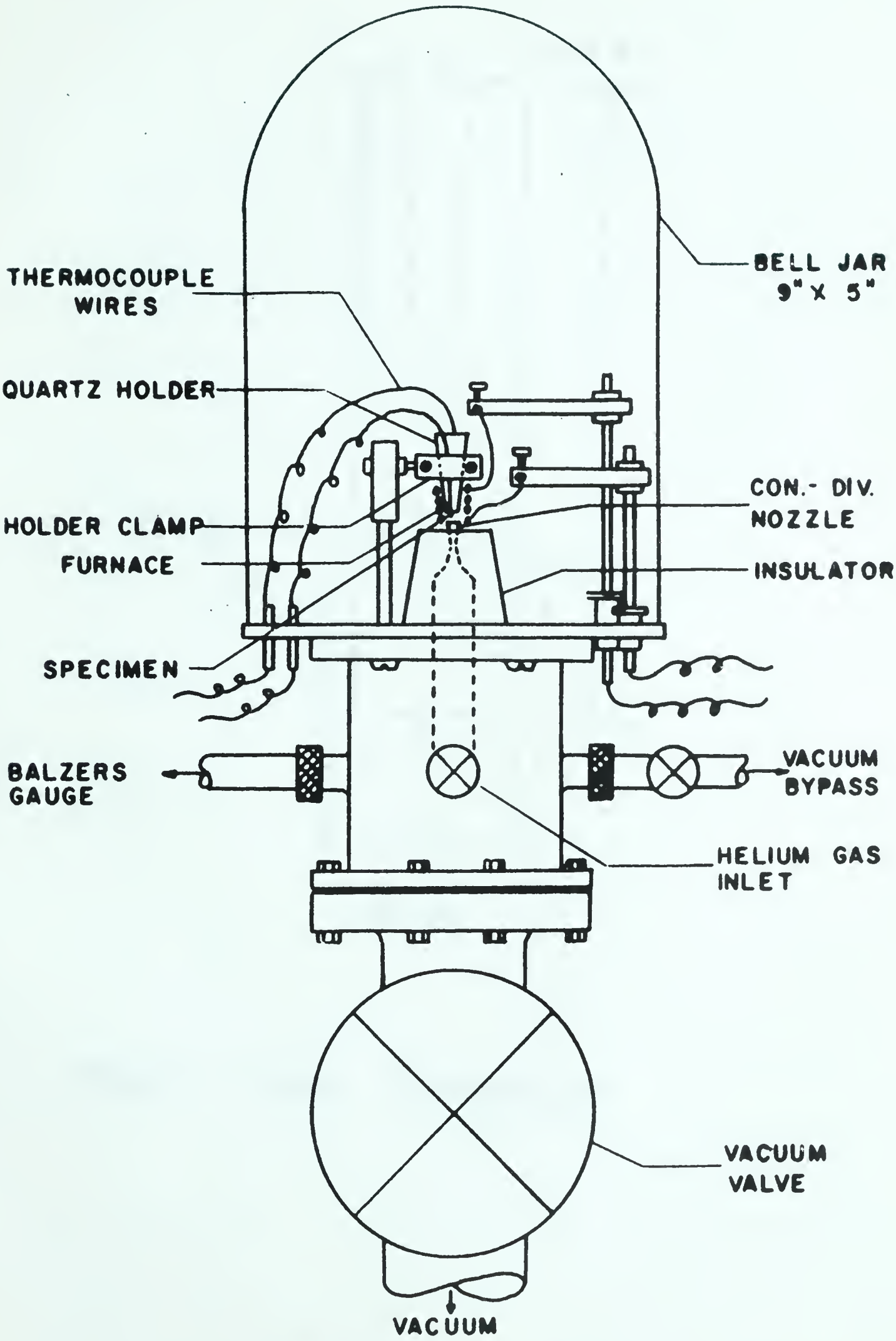

Schematic Representation of Quenching Assembly

Figure·4

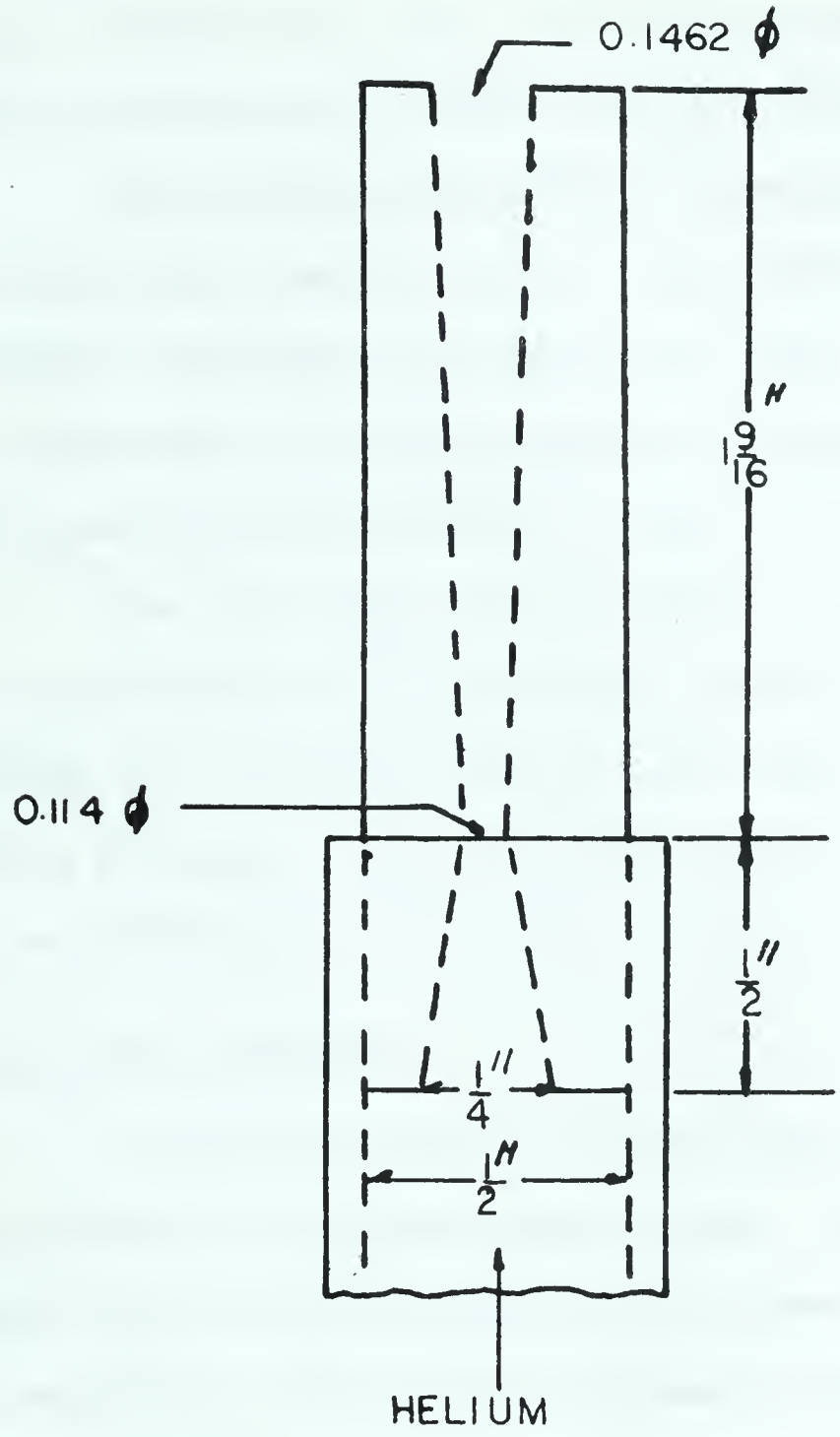

Figure 5 Helium Quenching Jet

between the Asco valve and the regulator is about 15 psi, so that the pressure differential across the valve is almost 30 psi. The Asco valve itself is controlled by a switch from a 110 volt source.

The solenoid valve offered a great improvement over the conventional hand valve used by previous investigators. However, the most significant improvement was made in the nozzle design. The quench nozzle is a convergent - divergent arrangement designed to give supersonic gas velocities and low temperatures. Figure 5 is a line diagram of the jet.

One other modification remains to be explained. Between the nozzle and heating coil is inserted a ceramic crucible for the purpose of shielding the jet against radiation from the resistance heater. With crucible shielding, alone, the maximum cooling rate is increased by as much as 5,000°C/sec.

D. RECORDING APPARATUS

A Tektronix 545A oscilloscope with a type D plug-in preamplifier unit was used to record the cooling curves. The voltage range of the unit is from 1 mv/cm to 20 volts/cm; the time base range is 0.5 microseconds/cm to 5 seconds/cm. The rise time response of the instrument is 0.012 microseconds. Often, it is advantageous to use the type 502 oscilloscope which has a finer voltage scale range 200 micovolts/cm to 50 volts/cm. The time base range of this instrument is 5 sec/cm to 1 microsecond/cm. The voltage base is accurate to 3% and the risetime response is 0.1 microseconds.

A potentiometer is required to calibrate the voltage scale of the oscilloscope. The potentiometer is a Leeds and Northrup instrument that can be read to 0.025 millivolts. The cold junction is usually room temperature and is determined with a thermometer accurate to $\pm 1^{\circ}C$.

E. SAMPLES

Thin wafers of the sample material were cut from titanium, iron and cobalt barstock (See Appendix V for material used). The wafers were then either ground or rolled in a very thin sheet and wrapped around a 0.0031 inch chromel - alumel beaded thermocouple except in the case of titanium (See Appendix III). A spot weld secured the assembly, which was ground with a tungsten file to a 0.010 inch cube.

F. QUENCHING METHOD

The gas quenching unit was first outgassed by evacuating to a pressure of 10^{-5} mm Hg and by supplying heavy current to the tungsten heating coil.

After the specimen had been put into the system it was again evacuated to a pressure of 10^{-5} mm Hg or less. The heating coil was energized and the temperature of the specimen raised to a predetermined soaking temperature (1,000°C for most experiments). The specimen was soaked at 1,000°C for a specific length of time (5 minutes for most experiments). Current to the heater was then switched off and the helium quench valve simultaneously opened.

Before and after the quenching operation the oscilloscope voltage scale was calibrated with the potentiometer, and adjusted to the proper range depending upon the quenching speed. Just before quenching the sample, the shutter of Polaroid Land Camera was opened to the fluorescent screen. As the quench proceeded a polaroid trace was taken of the moving electron beam on the oscilloscope screen. One such curve is shown on Figure 6.

Various quenching rates are obtained by varying the size of the specimen or by using argon gas as well as helium gas. The size of the

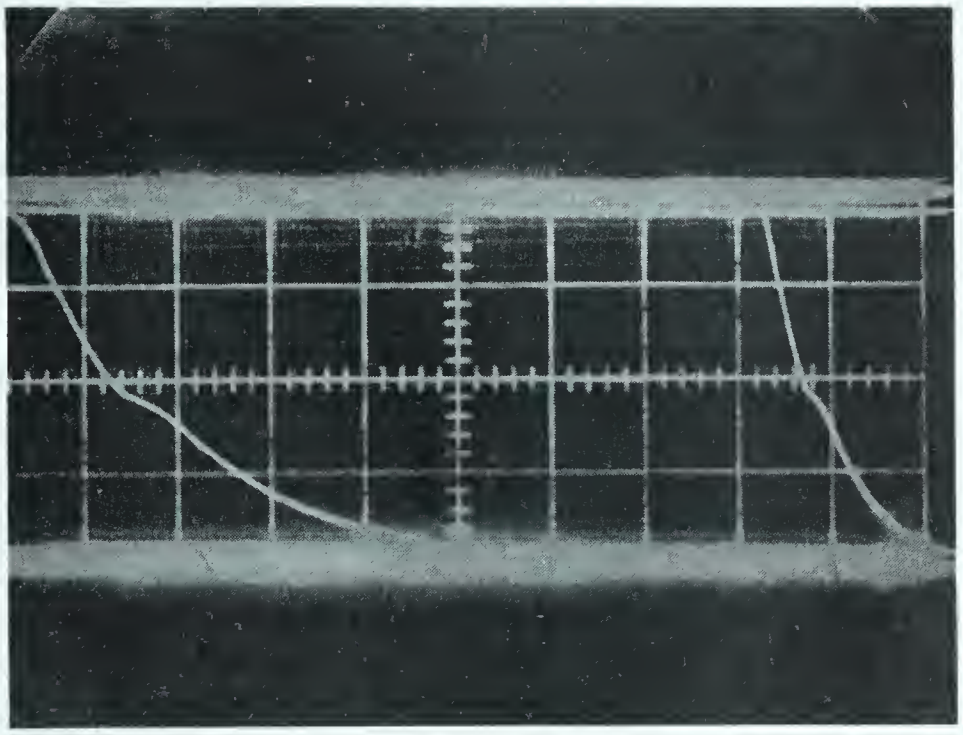

Fig. 6) Oscilloscope Trace of Cooling Curve
Pure Iron Rate (44,000° C/sec.

specimen is not an appealing variable since the transformation becomes masked as the size of the specimen increases, and, possibly, size affects the nature of the transformation. Rates slower than the maximum were also obtained by leaving the heater on during a quench operation, or by changing the position of the specimen. Very slow rates were obtained by turning down the variac with a variable speed reducer. The reducer has the following reduction steps:

(a) 1/5 revolution/second

(b) 1/60 revolution/second

(c) 1/600 revolution/second

G. CARBURIZING PROCEDURE

The effect of a carburizing atmosphere on the transformation temperature in pure iron was studied in the quenching unit. An Edwards leak valve was inserted into one of the vacuum inlets. This was, in turn, connected to a methane gas outlet; and a controlled atmosphere of methane obtained in the system. Iron samples were soaked at 750°C for predetermined lengths of time in a methane atmosphere at 1 inch of mercury. This atmosphere was measured on a J. H. Marsh pressure gauge. Atmospheres at 10^{-2} and 10^{-4} mm Hg were maintained for other experiments. These were measured on the Balzers high vacuum gauge. In addition to varying the carburizing atmosphere, the soaking temperature was varied until optimum conditions were obtained.

After carburizing the sample, the system was evacuated and the sample transformed with a helium quench.

H. HARDNESS MEASUREMENTS

Hardness measurements were taken on some polished specimens with the Reichert microhardness unit under a 20 gram load.

WHISKER TRANSFORMATION APPARATUS

Whiskers for this study from A. G. McMullen, (Department of Mining and Metallurgy, University of Alberta) were grown by the Cobaltous Bromide vapor reduction process.

The $\alpha \rightarrow \gamma$ transformation was studied by means of resistance -- temperature measurements. The whiskers used were from 1 to 9 microns in section and from 2 to 3 centimeters long. Some of the longest of these were removed from the growth crucible and clamped between soft copper knife edge contacts. The effective length between the contacts was about 0.5 cm.

A two volt battery source as well as two resistors, one a standard carbon drop resistor of 10 ohms accurate to $\pm$ 1% and the other a variable resistor 0-5000 ohms were connected in series. Potential leads were affixed to the sample contacts and across the standard carbon drop resistor. The emf across the sample, the emf across the standard resistor, and various furnace thermocouple emf's were all fed into a Honeywell multipoint strip chart recorder with a range from 0 to 45 millivolts, a speed range of 1 inch/min. to 4 inch/min. and a 2 second full scale response time. The emf across the standard resistor permitted the circuit current to be calculated and, hence, knowing the emf across the sample, the sample resistance was calculated.

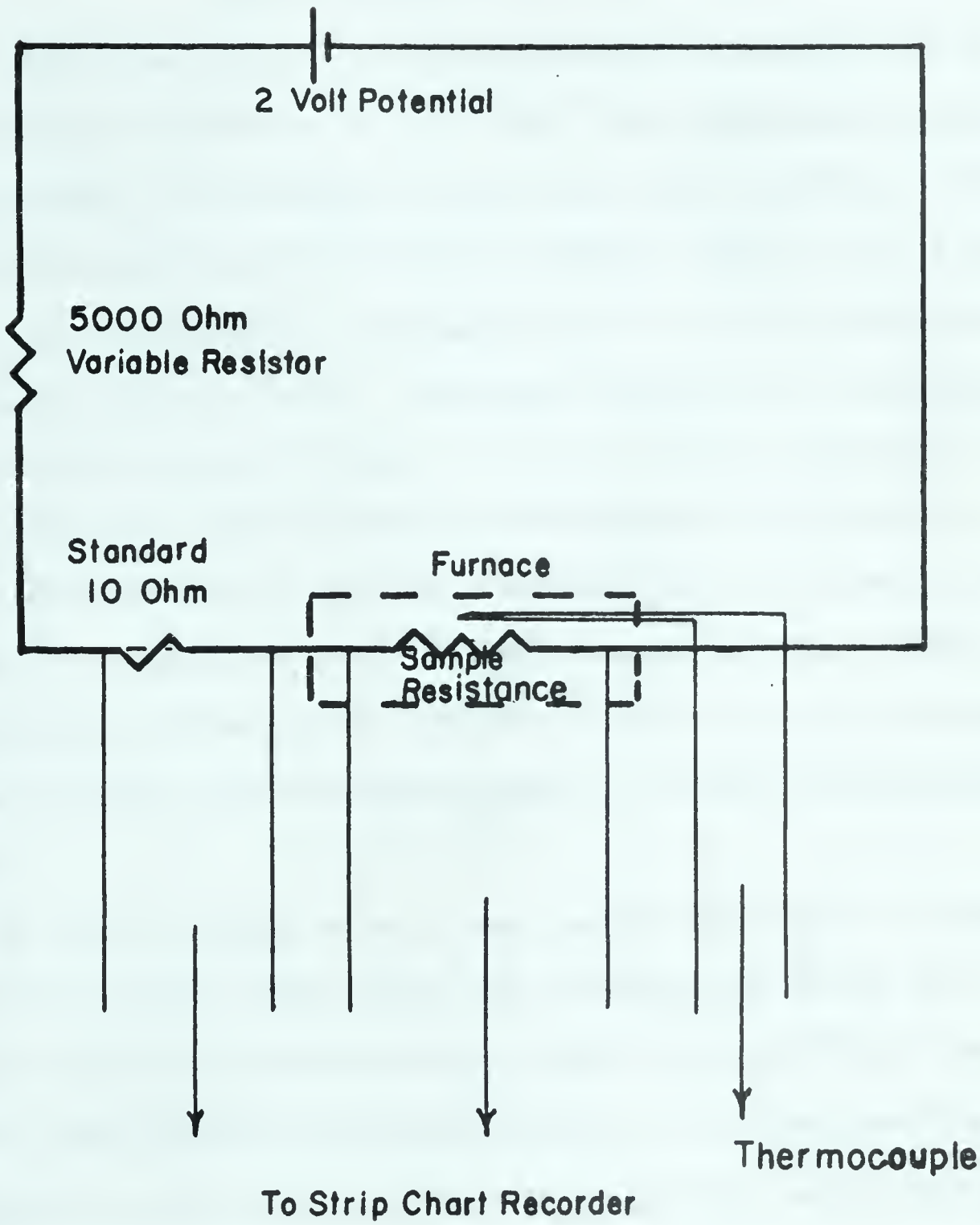

Circuit Diagram For Resistance
Measurements of Whisker Crystals

Figure 1

RESULTS

THE IRON RESULTS

Figure 8 and Figure 9 indicate the effect of cooling rate on the transformation temperature in pure iron. The transformation temperature is decreased with increasing cooling rate until 4,000°C/sec. The transformation temperature at this point is 742°C. There is only a slight decrease in the transformation temperature until a rate of 30,000°C/sec is reached where it drops to 695°C. The surface structure of a transformed specimen at 742°C is shown in Figure 12. The structure is equiaxed, with no surface rumpling. Many 120° grain boundaries are distinguishable.

Iron martensite is shown in Figure 13. This structure is obtained when a sample is quenched at a rate greater than 35,000°C/sec. However, samples quenched at rates greater than this critical value are not always entirely martensitic; only some grains appear to be entirely martensitic (Figure 14).

Of the as received material many samples were found to transform between 500°C and 695°C with critical rates between 5,000°C/sec for a sample that transformed martensitically at 500°C and 33,000°C/sec for a sample that transformed martensitically at 695°C. Two transformation ranges were predominant, a fact which is also evident from the work of Srivastava and Parr[35], who did not pursue the anomaly. There is a range from 700°C to 750°C in which the transformation is non-martensitic and is designated "massive" in accordance with the investigation of Owen and Gilbert[28]. Other specimens transformed under the same rate conditions (10,000°C/sec) in the range 500°C to 540°C and were martensitic as indicated by rumple on a polished surface (Figure 15). Any one sample, on repeated transformation inevitably transformed at the same transformation temperature ±5°C.

As a speculation, the variation in transformation temperature was attributed to the effect of carbon. Consequently, the curves of Figure 10 were obtained, in which a sample that transformed at 700°C (40,000°C/sec) was subjected to a methane atmosphere and subsequently quenched. Even though the exact concentration of carbon is not known Figure 11 shows the extreme effects of small carbon concentrations on the M_S temperature. To confirm that this was actually carbon, a sample was soaked at 750°C for a half hour, slowly cooled, polished and examined metallographically. A pearlitic structure resulted. The approximate amount of carbon absorbed by the specimen was assessed by measuring Ac_3 and assuming it to be lowered 10°C per 0.04 pct carbon. This assumes that differences in Ac_3 due to carbon represent differences in A_3 equilibrium temperature.

The M_S of iron obtained from the National Bureau of Standards containing less than 0.0015% carbon was found to be 754°C $\pm$5°C at a rate of 50,000°C/sec. A massive transformation temperature of 758°C was found at a rate of 10,000°C/sec.

The effect of changing specimen size between 0.1 inch cube and 0.005 X 0.01 X 0.01 inches had no effect on the transformation temperature at a given rate. Further soaking temperatures between 950°C and 1,300°C had no effect.

The $\gamma \rightarrow \alpha$ Transformation in Pure Iron
(Cooling Rate Range 0 → 50,000 °C/sec.)

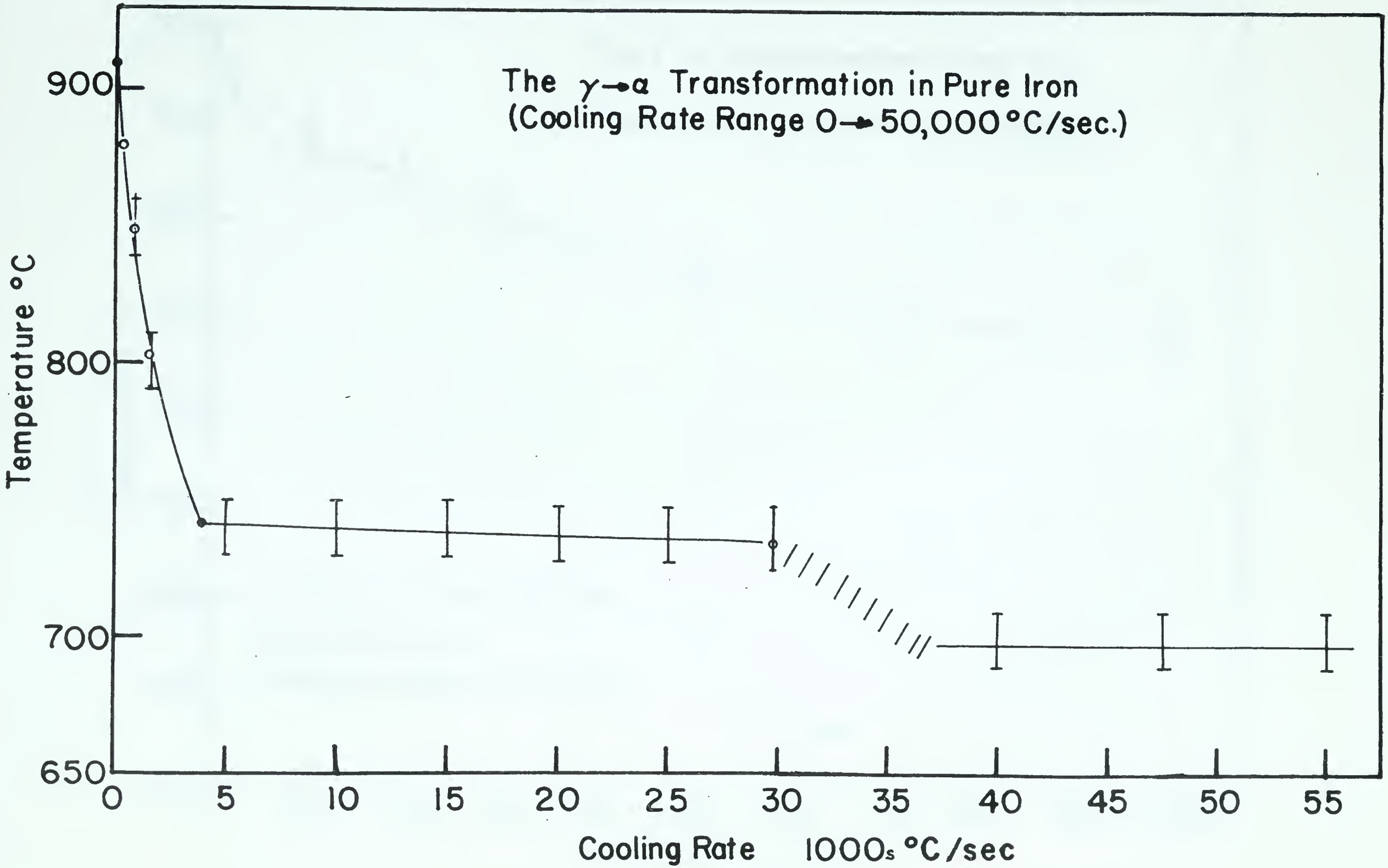

Figure 8

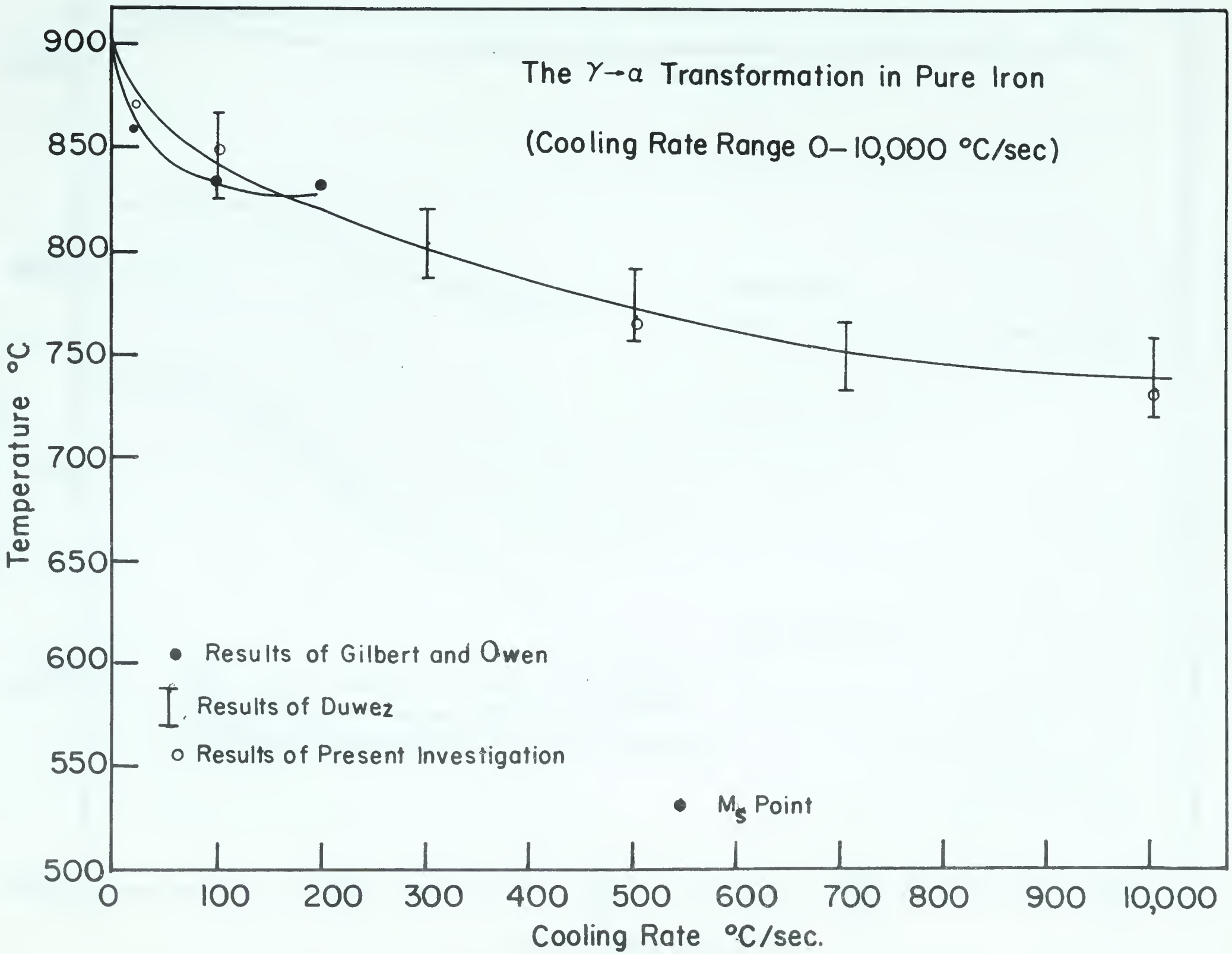
The γ→α Transformation in Pure Iron
(Cooling Rate Range 0–10,000 °C/sec)
Temperature °C
900
850
800
750
700
650
600
550
500
0
100
200
300
400
500
600
700
800
900
10,000
Cooling Rate °C/sec.
Results of Gilbert and Owen
Results of Duwez
Results of Present Investigation
M_S Point

Figure 9

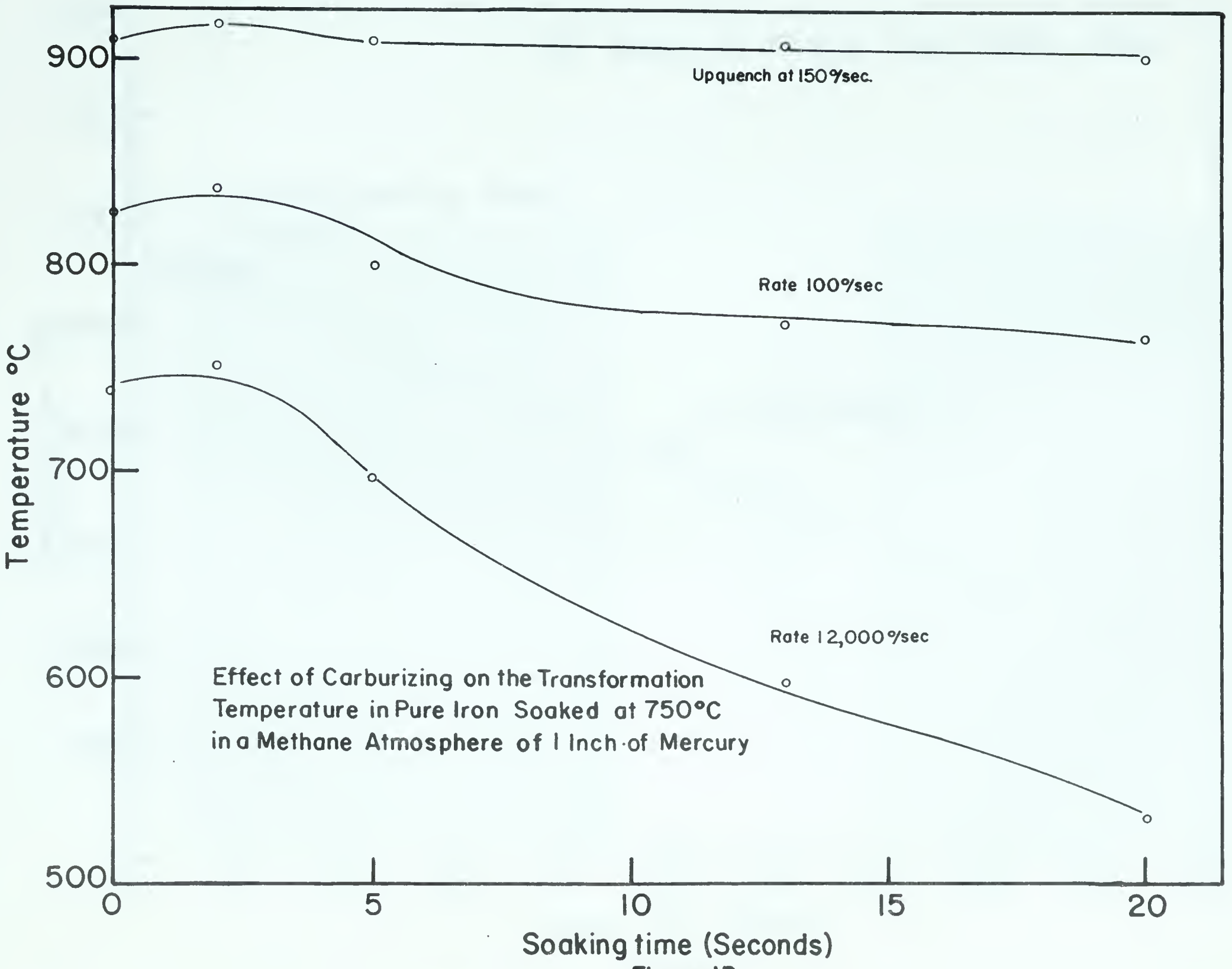

Effect of Carburizing on the Transformation Temperature in Pure Iron Soaked at 750°C in a Methane Atmosphere of 1 Inch of Mercury

Figure 10

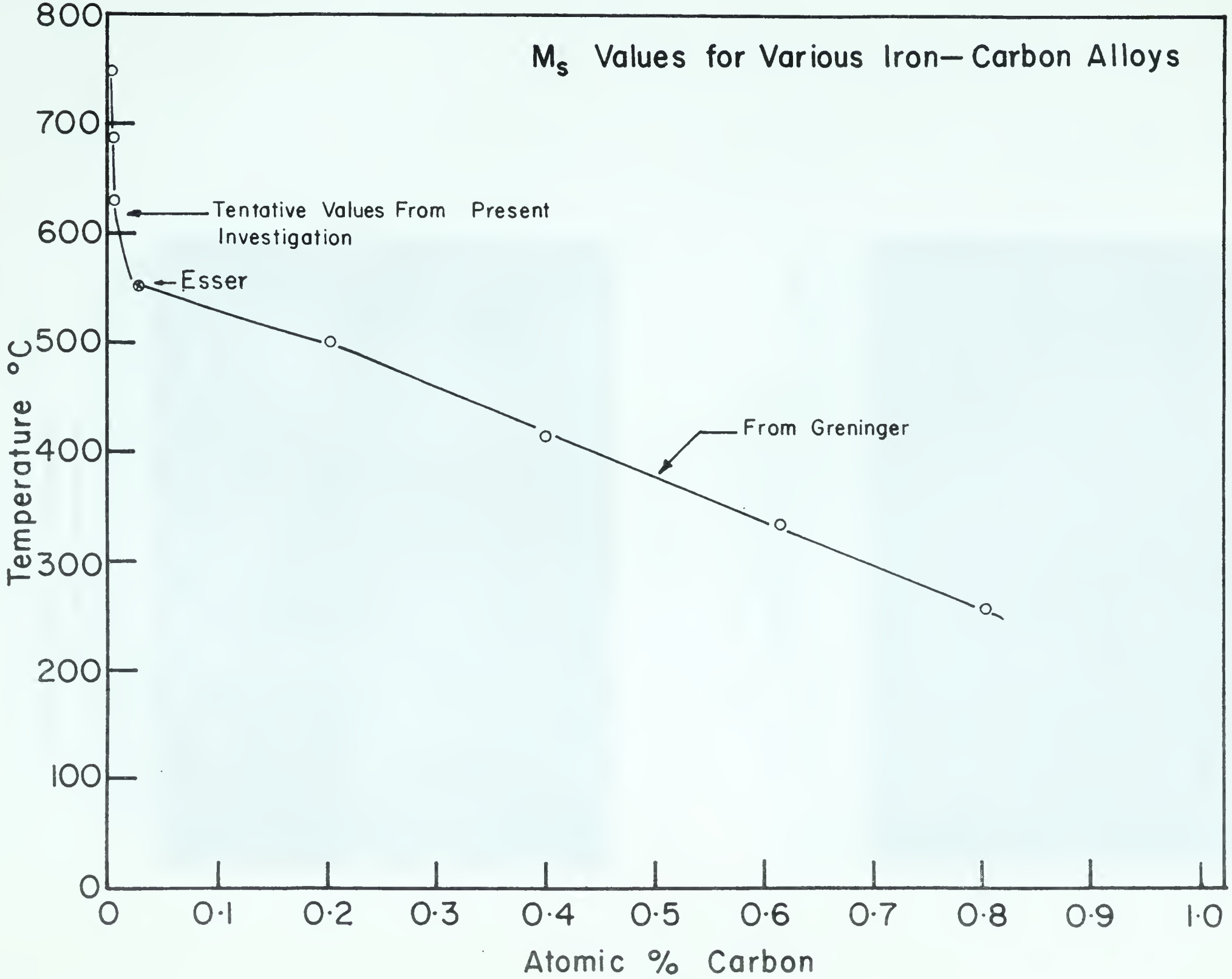
M_s Values for Various Iron—Carbon Alloys
Tentative Values From Present Investigation
Esser
From Greninger
Temperature °C
800
700
600
500
400
300
200
100
0
0
0·1
0·2
0·3
0·4
0·5
0·6
0·7
0·8
0·9
1·0
Atomic % Carbon

Figure 11

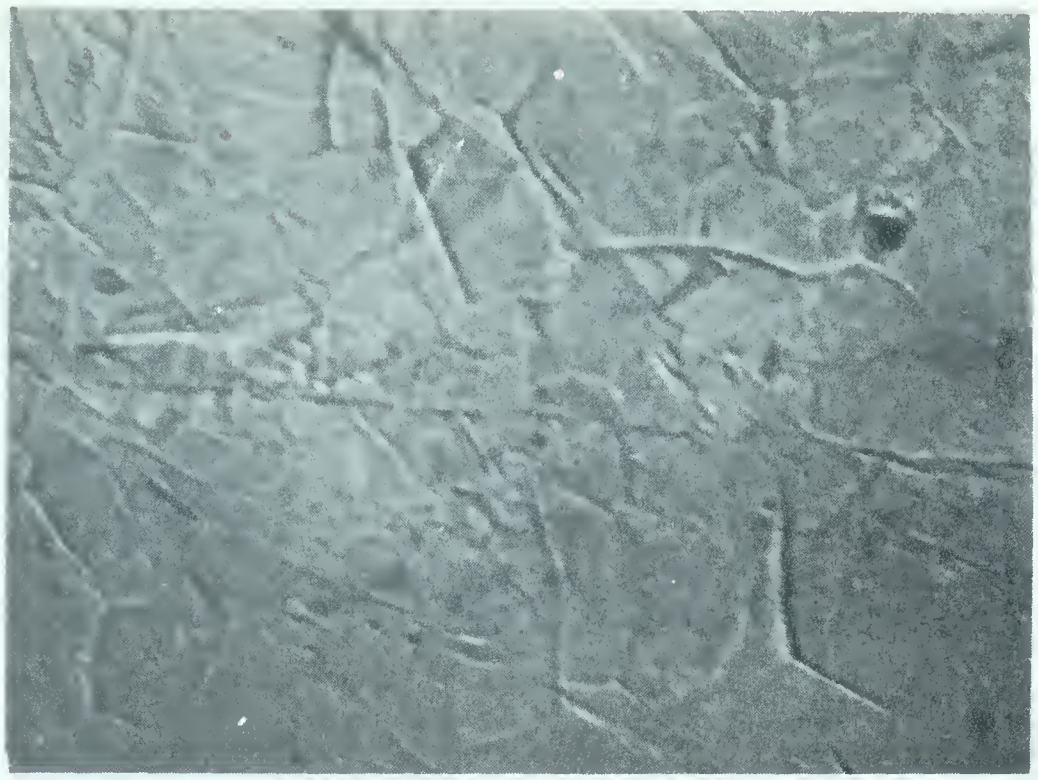

Figure 12 X750 Massive Equiaxed Surface Structure of Iron Cooled at 25,000°C/sec Transformation Temperature – 742°C

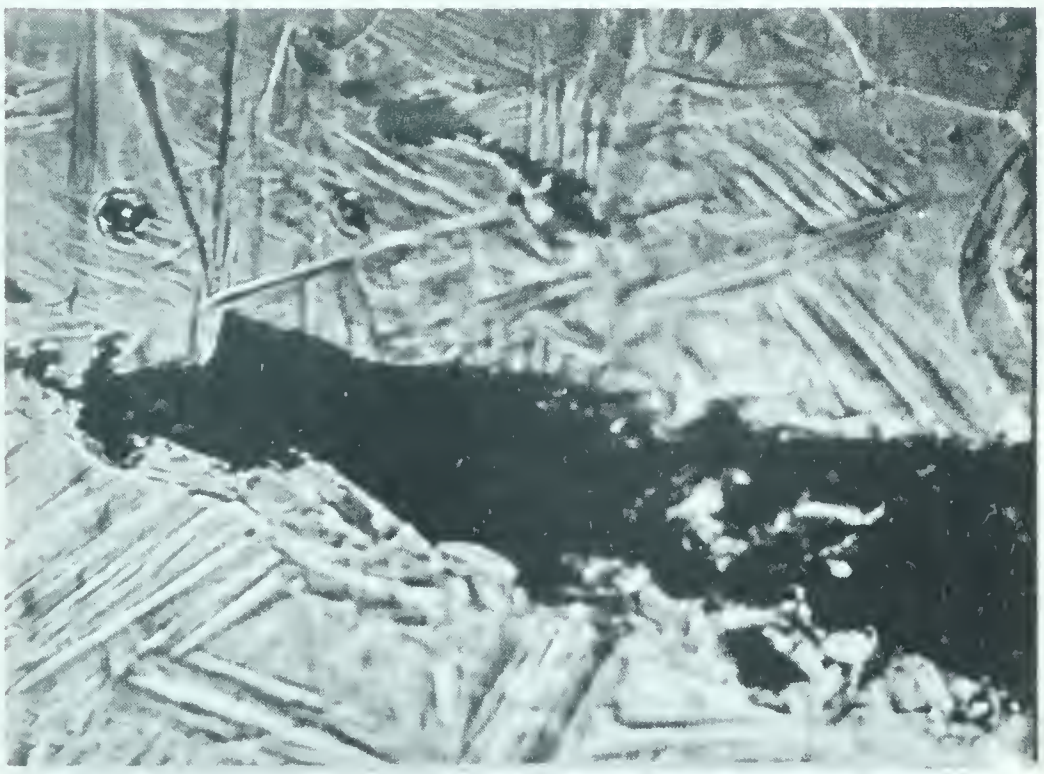

Figure 13 X750 Martensite Surface Structure of Iron Cooled at 50,000°C/sec Transformation Temperature – 694°C

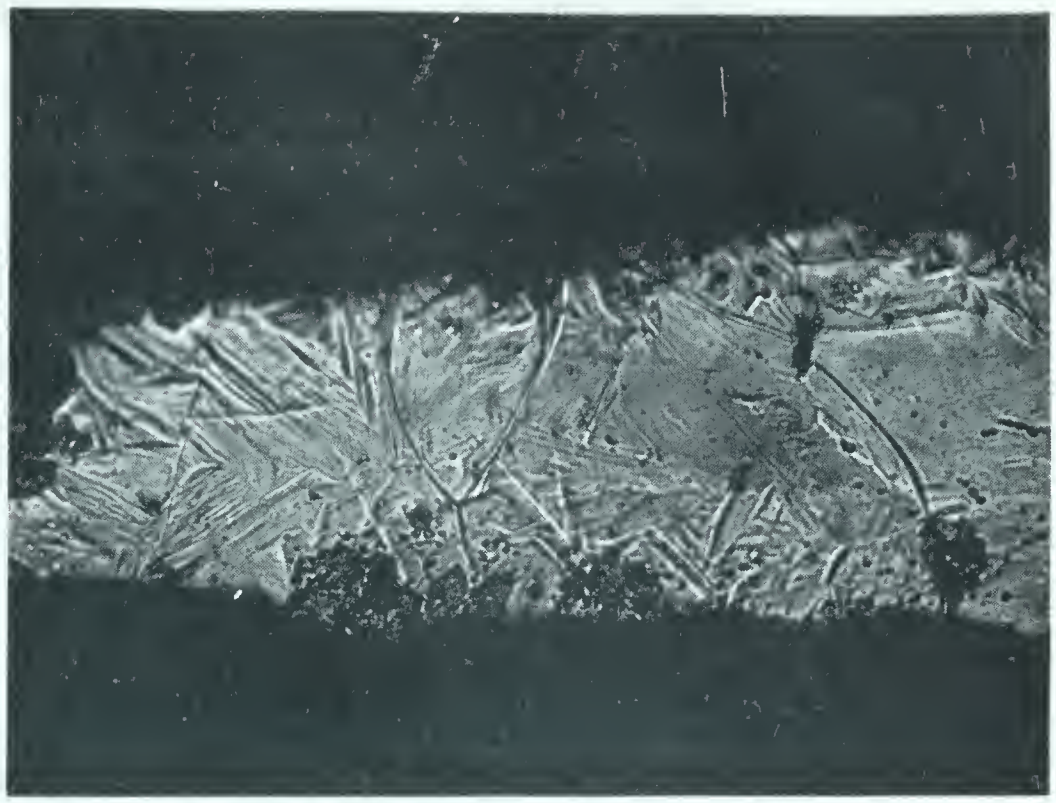

Figure 14 X300 Surface Structure of Iron Cooled at 53,000°C/sec
Transformation Temperature – 695°C

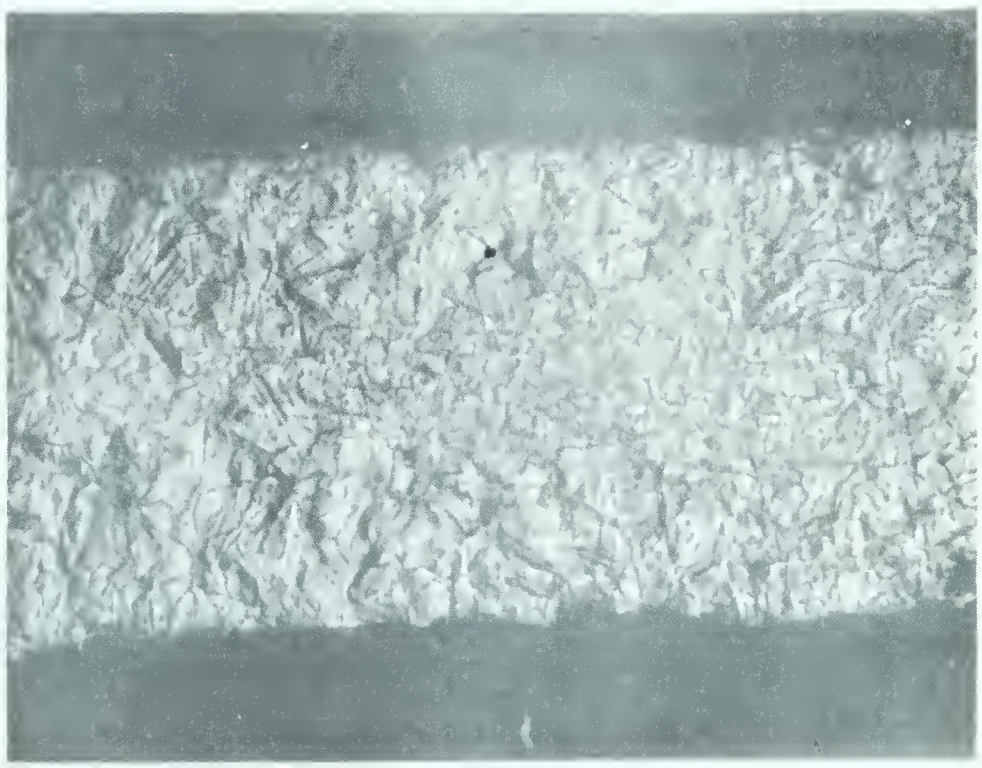

Figure 15 X300 Surface Structure of Iron Cooled at 10,000°C/sec
Transformation Temperature – 525°C

TABLE II MICROHARDNESS RESULTS IN PURE IRON

Heat Treatment	Average Microhardness VPN	Remarks
(1) Slowly Cooled ($100^{o}C$/sec)	112 ± 15	Average of 4 Specimens. Variation Across any one Sample ± 10
(2) "Massive" Iron Quenched at $25,000^{o}C$/sec Transformation Temperature - $742^{o}C$	142 ± 15	Average of 3 Specimens. Variation Across Any one Sample ± 10
(3) Quenched at $25,000^{o}C$/sec Transformation Temperature - $525^{o}C$	164 ± 25	Average of 3 Specimens T. T. Hardness (1) $540^{o}C$ - 164 ± 15 (2) 525 - 154 ± 10 (3) 530 - 175 ± 15
(4) Quenched at $53,000^{o}C$/sec	143 ± 30	T. T. Hardness (1) 695 - 136 ± 10 (2) 754 - 148 ± 10

THE TITANIUM TRANSFORMATION

The $\beta \rightarrow \alpha$ transformation plotted against cooling rate is shown in Figure 16: the transformation temperature is depressed from 872°C at a rate of 200°C/sec to 782°C at a rate of 60,000°C/sec. All samples cooled at rates greater than 200°C/sec were characteristically martensitic (Figure 22). A comparison of rate data obtained in this investigation with that of previous investigations is given in Figure 17. Figure 18 is a log plot of the transformation temperature against cooling rate to show the results of very slow cooling rates. Figure 21 is the surface structure of titanium sample cooled at a rate less than 100°C/sec.

Repeated experiments on any given sample led to the conclusion that experimental error was ± 5°C while the variation of transformation temperature from specimen to specimen was $\pm$ 5°C. Thus, the overall experimental error amounted to ± 10°C.

Since the curve of Figure 16 is approximately a straight line the equation $T_T = \frac{90}{60000} \frac{dT}{dt} + 872$ was assumed to represent the variation in transformation temperature T with the cooling rate $\frac{dT}{dt}$ where $\frac{dT}{dt}$ is a negative quantity.

The M_S depression with cooling rate indicates that the transformation is isothermal and will follow C curve kinetics. By solving for T in terms of t and plotting the results, C curve kinetics should be apparent.

$$(T_T - 872) = \frac{90}{60000} \frac{dT}{dt}$$

$$dt = \frac{90}{60000} \frac{1}{T_T - 872} dT$$

$$\int_0^{t_T} dt = \frac{90}{60000} \frac{1}{T_T - 872} \int_{T_i}^{T_T} dT$$

$$t_r = \frac{90}{60{,}000} \frac{(T_r - T_i)}{(T_r - 872)}$$

Because time to transformation varies with the soaking temperature the C curve is only determinable for that particular soaking temperature. If a T_i (soaking temperature) of 1000°C is chosen the curves of Figures 19 and 20 are obtained.

The size and shape of the specimen used in these experiments had little effect on the transformation temperature nor did soaking temperature alter the temperature of transformation. In all cases, the temperature of transformation on reheating at 150°C/sec was 890°C $\pm$ 10°C.

The results of microhardness measurements are given in Table 2.

The $\alpha-\beta$ Transformation in Pure Titanium
(Cooling Rate Range 0–64,000 °C/sec.)

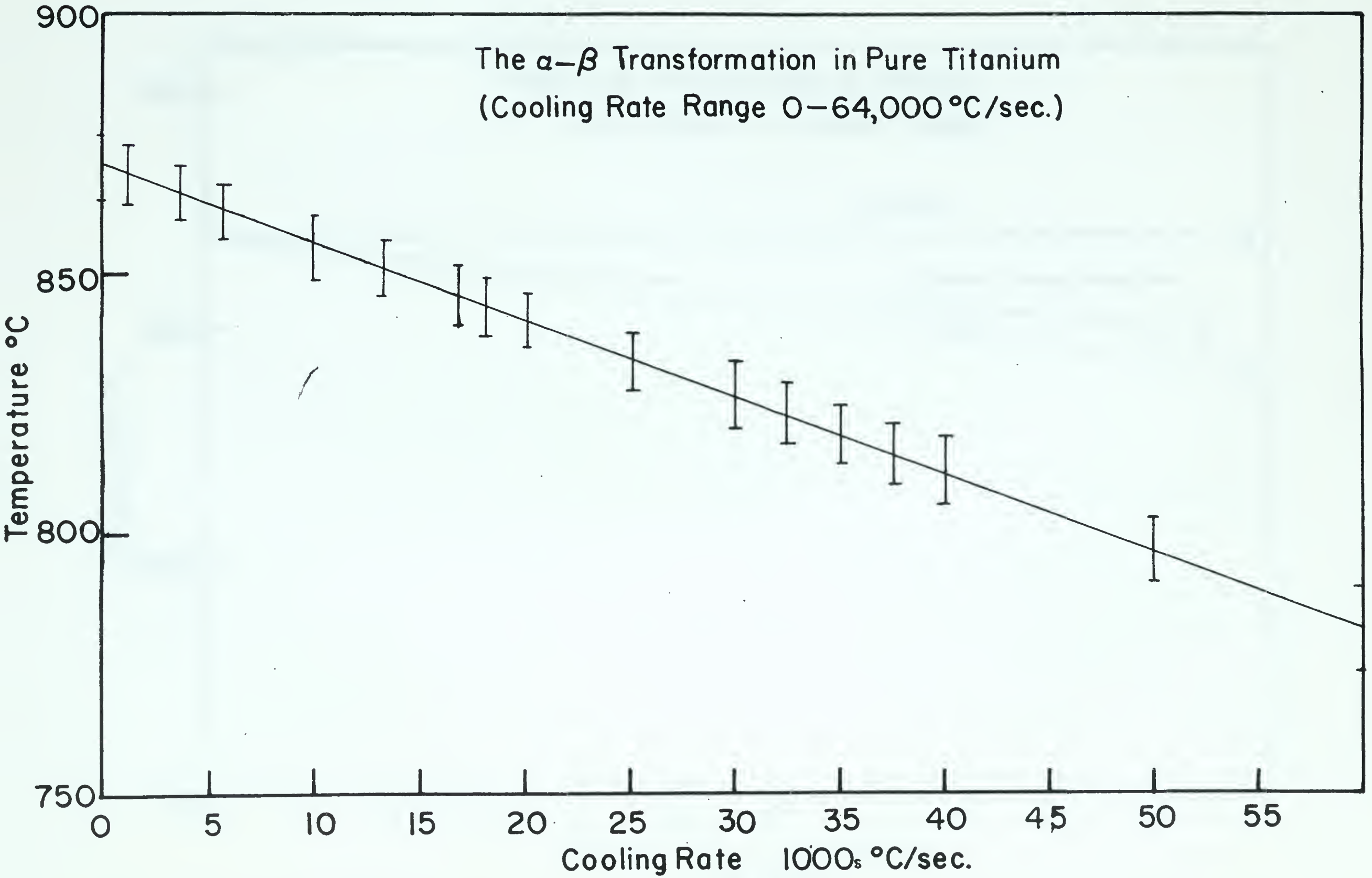

Figure 16

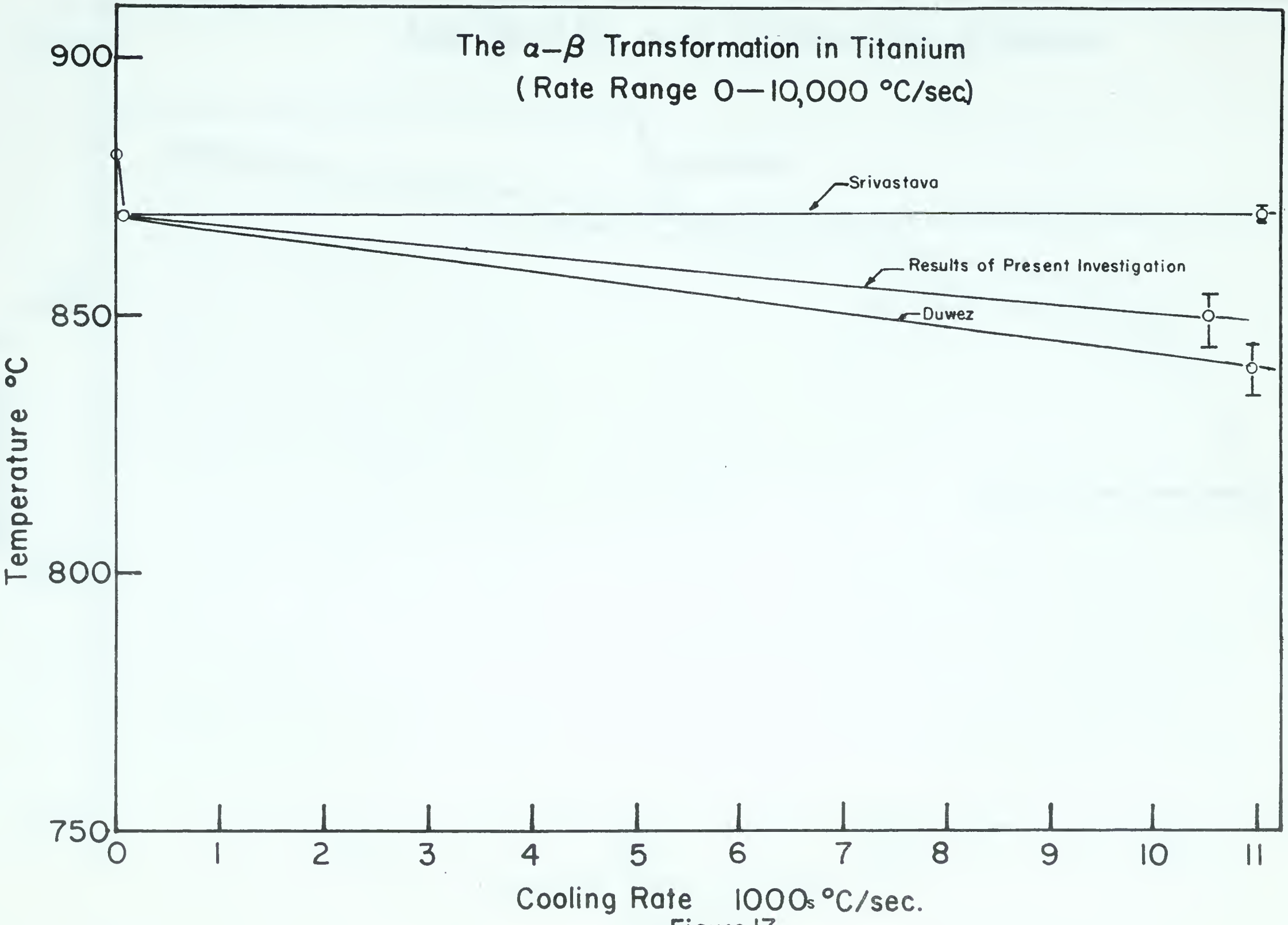
The α–β Transformation in Titanium
(Rate Range 0—10,000 °C/sec)
Srivastava
Results of Present Investigation
Duwez
900
850
800
750
Temperature °C
0
1
2
3
4
5
6
7
8
9
10
11
Cooling Rate 1000s °C/sec.

Figure 17

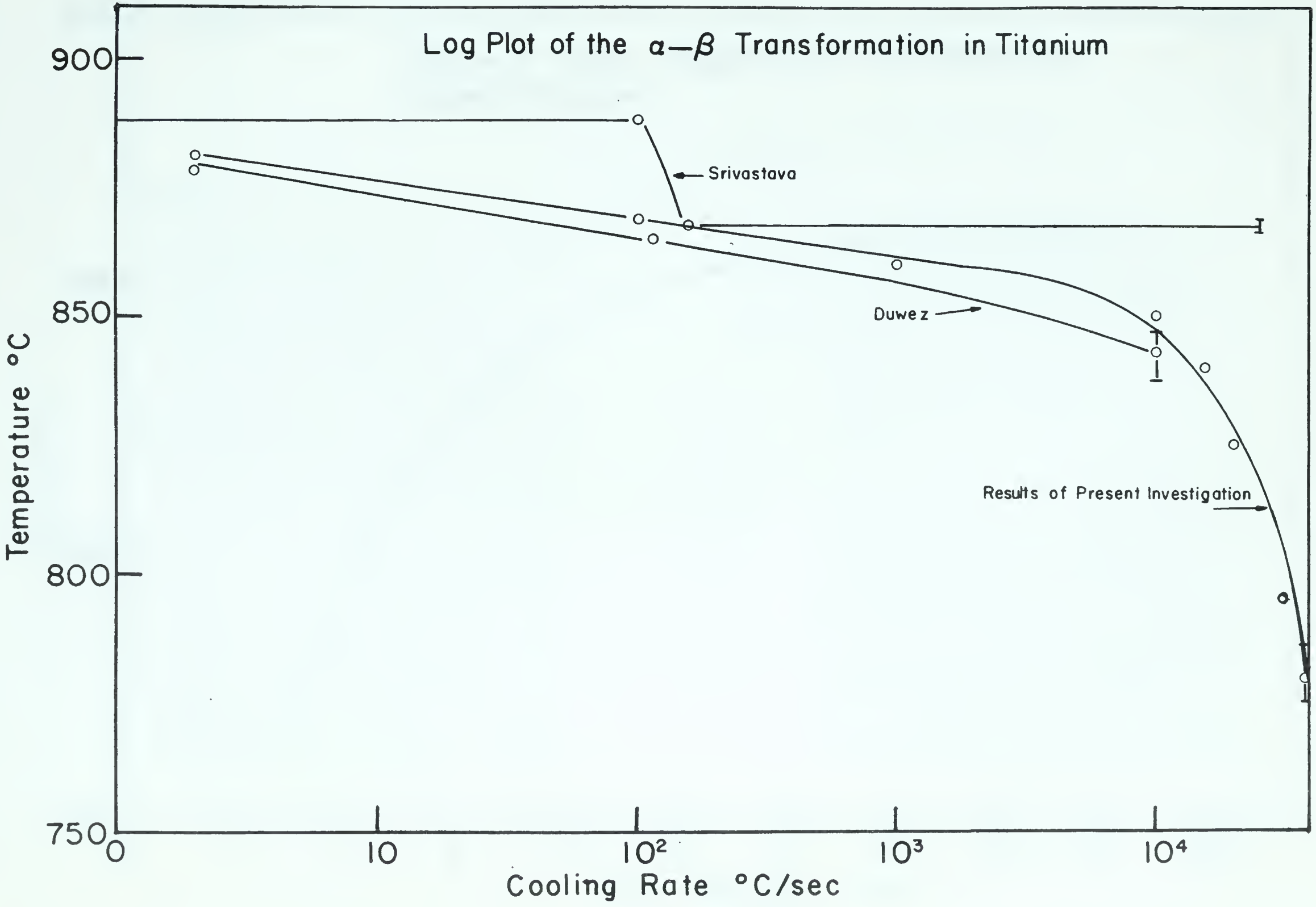
Log Plot of the α—β Transformation in Titanium
900
850
800
750
Temperature °C
Srivastava
Duwez
Results of Present Investigation
0
10
10²
10³
10⁴
Cooling Rate °C/sec

Figure 18

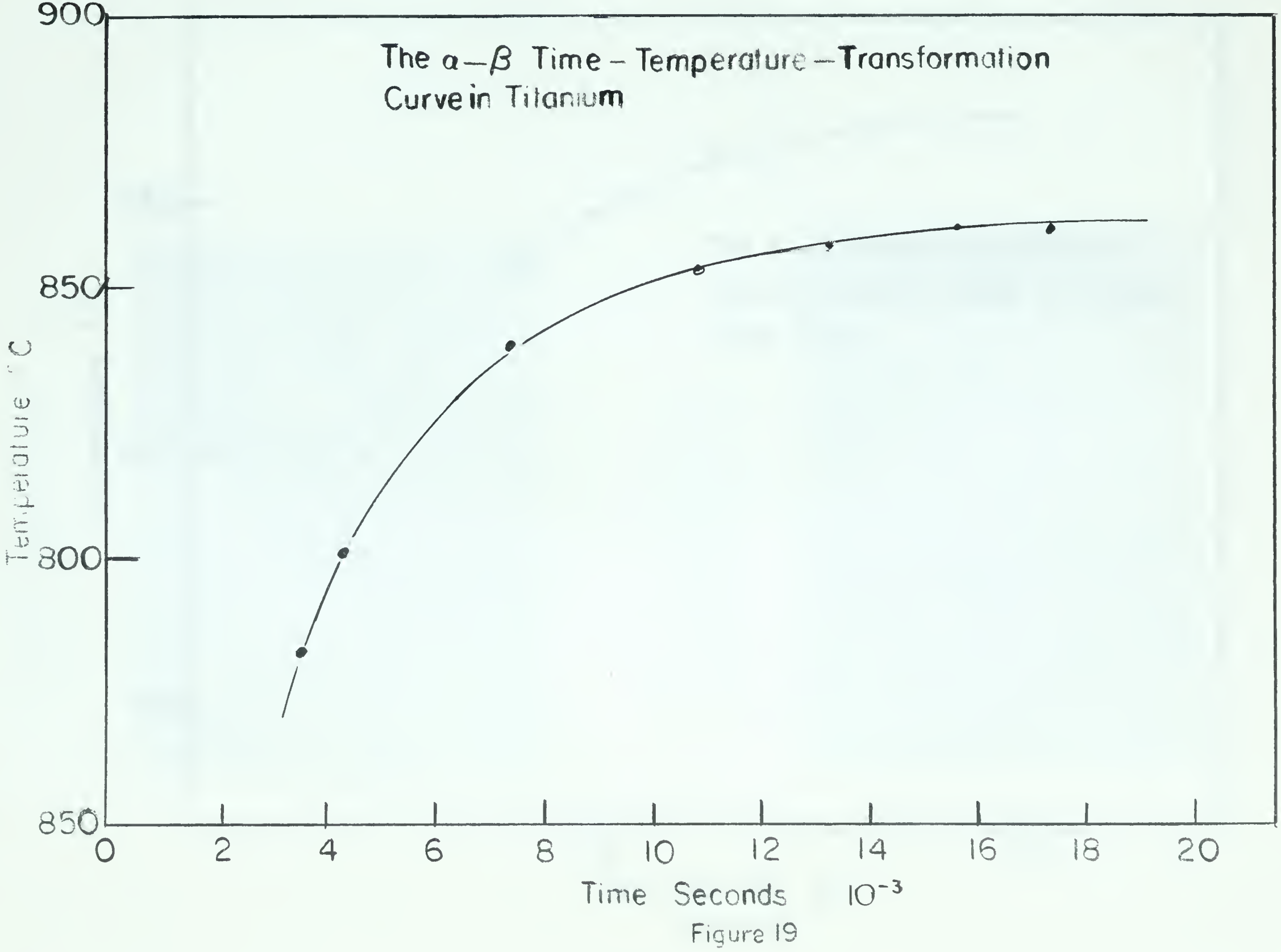
The α—β Time – Temperature – Transformation Curve in Titanium
900
850
800
850
Temperature °C
0
2
4
6
8
10
12
14
16
18
20
Time Seconds 10⁻³

Figure 19

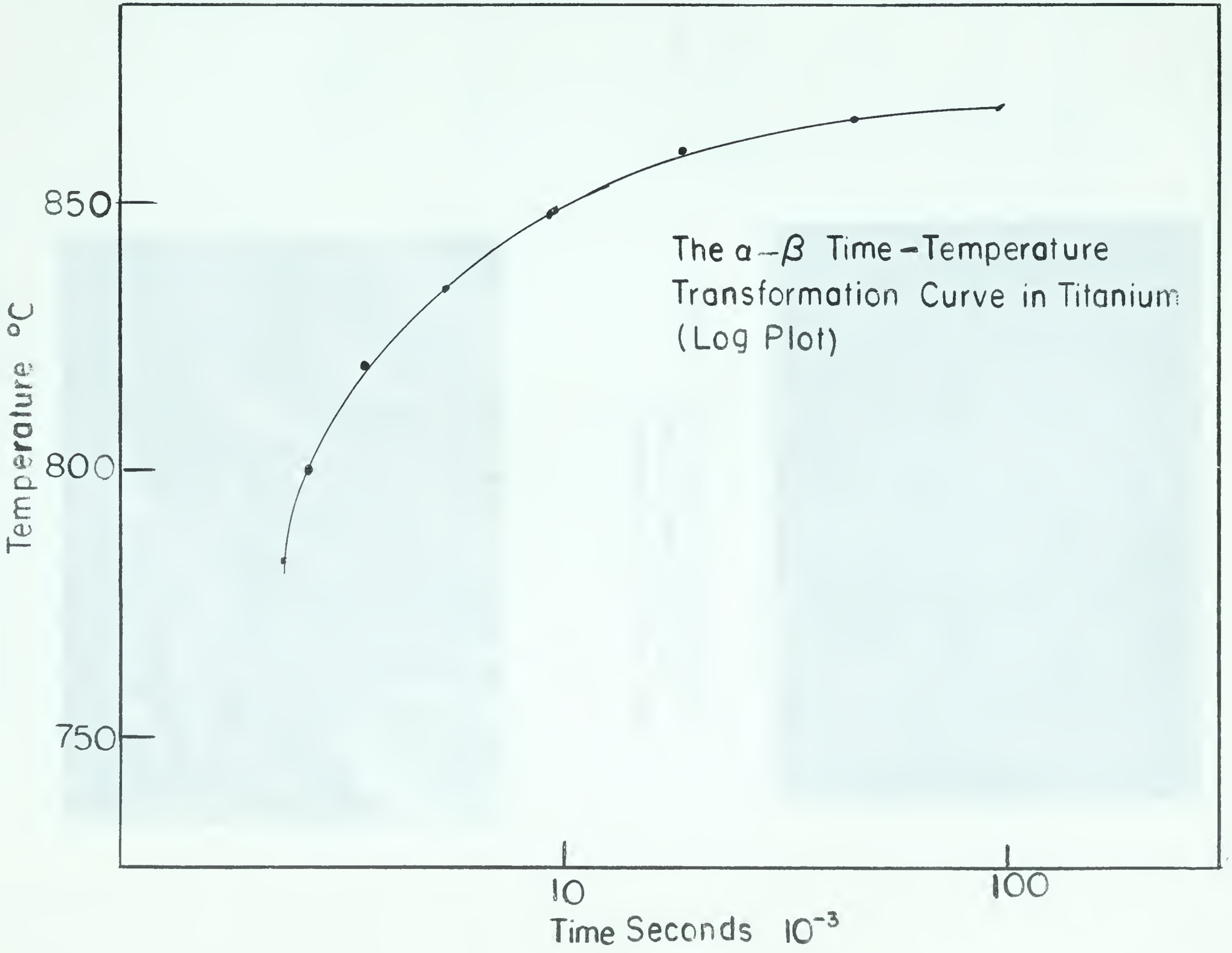
850
800
750
Temperature °C
The α–β Time–Temperature
Transformation Curve in Titanium
(Log Plot)
10
100
Time Seconds 10^{-3}

Figure 20

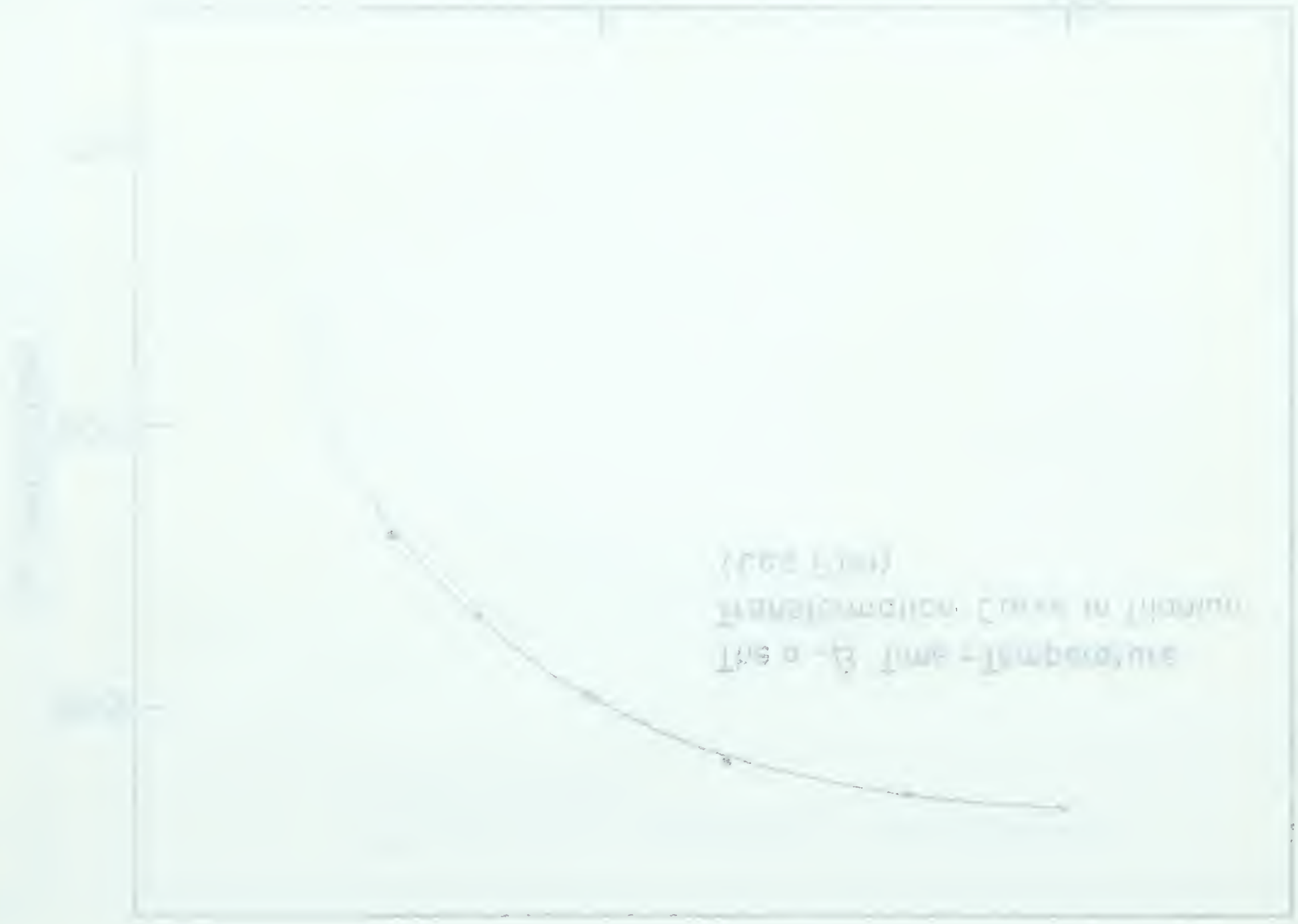

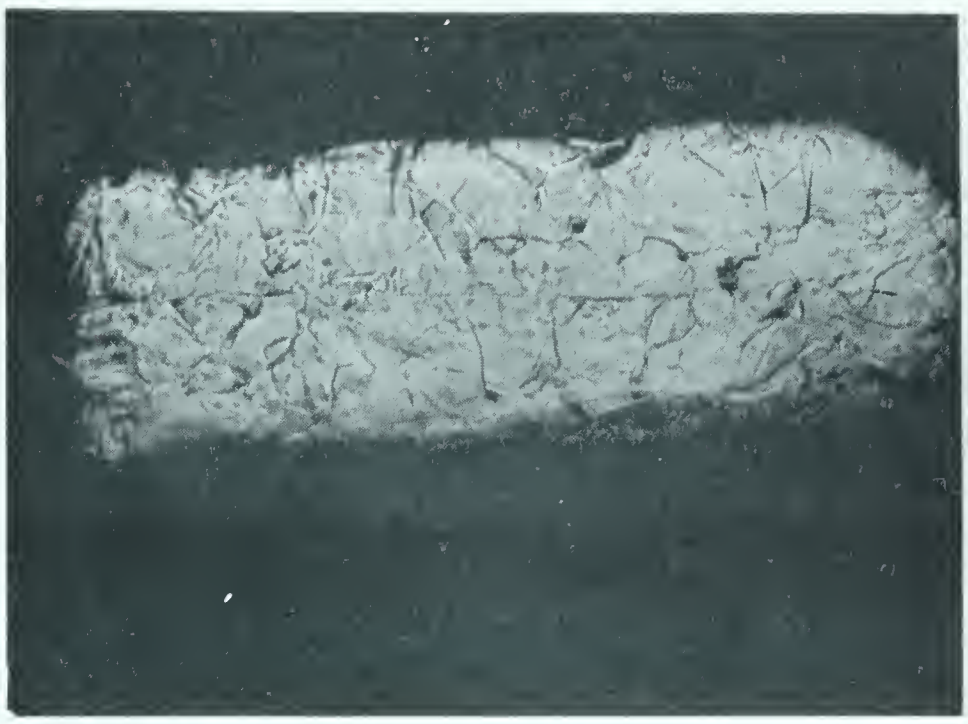

Figure 21 X150 Equiaxed Surface Structure of Titanium Cooled at 10°C/sec Transformation Temperature – 885°C

Figure 22 X300 Martensite Surface Structure of Titanium Cooled at 1,000°C/sec Transformation Temperature – 872°C

TABLE III MICROHARDNESS RESULTS IN PURE TITANIUM

Heat Treatment	Average Microhardness Load DPN	Remarks
As Received	10 Kgm - 89 20 gms - 106	Average of 3 samples maximum variation ± 5
Slowly Cooled $10^{o}C/sec$	20 gms - 110	Average of 2 samples max. variation ± 5
Quenched at $10,000^{o}C/sec$	20 gms - 121	Average of 2 samples ± 10
Quenched at $50,000^{o}C/sec$	20 gms - 125	Average of 2 samples ± 10

THE $\alpha \rightarrow \epsilon$ TRANSFORMATION IN COBALT

Figure 23 is a graph of transformation temperature against cooling rate. The transformation is depressed from 382°C at 100°C/sec to 345°C at 12,000°C/sec. The high quenching rates obtained in iron and titanium were not attainable in cobalt. This is reasonable since a cooling curve is characteristically a decay curve. Since cobalt, iron and titanium have nearly the same specific heat values almost identical cooling curves are obtained. However, the slope of the cooling curve (that is rate) around 350°C -- near the cobalt transformation point is much less than the slope near 800°C -- near the titanium transformation point.

There was a noticeable specimen size effect in cobalt. A 0.025 inch cubic specimen of cobalt transformed at 365°C (100°C/sec) while a 0.010 inch cube transformed at 382°C with the same cooling rate.

There was no evidence of any transformation in a cobalt cooling curve until the sample had been cycled above and below the transformation temperature several times. It was found that 900°C was the best soaking temperature if a clear delineation of the transformation was to be obtained on the cooling curve. At soaking temperatures between 900°C and the transformation temperature of 420°C no change of slope could be detected on the cooling curve.

Cobalt transformed at 432°C on reheating at 100°C/sec. In no case was the temperature of transformation affected by the previous mechanical or thermal history of the metal.

The surface structure associated with the transformation in cobalt is shown in Figures 25, 26, 27, 28 and 29. The cobalt surface structure is somewhat different from either the iron or titanium structure.

Among some of the thermally etched cobalt grains can be seen regions of triangular surface structure (Figure 29). The platelets are not lenticular in shape as in other martensites.

Microhardness measurements are given in Table IV.

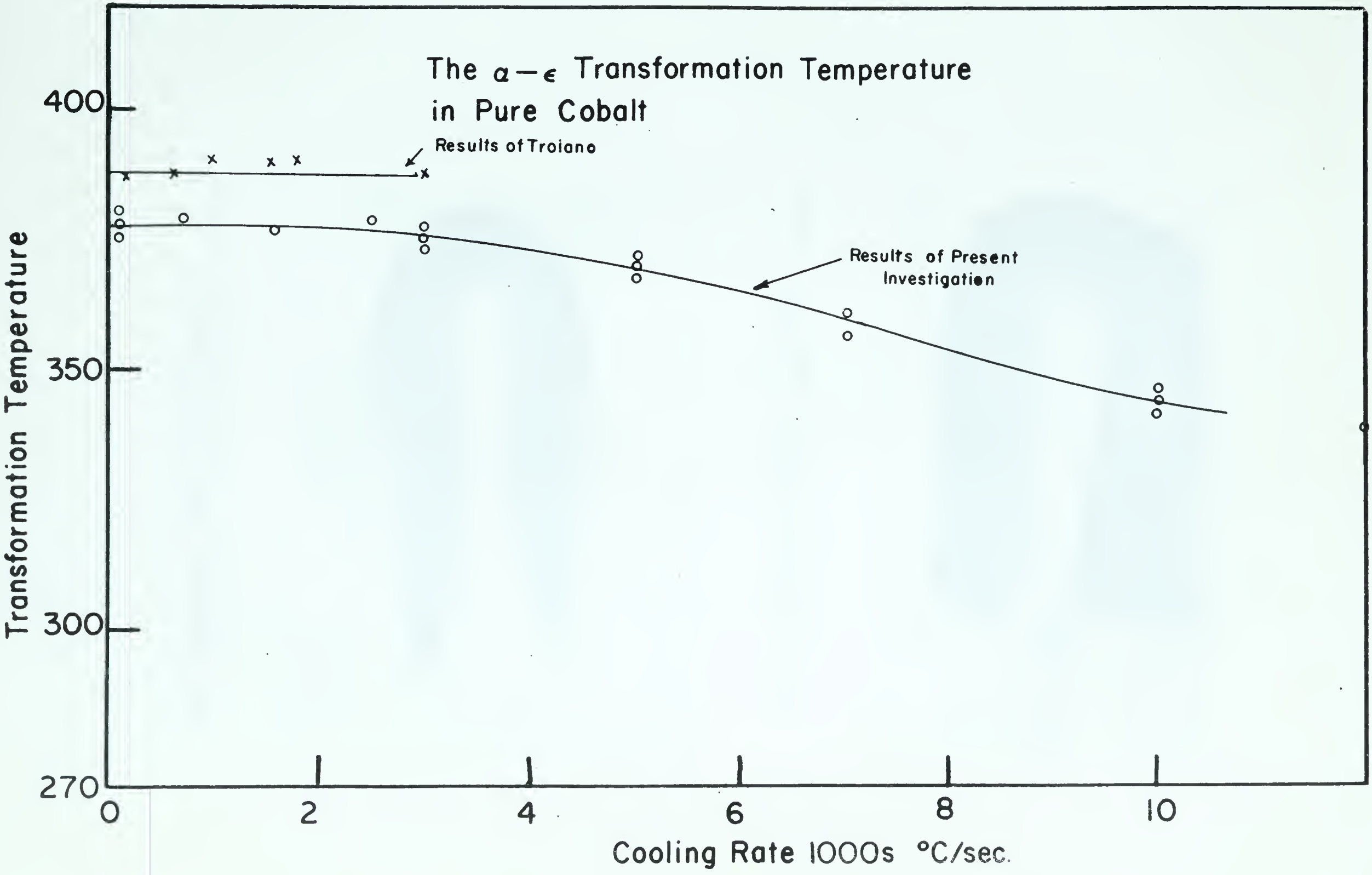
The α—ε Transformation Temperature
in Pure Cobalt
Results of Troiano
Results of Present
Investigation
Transformation Temperature
400
350
300
270
0
2
4
6
8
10
Cooling Rate 1000s °C/sec.

Figure 23

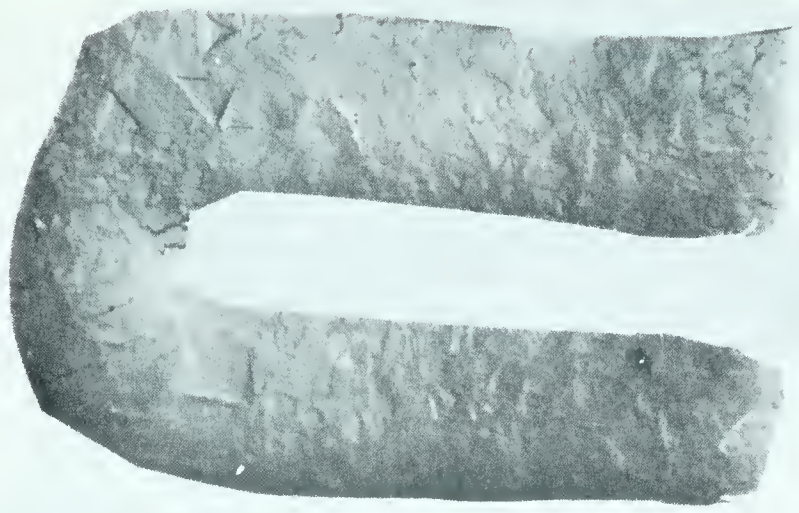

Figure 24 X150 Surface Structure of Cobalt Cooled at 100°C/sec. Transformation Temperature – 382°C

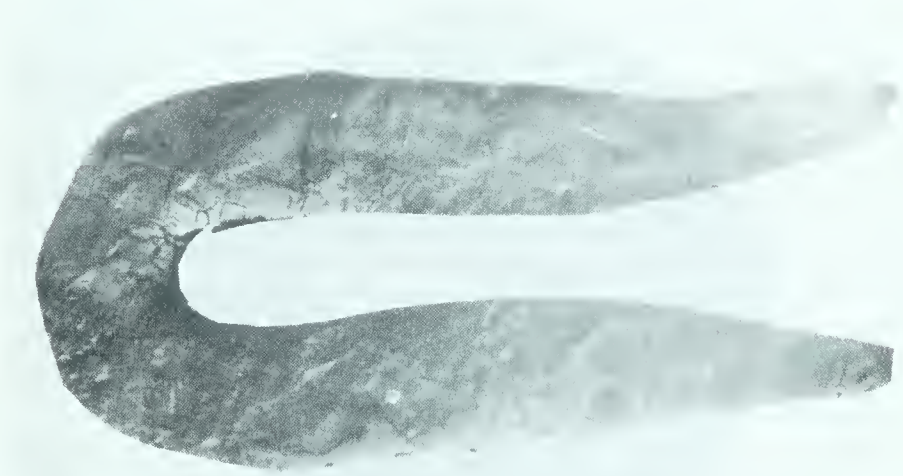

Figure 25 X150 Surface Structure of Cobalt Cooled at 2,000°C/sec. Transformation Temperature – 380°C

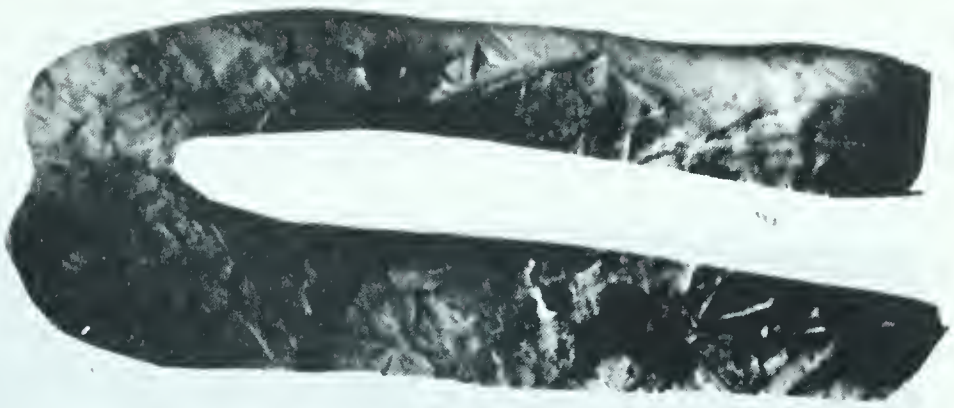

Figure 26 X150 Surface Structure of Cobalt Cooled at 10,000°C/sec. Transformation Temperature – 348°C

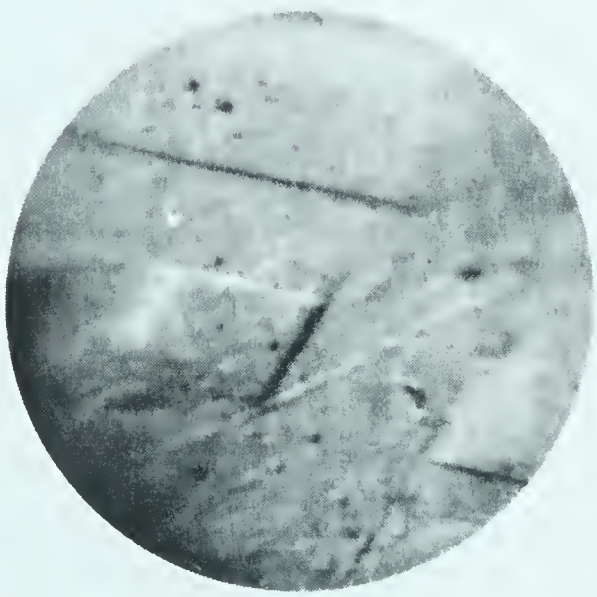

Figure 27 X750 Surface Structure of Cobalt Showing Transformed Region

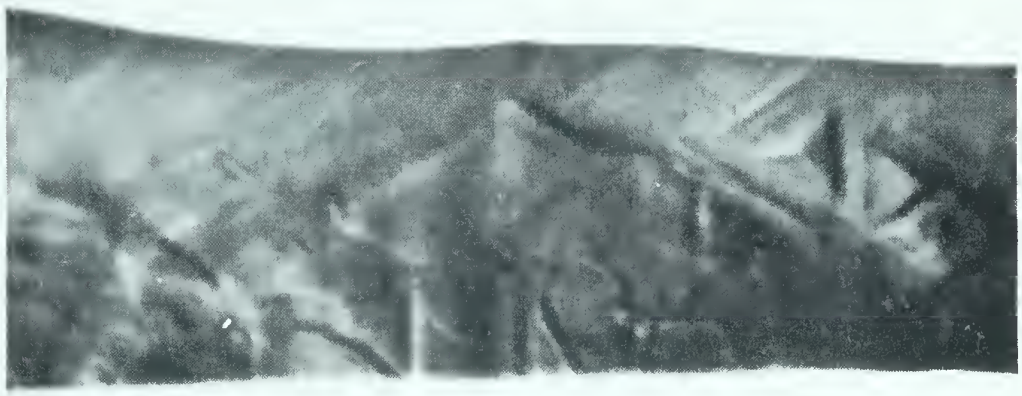

Figure 28 X800 Surface Structure of Cobalt Showing Relief Triangles

Figure 29 X150 Cobalt Whisker

TABLE IV MICROHARDNESS RESULTS IN PURE COBALT

Heat Treatment	Average Microhardness	Remarks
As Received	225 ± 10	Average of 3 Specimens variation with one sample ± 5
Quenched at 100°C/sec	195 ± 20	Average of 4 specimens variation within one sample ± 10
Quenched at 8,000°C/sec	190 ± 30	Rate — Hardness 10,000°C/sec - 195 ± 10 7,000°C/sec - 183 ± 10

COBALT WHISKERS

Various morphological observations on cobalt whiskers are reported in "Cobalt" by Bilby, McMullen and Parr [57]. It will suffice here to say that the whiskers were roughly hexagonal in section; the longest was about 2.5 cm long and they exhibited surface striations.

Two types of resistance curves were found to exist for cobalt whiskers. Figure 30 shows the resistance curve for a cobalt whisker in which the initial curve has a very definite resistance break at the transformation. The resistance remains almost constant for a small temperature range, and after transformation increases with a larger temperature coefficient than before. The resistance on cooling did not coincide with the initial resistance curve but fell at a higher value. On successive heating and cooling the resistance increased until it reached an equilibrium point (Figure 31 and Figure 33). This type of behavior is designated type (1). However, not all whiskers transformed in this manner. Some transformed as in Figure 32 without a resistance plateau or drop but merely a sharp change in slope at the transformation point. Notice the extreme linearity of the plot in the face centered cubic region. This type of transformation is designated type (2). Both types of whisker transformed at $408^{\circ}C \pm 3^{\circ}C$ on heating and at $405^{\circ}C \pm 3^{\circ}C$ on cooling. Thus, the hysteresis is probably less than $5^{\circ}C$. Figure 31 shows a clear delineation of the transformation in cycles 1 and 2 but the transformation is less easily seen in cycle 3 and cannot be seen at all in cycles 4 and 5. These curves become very smooth. However, the transformation temperature does not appear to change with the number of cycles - as long as it can be seen. Cycles 1, 2 and 3 all show a transformation at $408^{\circ}C$ on heating and $405^{\circ}C$ on cooling. Various values of

the temperature resistance coefficients are given in Table I.

Of seven whiskers tested, two had transformations characteristic of type 1 Figure 30, while the other five had characteristics typical of type 2 Figure 32.

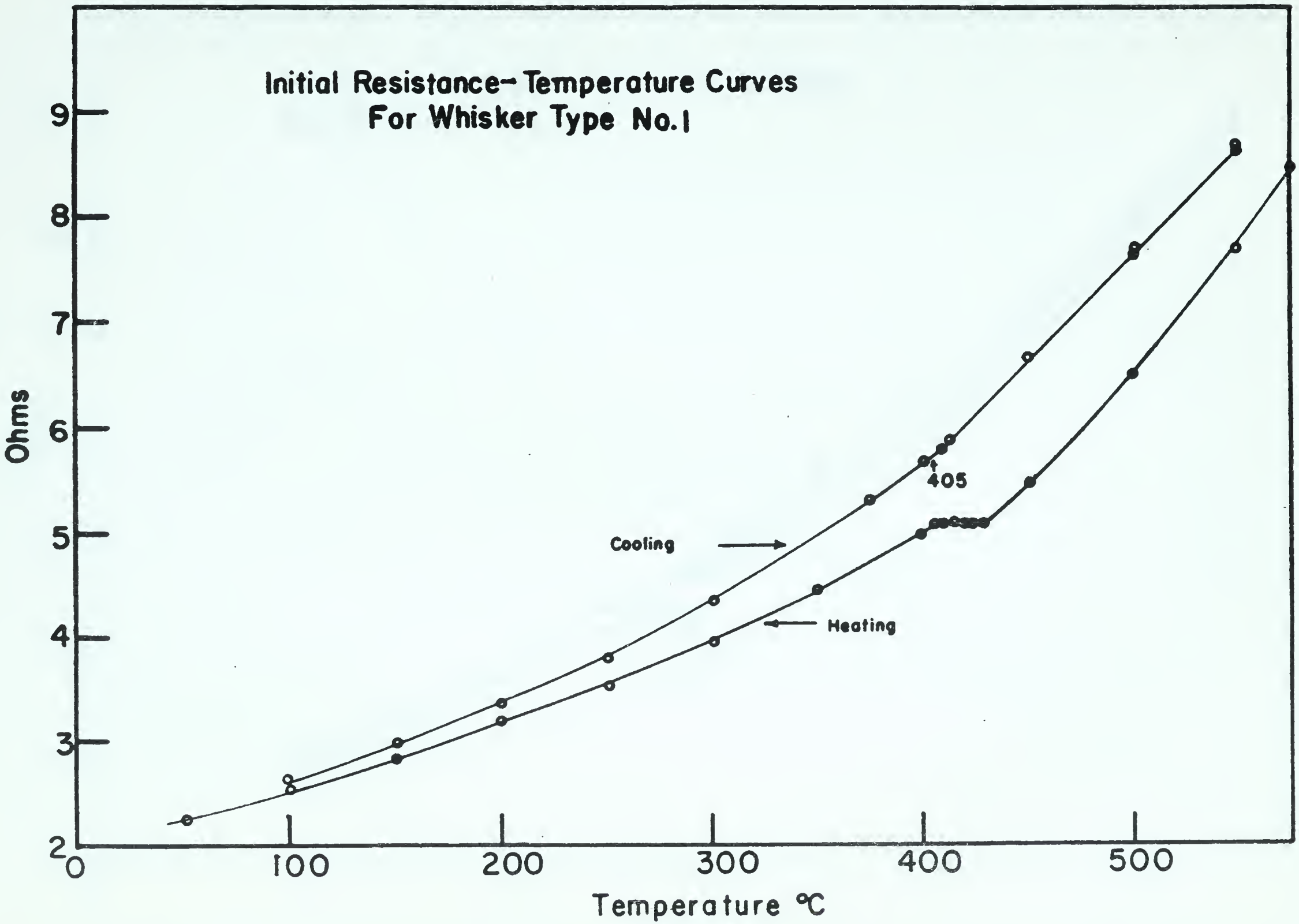
Initial Resistance-Temperature Curves
For Whisker Type No.1
Ohms
9
8
7
6
5
4
3
2
0
100
200
300
400
500
Temperature °C
405
Cooling
Heating

Figure 30

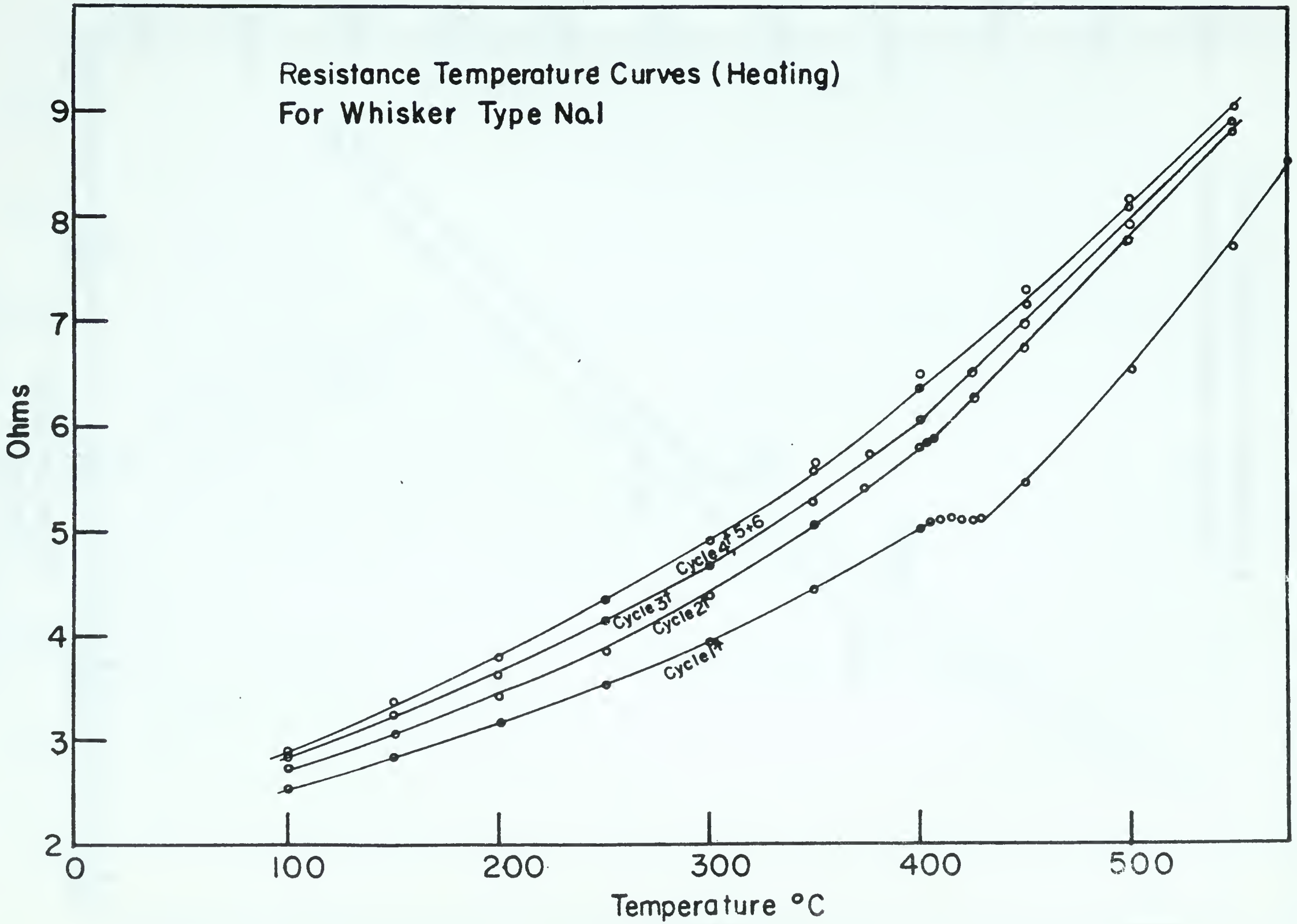
Resistance Temperature Curves (Heating)
For Whisker Type NaI
Ohms
9
8
7
6
5
4
3
2
0
100
200
300
400
500
Temperature °C
Cycle 4 & 5+6
Cycle 3
Cycle 2
Cycle 1

Figure 31

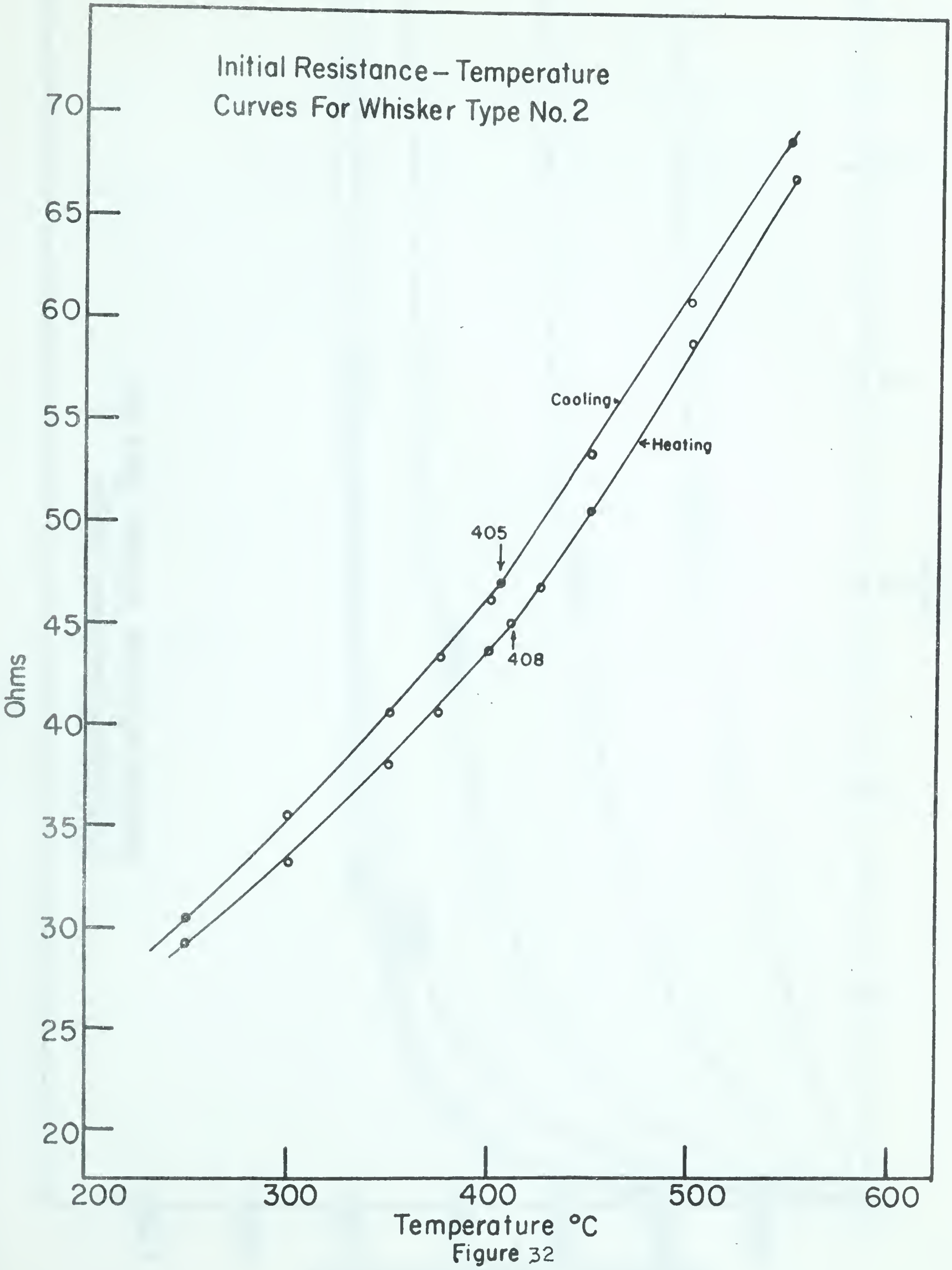
Initial Resistance – Temperature
Curves For Whisker Type No. 2
70
65
60
55
50
45
40
35
30
25
20
Ohms
Cooling
Heating
405
408
200
300
400
500
600
Temperature °C

Figure 32

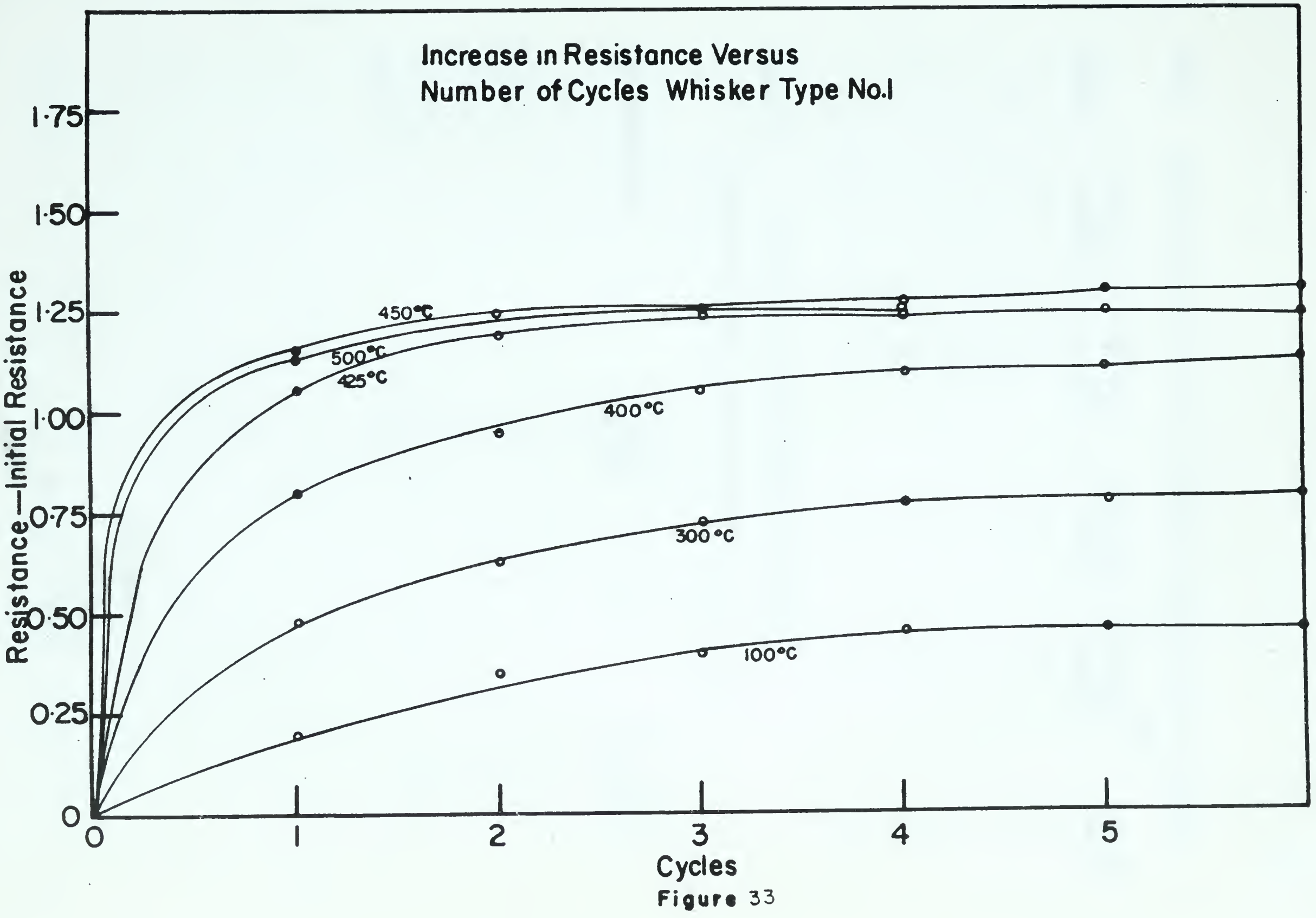
Increase in Resistance Versus
Number of Cycles Whisker Type No.1
Resistance—Initial Resistance
1·75
1·50
1·25
1·00
0·75
0·50
0·25
0
450°C
500°C
425°C
400°C
300°C
100°C
0
1
2
3
4
5
Cycles

Figure 33

TABLE V TEMPERATURE COEFFICIENT OF RESISTANCE (α) FOR COBALT WHISKERS

	TYPE 1				
CYCLE	0-100 x 10^3	100-200 x 10^3	200-300 x 10^3	300-400 x 10^3	425-500 x 10^3
1	2.5	2.8	2.2	2.9	4.23
2	-	2.78	2.5	2.9	3.32
3	-	2.77	2.7	2.92	3.29
4	-	2.75	2.9	2.95	3.25
5	-	2.75	2.9	2.95	3.25

TABLE VI COMPARISONS OF EQUILIBRIUM α VALUES FOR WHISKERS WITH α VALUES OF POLYCRYSTALLINE COBALT

TEMPERATURE °C	WHISKER x 10^3	BULK COBALT x 10^3
0-100	2.6	6.58
100-200	2.75	4.75
200-300	2.9	4.09
300-400	3.0	3.42
425-500	3.79	

GENERAL DISCUSSION

The results will be analysed; first, with respect to the individual transformations involved and, secondly, with respect to the general theories of martensite transformations. Thus, the discussion contains five sections:

(a) The Iron Transformation

(b) The Titanium Transformation

(c) The Cobalt Transformation

(d) Cobalt Whiskers

(e) A General Discussion of Martensite Transformation

A. THE IRON TRANSFORMATION

The high cooling rates obtained in these experiments have led to a much more complete picture of transformation rate data. For instance, both Owen and Gilbert[28] and Srivastava and Parr[35] determined only one M_s value for pure iron and assumed it martensitic because it agreed fairly well with extrapolated M_s data from the iron - carbon binary system. It might be pointed out that Owen and Gilbert[28] could not obtain experimental agreement in the intermediate rate ranges from 200°C/sec to 5,000°C/sec. This is prob ably due to the sensitivity of the transformation temperature to small amounts of carbon. Srivastava and Parr obtained two transformation ranges from 700°C - 750°C and from 500°C - 530°C at rates from 5,000°C/sec to 10,000°C/sec, but the fact seems to have been ignored. The existence of two transformation temperature ranges is almost certainly due to carbon segregation in the iron bar stock and the extreme sensitivity of M_s temperature to carbon concentration in the low carbon region. It should be emphasized that any one specimen had only one characteristic transformation

temperature which could be reproduced on repeated cooling, to ± 5°C. However, the variation from specimen to specimen was between 500°C and 750°C.

The iron used in this investigation contained 0.03 pct carbon and only trace amounts (less than 0.001 pct) other impurities. This iron contains less metallic impurities than does iron used by other investigators with the exception of Duwez[34]. Since there is about 30 times the amount of carbon in the iron than other impurity metallic, and since carbon is far more effective in depressing the transformation temperature than are other metallic elements, it is reasonable to suppose that the variation in M_s from specimen to specimen is attributable to carbon.

Iron from the National Bureau of Standards transformed on upquenching at 916°C. Iron obtained from Johnson, Mathey and Mallory transformed on upquenching anywhere between 895°C and 915°C. The upquench temperature of specimens that transformed on quenching at 742°C, however, was 915°C. Assuming that a difference of 10°C in the Ac3 temperature corresponds to 0.04 pct carbon, then iron, that has an Ms of 695°C, contains about 0.005 pct carbon. There was no indication of any surface rumple on samples that transformed at 742°C, and no indication that the transformation was significantly depressed with cooling rate from 3,000°C/sec to 33,000°C. These transformation features are characteristic of the so-called massive transformation proposed by Gilbert and Owen.[28] Any greater carbon content than 0.005 pct serves to depress the transformation from 742°C to 500°C when there is a sharp inflexion point. Thus, many samples transform at the 0.005 pct carbon content while others transform near the inflexion point with only the occasional sample transforming in between the two ranges.

Thus, Duwez[34] found that he could depress the transformation temperature in iron to 750°C at a rate of 10,000°C/sec using iron with a residual carbon concentration of 0.001 pct. This corresponds to the massive transformation temperature of 742°C found in this investigation. Further, Duwez's work shows a large experimental scatter (40°C) which can be associated with the carbon sensitivity of the transformation. On the other hand, the M_s temperature determined by Owen and Gilbert of 560°C is reasonable because the iron contained 0.010 pct carbon. The value obtained by Esser of 520°C is also reasonable as the iron he used contained 0.017 pct carbon.

In the above discussion, it should be kept in mind that the critical rate is extremely sensitive to carbon concentration, so that a rate of 35,000°C/sec is needed to obtain martensite in iron containing 0.005% carbon, whereas, only 5,000°C/sec is needed to obtain martensite in iron with 0.01% carbon.

Recently, Yeo[51] in an investigation of the iron - nickel - carbon system, found a sharp increase in transformation temperature with decreasing carbon content. This is probably similar to the situation in iron - carbon alloys.

It should be pointed out that the thermodynamics of martensites do not permit any discontinuity in the relationship between carbon content and M_s temperature. Since the results of this investigation do not agree with proposed theories, based on thermodynamic considerations, the thermodynamics of martensites will be discussed.

A quantitative understanding of the relative stabilities of atomic configurations would have widespread applicability in both theoretical and practical areas of solid state science. Unfortunately, first principle calculations based on quantum mechanics do not have sufficient

accuracy to distinguish between various polymorphs. In fact, in most quantum mechanical calculations configuational differences are neglected.

Consequently, many investigators have resorted to an approach that comprises combining thermodynamics and various physical phenomena, in order to deduce the free energy change, $\Delta F(T)^{\gamma \to \alpha'}$. Such an approach has been taken, for example, by Cohen, Macklin and Paranjpe[22] in the case of iron base alloys and by Kaufman[58] in the case of titanium - base and zirconium - base alloys. The gist of their argument is outlined as follows:

Accompanying the $\gamma \to \alpha'$ change, in iron carbon alloys (γ is austenite and α' is martensite) is a free energy decrease, ie: $F^{\gamma} - F^{\alpha'} > 0$

Consider the free energy change:

$$\gamma \to \alpha \to \alpha' \qquad \text{where} \quad \alpha = \text{Ferrite}$$

On a one mole basis:

$$F^{\alpha'} - F^{\alpha} = (F^{\alpha} - F^{\gamma}) + (F^{\alpha'} - F^{\alpha}) \quad (3)$$

Now:

$$F^{\alpha'} - F^{\alpha} = (N_{Fe}\mu_{Fe}^{\alpha} + N_C\mu_C^{\alpha}) - (N_{Fe}\mu_{Fe}^{\gamma} + N_C\mu_C^{\gamma}) \quad (4)$$

Where:

F^{α} = free energy of α iron

F^{γ} = free energy of austenite

N_{Fe} = mole fraction of iron

μ_{Fe} = chemical potential of iron

N_C = mole fraction of carbon

μ_C = chemical potential of carbon

The standard states are chosen to be pure body centered cubic iron, pure face centered cubic iron and pure graphite.

Noting that $\mu = \mu_0 + RT \ln a$ - (4)

we can write: $F^{\alpha'} - F^{\gamma} = N_{Fe}(\mu_{Fe}^{o\alpha} - \mu_{Fe}^{\gamma}) + N_{Fe} RT \ln \frac{a_{Fe}^{\alpha}}{a_{Fe}^{\gamma}}$

$+ N_C RT \ln \frac{a_C^{\alpha}}{a_C^{\gamma}}$ - (5)

The first term of equation (5) is obtainable from the data Darken and Smith[59].

Carbon activities are obtained by extrapolating solid solution data (Smith[59]) into the martensitic range of temperatures. The iron activities for the second term of equation (5) are obtained with the aid of the Gibbs - Duhem equation.

There remains to evaluate the quantity of $F^{\alpha} - F^{\gamma}$. This quantity is assumed to arise entirely through the tetragonality of the lattice and is: $F^{\alpha} - F^{\gamma} = \frac{1}{2} V_m (\sigma_x \xi_x + \sigma_y \xi_y + \sigma_z \xi_z)$ where: V_m = Volume of martensite

σ = principal stresses values

ξ = principal strain values

Thus, the free energy change $F^{\alpha'} - F^{\gamma}$ can be calculated as a function of temperature. Cohen et al[22] evaluated equation (5) for carbon concentrations between 0% carbon and 1.2% carbon. The results are shown in Figure 34. M_s values always lie a distance of 290 cals/mole below the equilibrium free energy temperature. Thus, it is assumed that all iron - carbon martensites require a driving force of 290 cals/mole.

The non-chemical contributions were estimated so that they might be compared to the driving force of 290 cals/mole. An estimation of all non-chemical factors, however, totaled no more than 65 cals/mole. This led to the suggestion that there exists an energy barrier to transformation -- otherwise, the reaction would begin at a driving force of 65 cals/mole. Such a transformation barrier is shown in Figure 35.

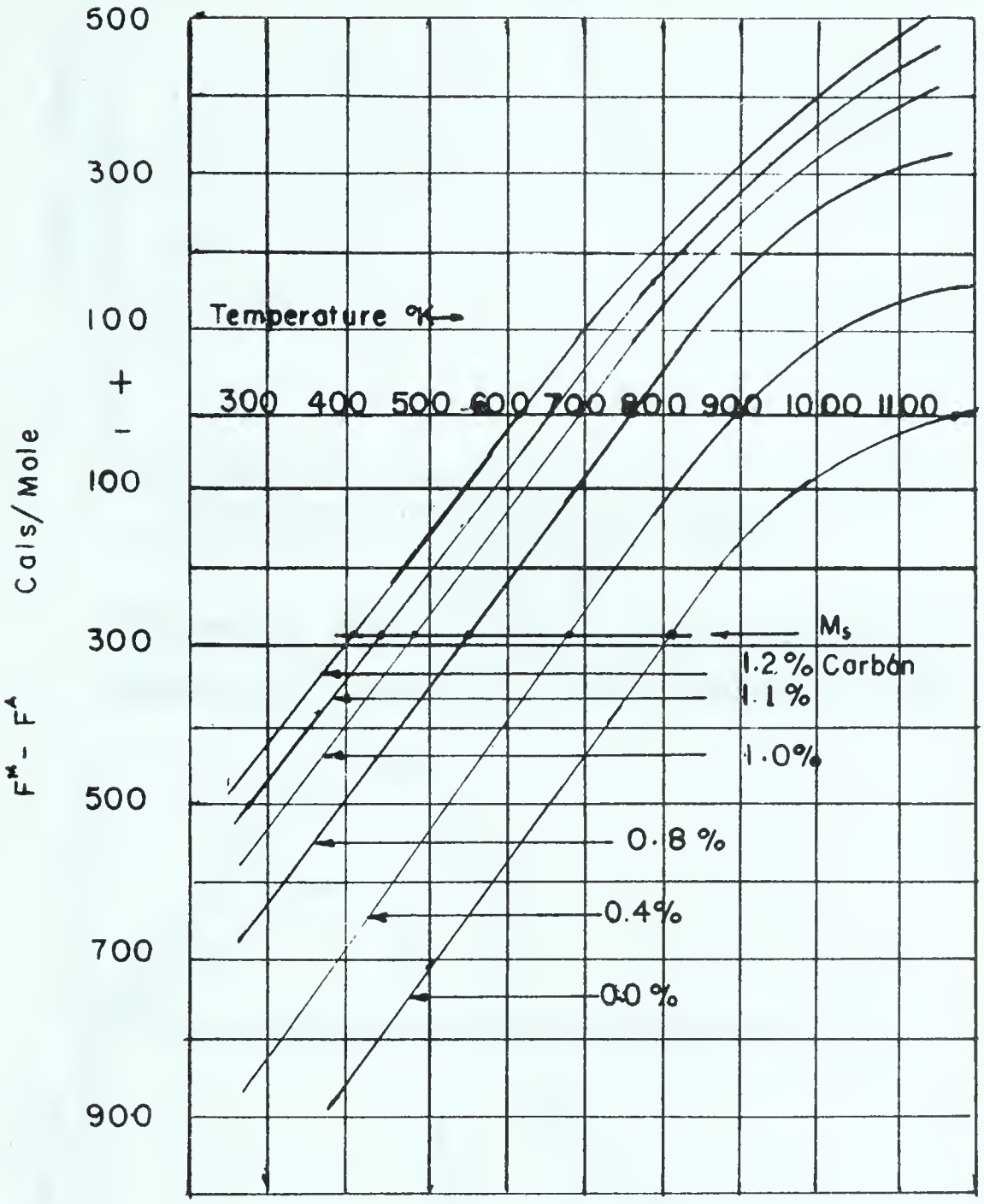

Figure 34 Free Energy Change Accompanying the Austenite-Martensite Transformation (After Cohen)

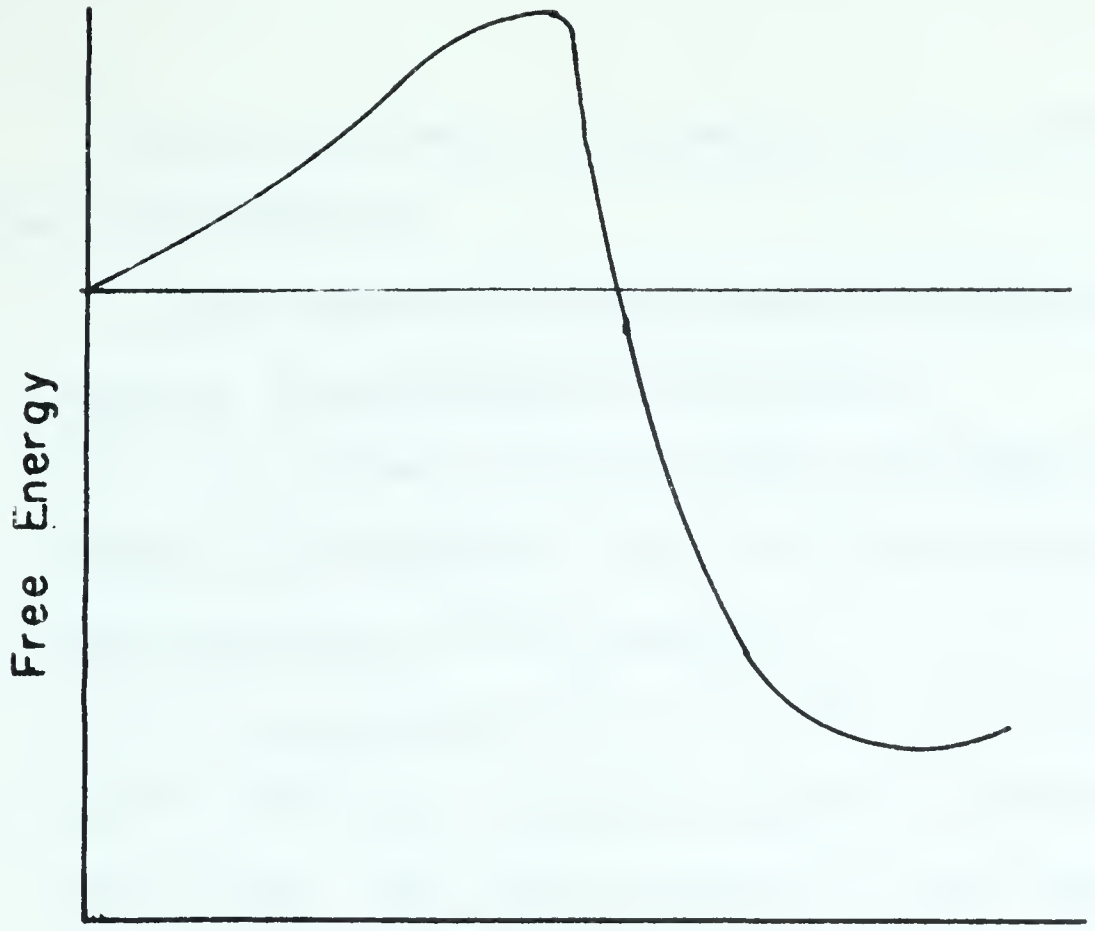

Figure 35

Schematic Representation of the Variation in Free Energy of Formation With Martensite Shear (After Cohen)

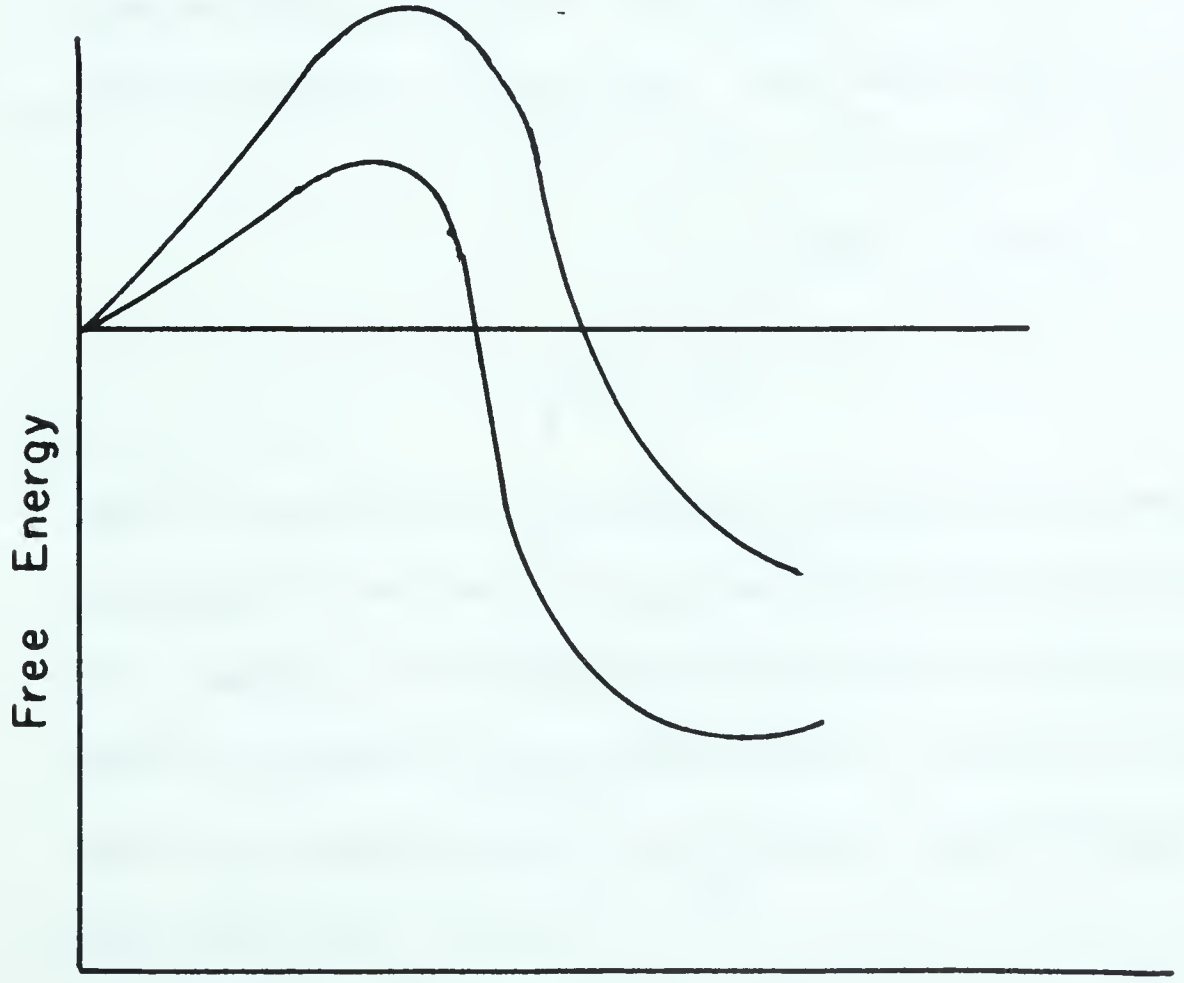

Figure 36

Effect of Matrix Constraints on the Free Energy of Martensite Formation (After Cohen)

While this theory is a pleasing rationalization, there are several inconsistencies.

(1) Since martensite is not an equilibrium phase, treatment by classical thermodynamics is questionable.

(2) It is implied in the theory that the height of the free energy barrier is 290 cals/mole. Yet, it is the quantity $F^{\gamma} - F^{\alpha'}$ that has been calculated to be 290 cals/mole.

(3) In the expression $F^{\alpha'} - F^{\gamma} = (F^{\alpha} - F^{\gamma}) + (F^{\alpha'} - F^{\alpha})$ -(1) the $F^{\alpha'} - F^{\alpha}$ term arises only through tetragonality induced by the carbon atoms. This term in pure iron is zero since pure iron is cubic.

$$F^{\alpha'} - F^{\gamma} = F^{\alpha} - F^{\gamma}$$

$$F^{\alpha'} = F^{\alpha}$$

However, Singh and Parr[60] have shown that $F^{\alpha'} - F^{\alpha}$ is 300 cals/mole ($\pm$70) cals/mole in pure iron. From equation (1) this implies:

$$F^{\alpha'} - F^{\gamma} = (F^{\alpha} - F^{\gamma}) + (F^{\alpha'} - F^{\alpha})$$

$$= -300 + 300 \text{ cals/mole}$$

$$= 0$$

$$F^{\alpha'} = F^{\gamma}$$

That is, austenite will transform to martensite when the free energy of austenite becomes equal to the free energy of martensite.

(4) Further, it has recently been pointed out that the experimental error in determining the thermodynamic functions of Darken and Smith could be translated into an experimental error of $\pm$ 700 cals/mole in the free energy calculations[61].

(5) The thermodynamic theory can not rationalize the rapid fall of M_s with very small carbon additions. On the contrary, it is assumed that M_s in iron can be obtained by extrapolating M_s values at higher

carbon concentrations to 0% carbon. But, if one accepts the theoretical derivation of Cohen and Kaufman[31] and applies it to the 750°C M_s found in pure iron, a driving force of less than 100 cals/mole is needed to nucleate martensite in pure iron.

In view of the doubtful validity of the thermodynamic approach, a quite different, though qualitative, approach is now submitted to account for the effects of small amounts of carbon. The approach is based on the relationship between atomic separation and energy. The relationship for nickel[52] takes the form of Figure 37. Data for iron are not available but are presumably similar to that for nickel, since the bonding energies of the two are nearly the same.

Any displacement from the point P results in a large increase in the internal energy of the martensite. The nature of the variation of lattice parameters with carbon suggests that this is a reasonable approach. From data by Kurdjumov

$$c = a_o + 0.118\ p$$

$$a = a_o - 0.015\ p$$

describe the change in unit cell dimensions of tetragonal iron - carbon martensites where:

a_o = cell dimensions

p = amount of carbon (wt pct)

"c" and "a" are the cell dimensions of the tetragonal lattice

The contration in a_o is almost an order of magnitude greater than the extension in $a_o \rightarrow c$. This indicates the interplay of interatomic forces since atomic compression forces are greater than are atomic tension forces.

A two-dimensional representation of the iron array with one carbon atom in an interstitial position is shown in Figure 38. The carbon atom tends to move the iron atoms out on either side of P and, thereby, increases the energy of the martensite lattice. Now consider the effect of a second carbon atom introduced into the lattice in a neighbouring position (Figure 39). Again the energy of the crystal is increased but the increase will not be as great as that caused by the first carbon atom. Therefore, this idealized model implies a sharp increase in energy with the addition of the first carbon atom, and a smaller energy increase with additional atoms. The sphere of influence of a dislocation is said to be about eight or ten atomic distances. If the same is true of interstitial carbon atoms, then the carbon spheres of influence will begin to interact at about one carbon atom for every twenty iron atoms linear distance. This corresponds a carbon volume concentration of about 0.0025 pct. Thus, one would expect the greatest energy changes in concentrations near this amount and subsequently a rapid decrease in M_s. Further carbon additions have less effect. It is important to realize, however, that this theory assumes a uniform distribution -- which is probably not the case.

A second hypothesis is a consequence of the observations of Smith[64], who observed by electron microscopy that carbon atoms migrate to vacancy sites in iron at 700°C. There are not sufficient data available to make precise computations but a vacancy concentration of 1 in 10^4 or 10^5 is not unreasonable. It is probable that the first atom initially added to the iron lattice will reside in these positions since they are potential wells. Thus, carbon up to 0.001 pct will migrate to vacancy positions. The transformation will, therefore, require less

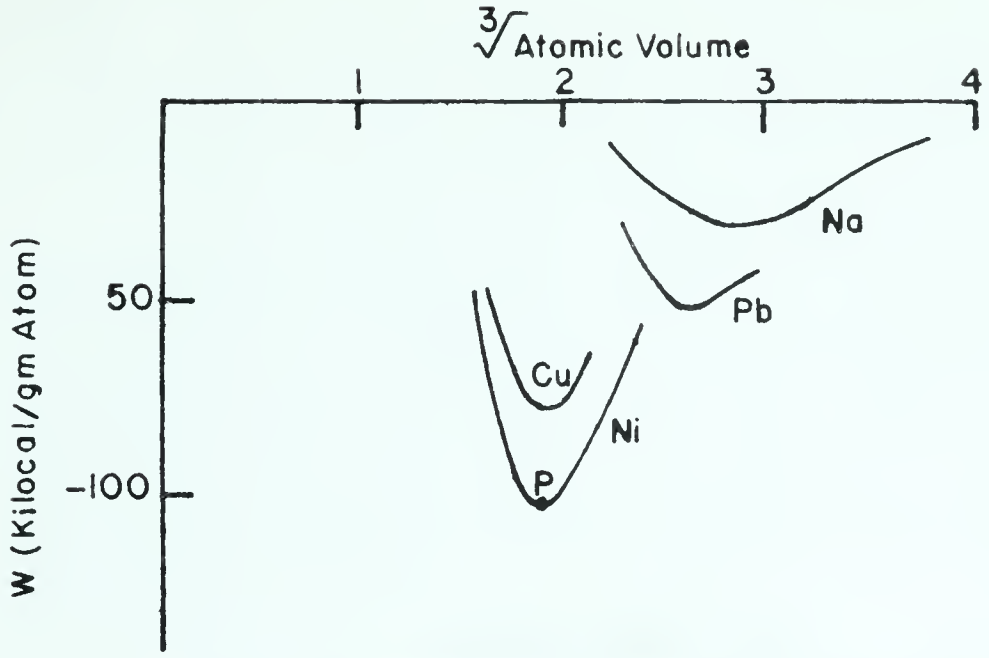

Energy Representation of a Nickel Atom as a Function of Atomic Separation (After Mott and Jones)

Figure 37

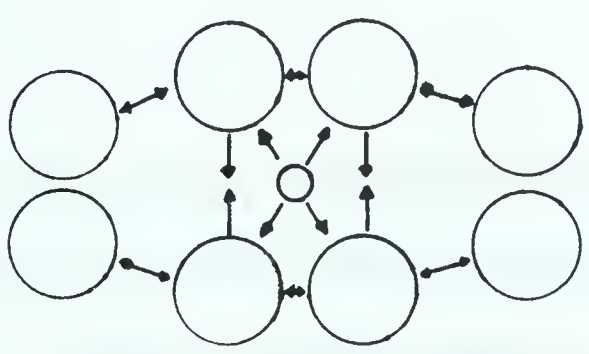

Two Dimensional Schematic Representation of The Iron Lattice After Addition of One Carbon Atom

Figure 38

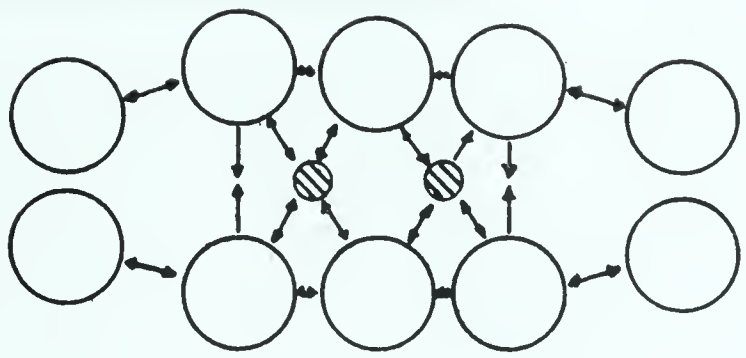

Two Dimensional Schematic Representation of the Iron Lattice After Addition of Two Carbon Atoms in Neighbouring Interstices

Figure 39

energy than if the carbon were retained interstitially, which becomes necessary at higher concentrates. Thus, one would expect a sharp change in transformation mechanism at 0.001 pct concentration.

This theory is also consistent with the fact that the critical rate is reduced at low carbon content. Assuming that carbon atoms reside in vacancy sites, a vacancy mechanism of diffusion will be rendered more difficult. Thus, the cooling rate necessary to suppress diffusion processes will be very sensitive to small additions of carbon as has been found in the experiments of this investigation.

THE TITANIUM TRANSFORMATION

The high cooling rates obtained in these experiments have led to a clearer picture of rate data. The results of Duwez[34] indicated that there might be a depression in the transformation temperature with increasing cooling rate; however, the amount of the depression was not much greater than experimental error and no conclusions could be made. The rate in these experiments was high enough to clearly indicate a depression in M_s of almost 90°C.

Although there have been numerous studies, both theoretical and experimental on martensites, there remain highly contentious fundamental questions. One such question is the mode of nucleation. Until 1947 it was an assumed fact that martensites formed athermally. (An athermal transformation will be understood to mean a transformation that is independent of thermal fluctuations.) However, since 1947 there have been many "isothermal martensites" found : that is, martensites that do depend upon thermal fluctuations.

Consequently, various theories now refer to the mode of transformation. Thus, Cohen et al[22] hypothesize the existence of strain embryo (clusters of atoms with insufficient energy to nucleate) in the high temperature phase region. Embryo are activated by either lowering the temperature which, thereby, reduces the critical size of nuclei, or by thermal fluctuations contributing to the extra energy necessary for an embryo to become a nucleus.

Fisher, Holloman, and Turnbull[53,61], on the other hand, suggest that martensite in iron nucleates at regions of impoverished carbon. Isothermal martensite is simply due to local variation of free enthalpy at the transformation temperature. Both theories have the advantage of simply

portraying identical end products.

From a consideration of nucleation modes there are two experimental corollaries that serve to determine whether a transformation is isothermal or athermal. The first of these is stabilization. That is, if the transformation is athermal the transformation ceases when cooling stops and does not begin again until some lower temperature M_s' has been reached. The second experimental feature of athermal martensites is the characteristic non-depressibility of M_s.

High temperature metallography or dilatometry are generally used to establish transformation characteristics at temperature. Rate data such as that obtained in this investigation are used to establish the second feature. But the two features are, in fact, one and the same. Consider the isothermal decay curves of Figure 40. Now suppose that before M_s is detected 1 pct of the parent phase must have transformed. Then, in order that M_s be detected, the specimen must be held a T_1 for a time t_1.

However, if the specimen is held for a time t_2 where $t_2 < t_1$, then the specimen will show an experimental M_s at temperature $T_2 < T_1$, as shown in Figure 40. If, on the other hand, one can measure any physical parameter that changes with the concentration of martensite then the decay curve could be established directly as a function of time at temperature. Thus, the two experimental methods of determining the mode of nucleation really reduce to measuring the same physical phenomenon.

A number of investigators believe all martensite transformations are isothermal[62]. They suggest that "so-called" athermal transformations only appear to stop transforming when cooling stops because the transformation is extremely rapid at temperature. Kurdjumov et al[14] were the first to find that by quenching an Fe-Ni-Mn alloy in liquid air from

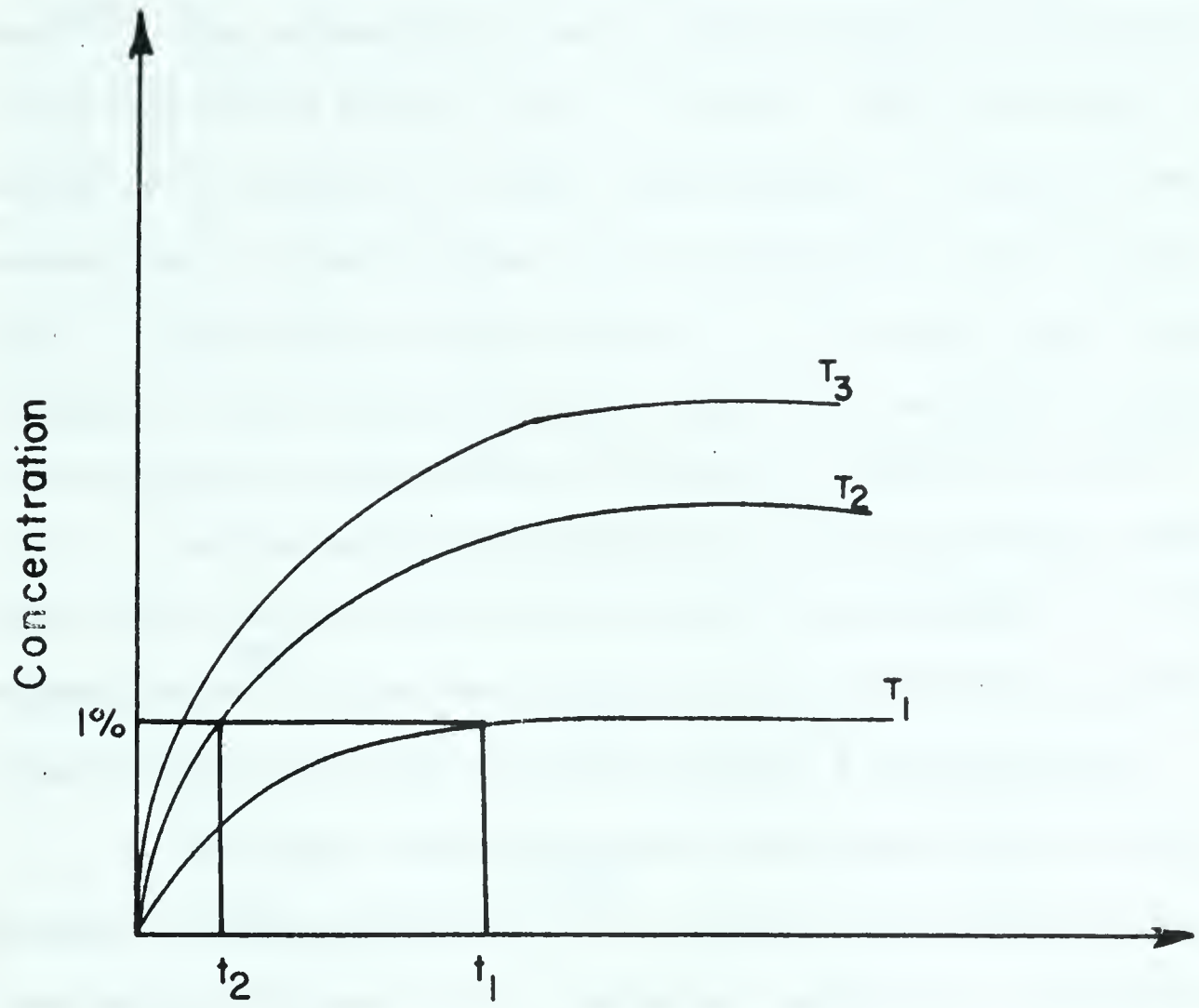

Figure40

Characteristic Isothermal Transformation Decay Curves

austenite he could suppress the transformation entirely. However, transformation was observed on reheating. Since then, other transformations of the same nature have been found, notably one in Ti - Ni by Polonis and Parr[55]. The proponents of such a theory regard the transformation as proceeding by the general laws of kinetics. They conjecture that low energy of activation for atomic displacements is involved when coherency between the original lattice and the martensitic lattice exists. However, when the coherency no longer exists, ie., the shear angle becomes large, no longer is the activation energy small and the growth process halts. This explains why the growth of martensite plates is limited.

At low temperatures where the energy of thermal vibrations is small, the rate of transformation should be measureable, as indeed it appears to be.[14] It has been found that for many binary ferrous alloys transformation rates follow normal kinetic C curve behavior.

The first isothermal martensites were found in 1947. This led Fisher, Holloman and Turnbull[54] to suggest that martensite transformations have both an athermal and an isothermal component. The athermal component of transformation could never be depressed but the isothermal component could be depressed with increasing cooling rate. They still prefer, however, to consider the martensite reaction in plain carbon steels as only athermal in nature. Crussard[62] in 1955 working with the Fe - Ni -C system showed that by controlled stabilization the athermal component of transformation could be rendered inoperative and the isothermal component slowed down. Crussard[62] was further able to show, using the Boltzman equation, that the characteristic depressibility of M_s in plain carbon steels is reasonable assuming an isothermal behavior, even at cooling rates of 12,000°C/sec.

Normally, the two experimental techniques mentioned above do not lend themselves to detecting isothermal transformations that take place extremely rapidly. However, the isothermal nature of the titanium transformation was exposed as a result of the high cooling rates obtained in this investigation. It has further been demonstrated here that the nature of the time - temperature - transformation curve can be computed from rate data. Typical C curve behavior is implied for titanium although only a small portion of the C curve could be obtained. Such time - temperature - transformation curves are at present impossible to determine by any other means because of the very short time intervals involved. For instance, the time between the initial point and last point at 872°C is only 1.33×10^{-3} seconds. Although the nose of the C curve has not been determined it is unlikely that it will extend more than a few milliseconds, while all previously determined isothermal time - temperature - transformation plots extend more than minutes for a typical martensite isothermal alloy. Isothermal measurements in this short space of time are extremely difficult.

There are not sufficient data available to carry out a calculation of the transformation depression as did Crussard for the iron - carbon system. However, the depression obtained is qualitatively consistent with isothermal theories of nucleation.

THE COBALT TRANSFORMATION

The nucleation considerations of the previous section apply, as well, to the cobalt transformation.

On the one hand, there are some investigators who feel that embryos are retained during rapid cooling, and since the critical size is smaller at lower temperature, they become nuclei[53]. On the other hand, another group suggest that martensite forms in a series of isothermal steps. However, isothermal characteristics may be masked by very rapid transformation rates. A criterion of such a transformation is the depression of transformation temperature at increased cooling rate: such a depression is not consistent with an athermal mechanism.

Although transformation temperature depressions in cobalt have not been detected previously (Troiano 1949[47]) cooling rates did not exceed 3,000°C/sec; and up to this rate the depression observed in the work repeated here is the same order of magnitude as is the experimental error.

At higher rates of cooling the depression is substantial (40°C at 12,000°C/sec), and is consistent with isothermal theories of martensite.

The triangular relief markings are presumably related to the geometry of shearing (111) planes in the cubic system to produce the basal (0001) hexagonal planes of the low temperature phase. The greater amount of surface relief observed after high quenching rates could be caused by the greater amount of high temperature transformation. Further, the relief triangles are not independent of prior stress -- as the bent sample in Figure 24 indicates.

The geometry of the transformation is consistent with a shear of pairs of (111) planes in the $[\bar{1}\,\bar{1}2]$ direction. Seeger[55] has suggested that cobalt transforms by the rotation of two half dislocations in the (111)

plane about the [111] direction and moving a distance along [111] of $2\,d_{(111)}$ at each revolution. As the temperature falls, the stacking energy decreases and the screw component about the dislocation line in the [111] direction begins to move through the structure causing the change in stacking sequence to produce the (ϵ) close packed hexagonal phase. Seeger attributes the retention of α at low temperatures to unfavorably oriented dislocations that can not initiate transformation. The transforming revolving dislocation has to break through these dislocations, requiring energy to do so.

The surface transformed regions do not have the lenticular shape that is typical of so many martensites and which arise through the restrictive effects imposed by the surface energy of the plate matrix interface and by other matrix stresses induced by the volume change associated with the formation of martensite. The less inhibited growth of cobalt martensite implies that such restrictions are minimal. This is reasonable: the volume change is small, the similarity of the martensite and the matrix structure might be expected to induce smaller surface energy terms than would be found in less compatible pairs of structures, and the martensite is formed by a simple, homogeneous shear -- in contrast to the more complex movements of shear compounded by secondary shear or "shuffling", in other systems.

COBALT WHISKERS

Few resistance measurements have been made on cobalt whiskers . This is largely due to the difficulty of handling whiskers and in measuring cross-sectional area to obtain an absolute resistivity. The curves of Figure 30, 31 and 32 imply a transformation at 405°C (cooling) and at 408°C (heating). This small hysteresis is significant for it has been pointed out by Seeger[55] that transformation characteristics are greatly affected by the grain size of the material.

Two alternatives may be offered to explain the small hysteresis of cobalt whiskers. It is small either as a result of the small number of grains or as a result of fewer dislocation modes. The effect of the number of grains arises because the activation barrier is decreased due to unrestricted movement of atomic planes at the boundary. Such freedom would encourage the whisker to return to its low temperature structure which is thermodynamically stable below 405°C. Thus, the hysteresis is small.

If, on the other hand, Seeger's[55] mechanism is correct then the lack of dislocations could account for the small hysteresis. There must, in fact, be an optimum dislocation density for which the transformation mechanism takes place most easily. This arises from the fact that while some dislocations are needed to initiate transformation other dislocations impede the transformation; that is, additional energy is required for the transforming combination of screw and partial dislocations to cross other imperfections. Since imperfect polycrystalline cobalt has many more dislocations that impede transformation than does a whisker, we would expect whiskers to transform with less hysteresis.

The comparatively sluggish nature of the transformation may

also be rationalized on the basis of the following qualitative argument. Consider the Burger's mechanism of transformation -- a shear of paired planes. Suppose that a pair of planes in the face centered cubic system shears by co-operative atomic propagation as the temperature is lowered. If these planes encounter a dislocation then the shear process will be stopped or retarded. This must be so because the transformation process is co-operative and involves a translation of $\frac{a}{\sqrt{6}}$ in a $[\bar{1}\,\bar{1}2]$ direction where "a" is the lattice parameter of the face centered cubic cell. Partial dislocations in the path of shear movement cancel out the other movement that is propagated by the motion of a partial. One would expect this to be less prominent in whiskers than in "normal" polycrystalline cobalt.

The resistance increase of the cycled structure may be attributed to an increase in the number of defects with each cycle, or to the increased number of grains after transformation. The latter is less likely, however, because the mean free path of electrons at room temperature is very small compared to the size of grains, therefore, grain boundary effects are not likely to be large. The constancy of resistance after several cycles indicates that the number of imperfections reaches a plateau. If this sort of qualitative argument is acceptable then type (2) transformation may be said to differ from type (1) in that the type (2) sample has initially a higher concentration of dislocations.

GENERAL DISCUSSION OF MARTENSITE

During past years interest has been expressed in the possibilities afforded by a wave model of martensite formation. Crussard[62] feels that martensite is the result of a shock wave propagation through the lattice. As a result, there is, first, a cooling and, after transformation, a heating of the metal. The wave produces a very thin layer of highly distorted metal, after which there is a period of plastic accommodation. Such a model is quite in line with the adiabatic theory of martensite formation.

Krisement et al[63] conjecture that there is not time for the heat of transformation to escape from the newly-formed martensite plate before the formation of neighbouring plates. Thus, the process should be considered adiabatic rather than isothermal. Crussard's shock wave model is in good agreement with the calculations of Krisement et al[63], if, in addition to the thermodynamic quantities involved, a kinetic energy term is added.

This sort argument has been carried a step further as a result of discussions with J. A. Goldak. It is well known that solutions of wave forms in a lattice are of the type $\psi = A(e^{-i\omega t + ikna})$ where:

ψ = wave displacement

A = amplitude

ω = frequency of wave

t = time

k = wave vector

a = lattice spacing

n = 1,2,3 . . .

Born[65] has shown that if ω is positive and complex a resonant condition is set up in the lattice such that the amplitude of vibration becomes infinite and the lattice breaks down.

Such a theory is consistent with martensite formation in that growth only occurs when the lattice is coherent with the parent phase. A wave exists in the lattice only as long as there is a regular array. There is increasing resistance to energy transfer as the coherency becomes less. This readily accounts for the high rate of energy transfer and, at the same time, shows why martensitic plate growth is limited.

Consider a γ/α' interface such as that shown in Figure 41. Energy is transferred across the boundary in the form of elastic waves. However, a transmission problem arises: not all of the wave energy is transmitted from the γ to the α' phase field but, presumably, some is reflected. The same is true of the wave travelling from α' to γ. The problem then reduces to finding the relative magnitudes of energy reflected and of energy transmitted as functions of time, temperature and shear angle.

This sort of theory does not suffer nucleation semantic problems as wavelengths from $2a$ to $2L$ are ever present in the lattice, where a = mean distance between atoms and L = length of the specimen. Martensite will form when precisely the correct frequency spectrum, determined by the temperature of the metal, presents itself. It is also well able to account for the characteristic crystallography associated with the transformation, because atomic vibrations are anisotropic. A vibration spectrum must then be associated with a crystallographic direction. It is, therefore, reasonable to expect that martensite will grow in preferred directions.

There is no easy and direct way of substantiating such a theory experimentally since spectrum data are not available and are difficult to obtain. However, the same can be said of all theories of martensite formation because the production of martensite involves undercooling into unstable regions. Thus, any direct measurement must be made while the metal

is being cooled. Such measurements would be of great value since most martensite theories depend upon relatively long extrapolations into undercooled regions. Indeed, experimental indications obtained from such experiments might well advance the theory of martensites very rapidly.

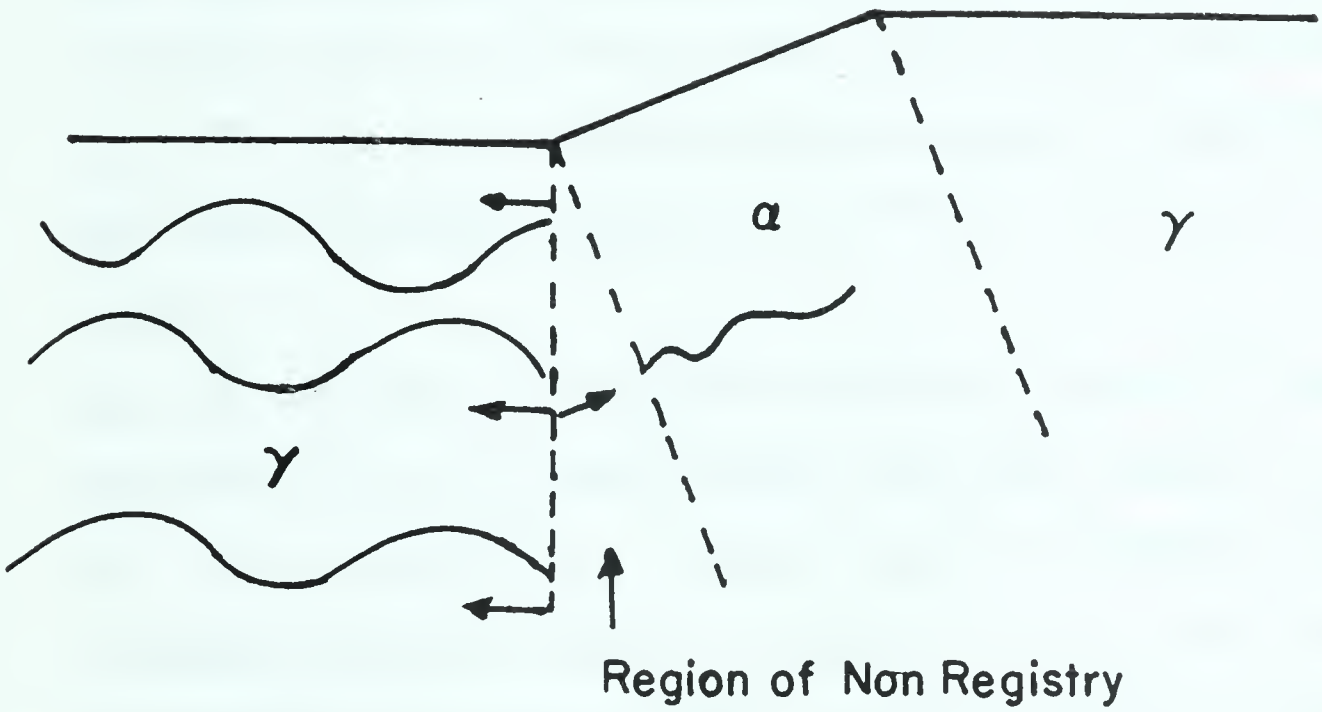

Figure 41

Schematic Representation of Lattice Wave Propagation During The Martensite Transformation. The Amount of Energy Depends Upon The Degree of Non Registry

CONCLUSIONS

(1) Iron containing 0.005 pct carbon transforms martensitically at 695°C 10°C. The critical rate for transformation is 33,000°C/sec 3,000°C/sec. At intermediate cooling rates, iron transforms as a massive structure at 742°C 10°C. At rates less than 3,000°C/sec the transformation is diffusion controlled. The M_s of iron with a carbon concentration of less than 0.0017 pct is 754°C 10°C.

(2) Small amounts of carbon lower the M_s temperature. An increase from 0.005 pct carbon to 0.010 pct carbon lowers the M_s temperature from 695°C to 560°C. The critical rate of transformation is reduced from 33,000°C/sec for iron with 0.005 pct carbon to 5,000°C/sec for iron with 0.010 pct carbon.

(3) The hardness of the massive structure is higher than equiaxed iron while martensitic iron is slightly higher than either massive or equiaxed iron.

(4) The transformation in titanium cooled at 200°C/sec is 872°C 10°C. A rumpled martensite surface is observed at this point. The transformation is depressed from 872°C to 782°C for titanium cooled at 64,000°C/sec. This suggests that titanium transforms isothermally. Titanium transforms at 890°C 10°C on reheating at 100°C/sec.

(5) There is only a slight increase in the hardness of titanium transformed martensitically.

(6) The transformation temperature of cobalt cooled at rates less than 200°C/sec is 382°C ± 5°C. The transformation temperature of cobalt cooled at 12,000°C/sec is depressed to 345°C ±10°C. Cobalt transforms at 432°C ± 5°C on reheating.

(7) There is a characteristic surface rumple effect associated with the cobalt transformation that is generally triangular - not lenticular. There was no increase in hardness with transformation.

(8) Cobalt Whisker crystals transform at 408°C ± 5°C on heating and 405°C ±5°C on cooling. Thus, the hysteresis of transformation is about 3°C compared to 50°C for bulk cobalt.

(9) Two types of whiskers resistance curves were found to exist: one, showing a marked transformation and the other showing a marked change in slope at the transformation temperature.

(10) The resistance of whisker crystals increases with the number of heating and cooling cycles until after a few cycles a resistance plateau is reached.

(11) The temperature - coefficient of resistance in whiskers is very much less than that of bulk cobalt.

(12) The sharp change in behavior of iron at a critical carbon content is tentatively rationized on the basis of the effect of interstitial carbon atoms on bond energies, or by assuming vacancy sites for carbon atoms.

(13) The calculation of the general shape of the time - temperature transformation curve from cooling rate data has been demonstrated and applied to the martensite transformation characteristics of titanium.

(14) The isothermal behavior of both titanium and of cobalt is rationalized on the basis of existing nucleation theory.

(15) Since the thermodynamic approach is no longer consistent with the M_s temperature of 750°C in high purity iron, and, in view of the theory's other limitations, a suggestion is made which relates martensite formation to lattice resonance.

REFERENCES

1. Zener, C., Physics Rev. (1947) 71, p. 846
2. Metals Handbook, American Society of Metals Publication (1948) p. 1181
3. Zener, C., Journal of Metals Trans. AIME (1955) 203, p. 619
4. Cobalt Monograph, Published by Center D'information Du Cobalt (1960) p. 75
5. Seeger, A., Stacking Faults in Close Packed Structure in "Defects in Crystalline Solids" (Report on the Conference, University of Bristol, July 1954) The Physical Society, London 1955, pp. 328-339
6. Kurdjumov, C. V., Journal of the Iron and Steel Institute (1960) 195, pp. 26-48
7. Bilby, B. A., and Christian, J. W., Institute of Metals Monograph and Report Series No. 18 (1956) p. 121
8. Greninger, A. B., and Troiano, A. R., (1946) Metal Progress 50, p. 303
9. Greninger, A. B., and Troiano, A. R., Trans. AIME (1949) 185, p. 590
10. Frank, F. C., Acta Met. (1952) 1, p. 15
11. Bunshah, R. F., and Mehl, R. F., Trans. AIME (1953) 197, p. 1251
12. Kulin, S. A., and Cohen, M., Trans. AIME (1950) 188, p. 1139
13. Averbach, B. L., and Cohen, M. Trans. A.S.M. (1949) 41, p. 1024
14. Kurdjumov, G. V., and Maksimova, O. P., Dokl. Akad. Nauk. SSSR (1948) 61, p. 83
15. Kurdjumov, G. V., and Maksimova, O. P., Dokl. Akad. Nauk. SSSR (1950) 73, p. 95
16. Kurdjumov, G. V., and Maksimova, O. P., Dohl. Akad. Nauk. SSSR (1951) 81, p. 565
17. Kaufman, L., and Cohen, M., Trans. AIME (1956) 206, p. 1393; Journal of Metal (1956) 8, p. 1393

18. Lieberman, D. S., The Mechanism of Phase Transformations in Metals, Institute of Metal Monograph and Report Series No. 18 (1955) Discussion

19. Harris, W. J., and Cohen, M., Trans. AIME (1949) 185, p. 447

20. Macklin, E. S., and Cohen, M., Trans. AIME (1951) 191, p. 746

21. Barrett, C. S., Structure of Metals. Pub. - McGraw Hill (1952) p. 559

22. Cohen, M., Macklin, E. S., and Paranjpe, V. G., Thermodynamics of the Martensitic Transformation in the "Thermodynamics of Metallurgy" A.S.M. publication (1952) p. 242

23. Kulin, A., Cohen, M., and Averbach, B. L., Trans. AIME (1952) 4 p. 661

24. Troiano, A. R., and McGuire, F. T., Trans. A.S.M. (1943) 31, p. 340

25. Fisher, J. C., Acta Met (1953) 1, p. 32

26. Kurdjumov, G. V., Phenomena Occurring in the Quenching and Tempering of Steels, Journal of the Iron and Steel Institute May 1960 p. 26

27. Massalski, T. B., Acta Met. (1958) 6, p. 243

28. Owen, W. S., and Gilbert, A., Journal of the Iron and Steel Institute (1960) 196 p. 142

29. Carpenter, H. and Robertson, J. M., Oxford University Press Second Impression (1944) p. 28

30. Saveur, H., and Chou, C. H. Trans. AIME (1929) 84 p. 350

31. Kaufman, L., and Cohen, M., Progress in Metal Physics, Pergamon Press, London (1958) 7 p. 165

32. Swanson, W. D. - MSc Thesis, University of Alberta, May 1962

33. Esser, H., Elender, W., and Spenel, E., Archiv Fur der Eisenhutten wesen (1933) 6 p. 389

34. Duwez, P., Journal of Metals (1951) 3, p. 765

35. Srivastava, L. P., and Parr, J. G., Trans AIME (1962) 224 p. 1295

36. McQuillan, A. D., Journal Inst. Metals (1950-51) 78, p. 249

37. McQuillan, A. D., Nature (1949) 164 p. 24

38. McQuillan, A. D. Proc. Roy. Soc. (1950) 204, p. 309

39. Burgers, W. G., Physics (1934) 1, p. 561

40. Newkirk, J. B., and Geisler, A. H., Acta Met. (1953) 1, p. 370

41. McHargue, C. J., Acta Cryst. Canb. (1953) 6, p. 529

42. Hess, J. B., and Barrett, C. S., Trans AIME (1952) 194, p. 645

43. Metcalfe, A. C., Acta Met. (1953) 1 p. 609

44. Marick, L., Physics Rev. (1936) 49, p. 831

45. Sebilleau, F., Bibring, C., and Buckle, C., Journal of Institute of Metals (1958-59) 87, p. 71

46. Sakae Takeuch, and Toshio Honma, Science Reports of Research Institute Tohoku University (Sandai Japan) December 1957 p. 492

47. Troiano, A. R., Tockich, J. L. Trans. AIME (1948) 175, p. 728

48. Edwards, O. S., Lipson, H., Journal Institute Metals (1943) 69, p. 177

49. Greninger, A. R., Trans. A. S. M. (1942) 30 p. 1

50. Bibby, M. J., McMullen, A. G., and Parr J. G., to be published in "Cobalt". (1963)

51. Yeo, R. B. G., Trans AIME (1962) 224, p. 1222

52. Mott, N. F. and Jones, H., The Theory of the Properties of Metals and Alloys, Dover Publications Inc. (1958) p. 24

53. Fisher, J, C., Holloman, J. H. and Turnbull D., J. App. Physics (1948) 19, p. 775

54. Fisher, J. C., Holloman, J. H., and Turnbull, D., Trans. AIME (1949) 185, p. 691

55. Seeger, A., Z Metallkunde (1956) 47, p. 653

56. Brenner, S. S., Properties of Whiskers and Whisker Crystals in Growth and Perfection of Crystals, John Wiley and Sons (1958)

57. Bibby, M. J., and Parr, J. G., The Spurious Titanium Transformation accepted for Publication AIME (1963)

58. Kaufman, L., Acta Met. (1959) 7 p. 575

59. Darken, L. S., and Smith R. P., Inc. Eng. Chem. (1951) 43, p. 1815

60. Singh, K. P., and Parr, J. G., Acta Met. 9 No. 12 p. 1073

61. Anderson, P. D., and Hultgren, H., Trans. AIME (1962) 224, p. 842

62. Crussard, C., and Philibert, J., Journal Iron and Steel Institute (1955) 180, p. 39

63. Krisement, O., Hourdremout, E., and Wever, F., (1954) Revue De Metallurgie 51, p. 401

64. Smith, E., from "Direct Observation of Imperfections in Crystals" Interscience Publication of John Wiley and Sons (1962) p. 203

65. Born, M. and Huang, K., From "Dynamical Theory of Crystal Lattices" Oxford Clarendon Press (1954) p. 153

APPENDIX I TABLE V

THE $\gamma \rightarrow \alpha$ TRANSFORMATION IN IRON

COOLING RATE $^{o}C/SEC$	TRANSFORMATION TEMPERATURE $^{o}C \pm 10^{o}C$
1	882
31	862
50	850
150	835
1500	795
2600	774
3100	754
3600	735
4200	742
5000	744
5600	741
6300	732
8500	742
9200	738
11,000	742
13,000	744
16,600	740
19,200	738
24,000	742
32,000	721
33,000	733
36,200	709
41,000	700

COOLING RATE °C/SEC	TRANSFORMATION TEMPERATURE °C ±10°C
43,300	704
50,000	688
53,000	694
57,000	695

TABLE VI

TRANSFORMATION TEMPERATURE OF CARBURIZED IRON

Specimen Treatment	Cooling Rate	Transformation Temperature °C ± 5°C
As Received	100°C/sec	825
	12,000°C/sec	742
	upquench - 150°C/sec	912°C
Soaked in a methane atmosphere of 10^{-3} mm mercury for $\frac{1}{3}$ hr. at 750°C	100°C/sec	830
	12,000°C/sec	745
	upquench 150°C/sec	912°C
Soaked in a methane atmosphere of 10^{-2} mm mercury for $\frac{1}{3}$ hr. at 750°C	100°C/sec	830
	12,000°C/sec	745
	upquench 150°C/sec	912°C
Soaked in a methane atmosphere of 1 inch mercury for 2 seconds ± 1 second at 750°C	100°C/sec	835
	12,000°C/sec	750
	upquench 150°C/sec	912°C
Soaked in a methane atmosphere of 1 inch of mercury for 5 seconds at 750°C	100°C/sec	805
	12,000°C/sec	698
	upquench 150°C/sec	910°C
Soaked in a methane atmosphere of 1 inch of mercury for 13 seconds at 750°C	100°C/sec	774
	12,000°C/sec	595
	upquench 150°C/sec	905°C
Soaked in a methane atmosphere of 1 inch of mercury for 20 seconds at 750°C	100°C/sec	760
	12,000°C/sec	520
	upquench 150°C/sec →	900°C

APPENDIX II

TABLE VII

THE $\beta \rightarrow \alpha$ TRANSFORMATION IN TITANIUM

COOLING RATE °C/SEC	TRANSFORMATION TEMPERATURE °C ± 10°C
5	885
100	872
1100	868
1500	865
2600	864
3400	865
5500	864
7800	860
10,500	858
11,000	855
14,000	851
18,000	844
19,200	838
21,500	840
24,000	830
26,000	832
29,200	826
31,500	825
36,000	820
38,000	817
42,000	815
50,000	802
63,600	782

APPENDIX III

THE SPURIOUS TITANIUM TRANSFORMATION

In addition to the β (body centered cubic)$\rightarrow\alpha$close packed hexagonal transformation at 882°C, a second distinct change of slope has been observed on a titanium cooling curve between 905°C and 960°C . Duwez[34] commenting on work by McQuillan[37] attributed this arrest to contamination of the specimen with oxygen --- a possibility that existed even at the reduced pressure of 10^{-5} mm Hg at which the experiments were conducted.

Cooling curves similar to those obtained by Duwez were reproduced by the authors using chromel - alumel thermocouple wires spot welded to a small titanium sample[67]. Both arrests during cooling are shown in (Figure 42). However, when platinum - platinum rhodium thermocouple wires were used there was no indication of the high temperature arrest,(Figure 43). Further, on examination of polished surfaces before and after quenching revealed a cavity at the surface between base metal thermocouple and titanium of a size greater than the thermocouple junction,(Figure 44). There was, however, very little disturbance around the platinum - platinum rhodium thermocouple,(Figure 45). Microhardness measurements (20 gm load) on the polished surface of the transformed sample attached to the chromel - alumel wires were found to increase from a value of 106 DPN near the periphery of the sample to values of 185 DPN near the chromel - alumel thermocouple wires,(Figure 46). Tests on larger samples of titanium from which the specimens for thermal analysis were cut gave hardness values of 106 DPN with a 20 gm load and 89 DPN with a 10 Kgm load.

These observations imply that the high temperature arrest is a result of alloying between the chromel - alumel thermocouple and the sample, rather than oxygen contamination. In order that the second transformation

take place at 945°C as indicated by the cooling curve, a concentration of at least 2% oxygen would be required. If this concentration existed only at the surface, a surface hardness of something greater than 350 DPN would result, in contrast to our value of 106 DPN. On the other hand, a large concentration of either nickel or aluminum in the immediate vicinity of the thermocouple would account for the additional arrest. The lower temperature arrest of 882°C can, of course, be attributed to the mass of pure titanium outside the alloy zone.

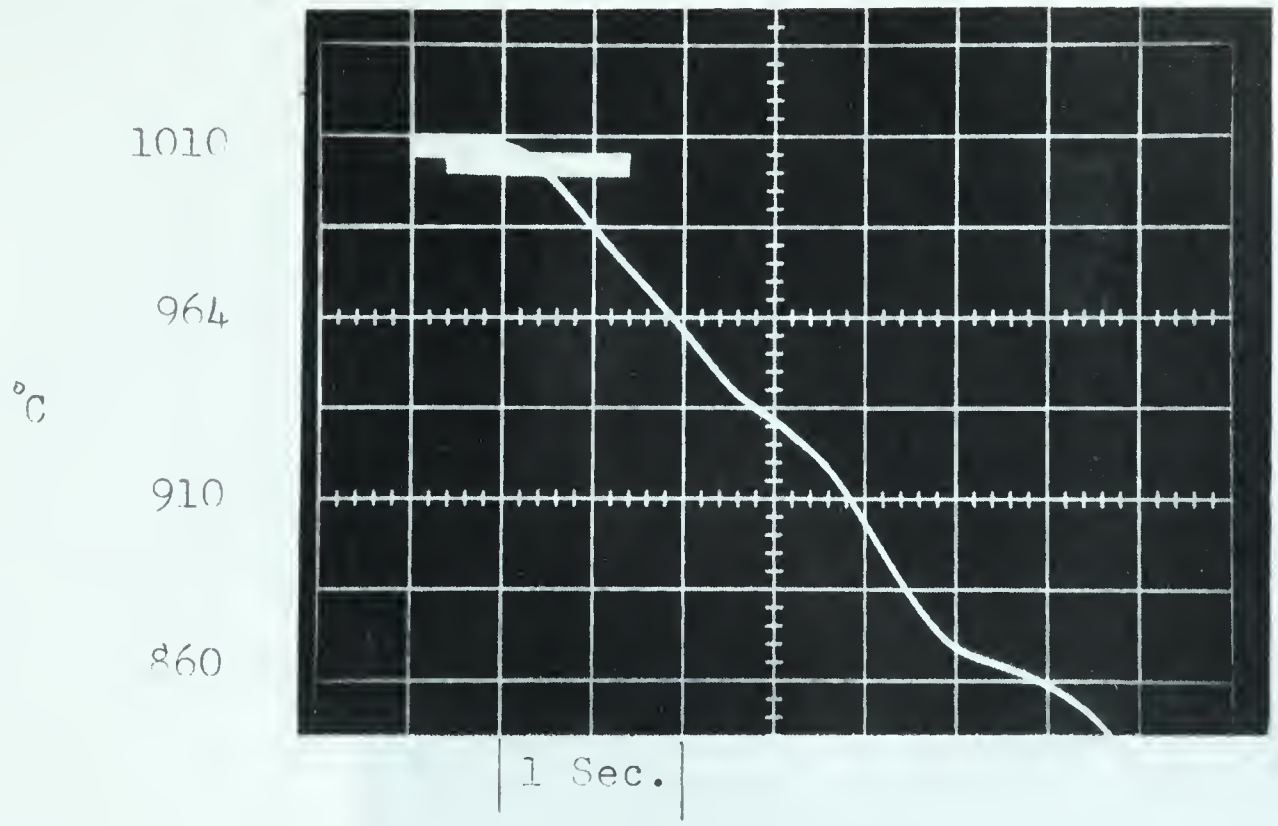

Figure 42 Oscilloscope Trace of Titanium Cooling Curve using Chromel – Alumel Thermocouple Wire

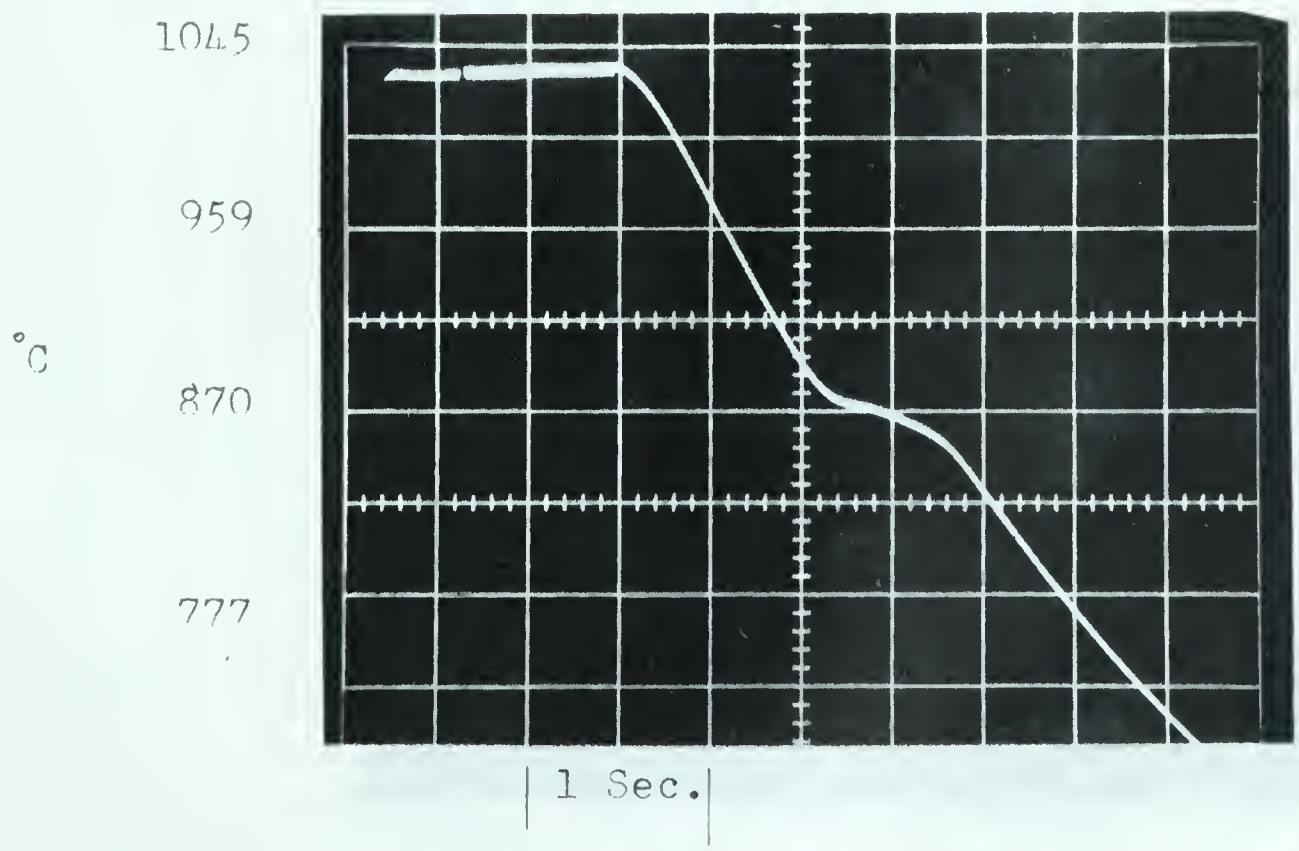

Figure 43 Oscilloscope Trace of Pure Titanium Cooling Curve Using Platinum – Platinum Rhodium Thermocouple Wire

Figure 44 X200 Transformed Surface of Polished Titanium Showing Base Metal Thermocouple Region

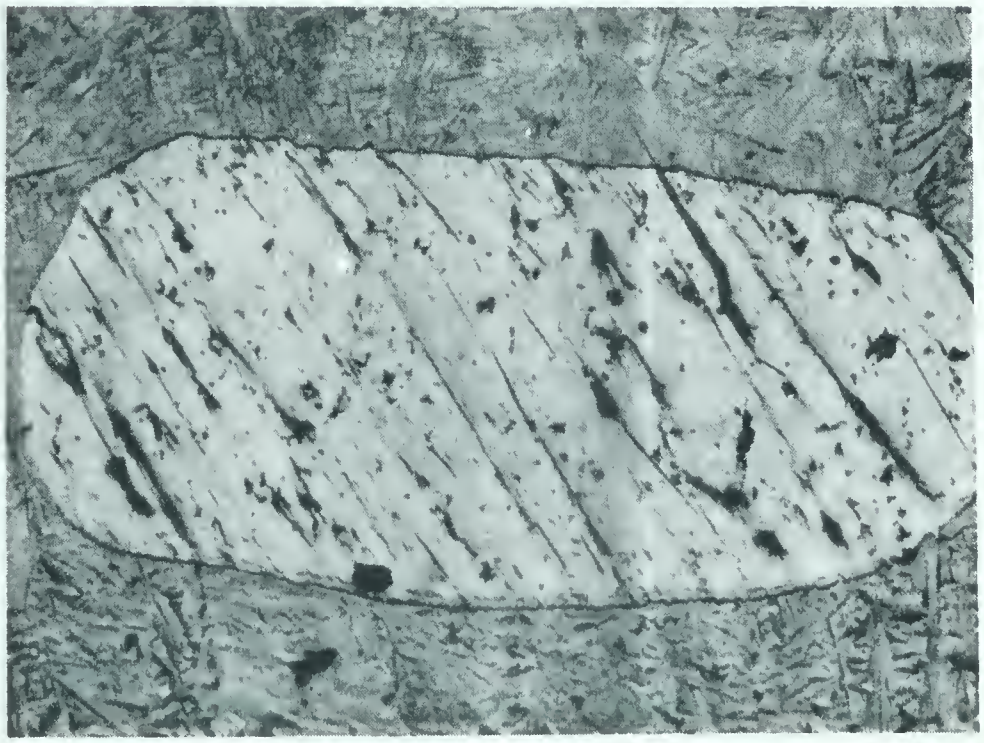

Figure 45 X200 Transformed Surface of Polished Titanium Sample Showing Platinum – Platinum Rhodium Thermocouple Region

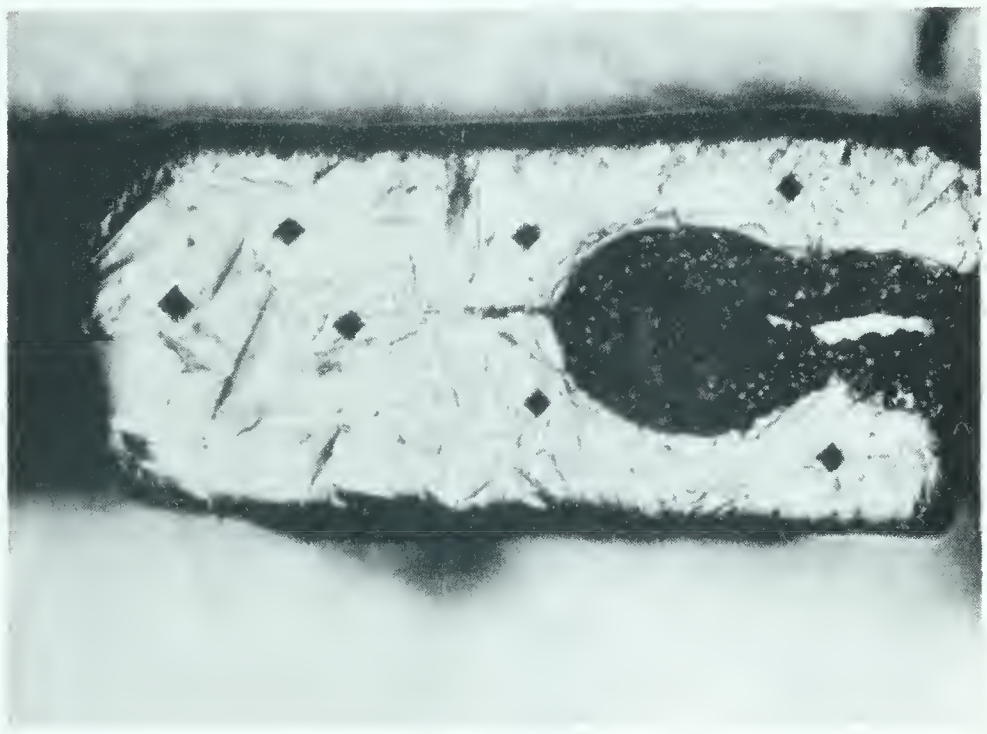

Figure 46 X150 Transformed Surface of Polished Titanium Showing Hardness Indentations in the Base Metal Thermocouple Region

APPENDIX IV TABLE VIII

THE $\alpha \rightarrow \epsilon$ TRANSFORMATION IN COBALT

COOLING RATE °C/SEC	TRANSFORMATION TEMPERATURE °C ± 5°C
5	382
100	380
1000	382
1100	382
2100	380
2200	382
3400	377
5000	370
7000	362
7200	360
10,000	352
12,000	345

APPENDIX V TABLE IX

THE $\alpha \rightarrow \epsilon$ TRANSFORMATION IN COBALT WHISKERS

WHISKER TYPE (1)

TEMPERATURE °C ±3°C	RESISTANCE (INITIAL) OHMS	
	HEATING	COOLING
100	2.54	2.82
150	2.34	3.16
200	3.17	3.66
250	3.51	4.15
300	3.94	4.78
325	4.22	5.12
350	4.41	5.42
375	4.64	5.78
400	4.97	
402	5.00	
403	5.01	
404	4.03	6.12
405	5.04	6.19
406	5.04	
410	5.06	6.24
412	5.07	
415	5.05	6.33
420	5.03	
425	5.46	6.46
450	5.46	6.86
475	6.00	7.21

TEMPERATURE °C	RESISTANCE (INITIAL) OHMS	
	HEATING	COOLING
500	6.50	7.60
550	7.67	8.35
575	8.49	8.80
600	9.10	9.10

TABLE X

THE CYCLED RESISTANCE OF COBALT WHISKERS

TYPE (1)

TEMPERATURE °C ±3°C	RESISTANCE (OHMS) (HEATING) CYCLE 1	CYCLE 2	CYCLE 3	CYCLE 4
100	2.54	2.73	2.96	3.015
150	2.84	3.05	3.22	3.36
200	3.17	3.41	3.63	3.78
250	3.51	3.84	4.14	4.29
300	3.94	4.37	4.64	4.90
325	4.22	4.69		
350	4.41	5.05	5.35	5.55
375	4.64	5.39	5.72	5.90
400	4.97	5.77	6.05	6.34
410	5.06	5.93	6.19	6.47
425	5.05	6.00	6.50	6.74
450	5.46	6.61	6.90	7.15
475	6.00	7.32	7.40	7.59
500	6.50	7.67	7.89	8.14
550	7.67	8.80	8.02	9.72
575	8.49	9.15		
600	9.10			

TEMPERATURE °C ±3°C	RESISTANCE OHMS CYCLE 5	CYCLE 6	CYCLE 7
100	3.10	3.14	3.13
150	3.38	3.41	3.42
200	3.80	3.85	3.83
250	4.33	4.32	4.36
300	4.92	4.90	4.94
325	5.33	5.32	5.35
350	5.58	5.58	5.58
375	5.95	5.96	5.90
400	6.38	6.40	6.41
410	6.49	6.55	6.55
425	6.80	6.82	6.85
450	7.20	7.22	7.27
474	7.70	7.71	7.69
500	8.20	8.19	8.19
550	9.31	9.35	9.35
575			
600			

TABLE XI

THE $\alpha \rightarrow \epsilon$ TRANSFORMATION IN COBALT

WHISKER TYPE (2)

TEMPERATURE °C ± 3°C	RESISTANCE (OHMS)(INITIAL)	
	HEATING	COOLING
25		
50		
75	18.25	20.55
100	19.15	
150	21.40	21.60
200	24.10	23.50
250	27.20	30.10
300	31.20	34.70
325	33.20	37.40
350	35.50	39.90
375	38.00	42.70
400	41.30	46.0
415	42.60	
420	43.10	48.60
425	43.70	50.00
450	50.2	52.40
500	55.0	58.70
550	64.7	64.7

APPENDIX VI TABLE XII

MATERIAL USED IN INVESTIGATION

I Iron - obtained from Johnson Mathey and Mallory

110 Industry Street

Toronto, Ontario

Impurity	PPM
Ni	10
Si	7
Mn	5
Cr	3
Mg	2
Ag	less than 1
Carbon	0.03 pct

II Iron - obtained from National Bureau of Standards

Washington, D. C.

Total metallics less than 15 ppm

Total non-metallics less than 15 ppm

Titanium - obtained from Foote Mineral Company,
18 West Chelten Avenue,
Philadelphia 44, Pa.

Metal	Concentration
Si	0.004
Al	0.003
Mg	0.005
Mn	0.003
Fe	0.002
Cr	Trace
Ni	Trace
Sn	0.006
Cu	0.002
Ca	0.008
Mo	N.D.
Zr	0.05

Cobalt - obtained from Sherritt Gordon Mines Ltd.,
Marketing Division,
25 King Street West,
Toronto 1, Ontario

	Concentration
Cobalt	99.9%
Cu	0.005
Fe	0.018
Ni	0.100
S	0.004
C	0.014

APPENDIX VII

LIST OF PUBLICATIONS

(1) Bibby, M. J., McMullen, R. G., and Parr, J. G., Cobalt Whiskers - accepted for publication in "Cobalt" 1963

(2) Bibby, M. J., and Parr, J. G. The $\alpha \rightarrow \epsilon$ Transformation in Polycrystalline Cobalt - accepted for publication in "Cobalt" 1963

(3) Bibby, M. J., and Parr J. G. The Spurious Titanium Transformation - accepted for publication in Transaction AIME 1963

B29805